Chapter 5

DETERMINATION OF STABILITY

5.1. The "Parcel" Theory as a Basis for Determining Stability and Instability. Nearly all the procedures routinely used to evaluate and analyze the stability of the atmosphere are manipulations of the so-called "parcel" method, which is a particular way of applying certain physical laws of hydrostatics and thermodynamics. It is simply a theory which assumes an over-simplified model of the behavior of the atmosphere. We do not yet know just how closely this model corresponds to reality. Only recently have serious attempts been made to analyze the physics of clouds and atmospheric convection in more realistic and quantitative detail. These studies provide some useful corrections and modifications to parcel-method procedures, as will be shown in Chapter 8 of this manual. The theory of the parcel-method will now be described briefly and qualitatively along with general indications of its unrealistic assumptions and their effects on the practical utility of the method.

The temperature of a minute parcel of air is assumed to change adiabatically as the parcel is displaced a small distance vertically from its original position. If the parcel is unsaturated, its virtual temperature (see pars. 4.13 and 5.8) is assumed to change at the dry-adiabatic rate; if the parcel is saturated, the change will occur at the saturation-adiabatic rate. In addition, it is assumed that the moving parcel neither affects, nor is affected by, the atmosphere through which it moves; i.e., the parcel does not "mix" with nor disturb the surrounding air.

If, after the vertical displacement, the parcel has a higher virtual temperature (i.e., lower density) than the surrounding atmosphere, the parcel is subjected to a *positive buoyancy force* and will be further accelerated upwards; conversely, if its virtual temperature has become lower than that of the surrounding air, the parcel will be denser than its environment (subjected to a *negative buoyancy force*) and will be retarded and eventually return to the initial or equilibrium position.

The atmosphere surrounding the parcel is said to be *stable* if the displaced parcel tends to return to its original position; *unstable* if the displaced parcel tends to move farther away from its original position; and *in neutral equilibrium* when the displaced parcel has the same density as its surroundings.

According to the parcel theory, the behavior of a parcel which, once it is saturated, becomes warmer than its environment through the release of the latent heat of condensation, is as follows. The parcel ascends under acceleration from the positive buoyancy force. If the saturated parcel continues to rise through an atmosphere in which the lapse rate exceeds the saturation adiabatic, the speed of the ascent increases. This acceleration persists until the height is reached where the saturation-adiabatic path of the parcel crosses the temperature sounding; i.e., where the parcel temperature becomes equal to the environment temperature. This height has been defined as the equilibrium level (EL) in paragraph 4.24. The rising parcel at this point has its maximum momentum. It now passes above the EL, becomes colder than the environment (negative buoyancy) and is decelerated in the *upper negative area*, until it comes to rest at some unspecified distance above the EL ("overshooting"). The acceleration and speed of the parcel at any point can be computed from the temperature excess of the parcel over the environment by the buoyancy formula — but it usually gives a very unrealistic result.

5.2. General Comment on the Effect of the Assumptions in the Parcel Theory on the Utility of Parcel-Method Techniques. Meteorologists of a generation ago experimented extensively with the use of parcel-method techniques for analysis and forecasting of air masses, fronts, and convection weather. There was, at that time, little knowledge of cloud physics and convection mechanisms. Ideas of air-mass and frontal analysis predominated in the forecaster's routine, and the forecasters were eager to use soundings in place of indirect aerology. In more recent years, experience has shown that while identification of air-mass type is no longer a problem requiring soundings, the analysis of the soundings for temperature, moisture, and stability characteristics of the air remains one of the basic tools for weather forecasting. But this kind of analysis *by itself* has not proved very useful for forecasts of over six hours, and the necessity of also considering circulation characteristics and dynamics is now generally recognized [2] (and *AWS TR200*).

Parcel methods are useful because there are definite empirical relations between the results of parcel computations and the observed atmospheric behavior. Also, the parcel computations can provide a sort of standard of reference against which various more realistic procedures or forecasts may be compared to see if they are an improvement over the pure parcel computations.

In Chapter 8, considerable information from recent observational, theoretical, and experimental studies of convection and cloud physics will be referenced that appears to have a practical value in adapting parcel procedures to the real atmosphere and in appreciating their limitations. At this point it will suffice to note that the main effects observed in real convection and clouds which are not accounted for by the parcel theory are:

a. Lateral mixing of the convection-thermal or cumulus cloud with its environment ("dynamic entrainment"), which reduces the water content and buoyancy — at least of the outer parts of the convection column.

b. Vertical mixing, within the convection-thermal or cloud cell itself and with the environment at the top; in the cumulus cloud this is manifested by downdrafts, "holes," etc., and causes redistribution of condensed water and departures from the saturation-adiabatic lapse rate locally and for the cloud as a whole — these effects may be more important than those of lateral mixing.

c. Cooling from evaporation of falling precipitation; e.g., the lapse rate in rising saturated air which is being cooled by melting of falling snow or hail is 9°C to 14°C per kilometer.

d. Skin-friction and form-drag (dynamical interaction) between the rising thermal or cloud and the surrounding winds — especially when there is strong vertical-wind shear in the environment.

e. The compensatory subsidence in the environment of a rising convection current (see par. 5.23).

f. Internal viscous friction (can be neglected).

g. Radiation to or from cloud boundaries (see par. 5.11.0).

h. Different effects for coalescence versus ice-crystal precipitation process.

i. Cellular structure.

j. Reduction in buoyancy due to weight of condensed water (see par. 5.3).

k. Drag of falling precipitation on upward vertical motion.

Although the theory for many of these effects permits estimates of the right order of magnitude, observations of most of the parameters required for such computations are either not routinely obtainable or are not specifiable in sufficient detail and accuracy. In empirical forecast studies, the effects of the above factors are often indirectly "built-in" by correlating the actual weather occurrences with parcel-method-derived parameters or with combinations of such parameters and synoptic parameters. In general, the parcel-theory assumption of solid, continuous, adiabatic ascents in clouds gives values of updraft speed, water content, and temperature much too high compared to observations. Nevertheless, since these departures have a largely systematic character, the parcel-method procedures are useful in an empirical way. This relation is probably fortuitous, but a very fortunate one for the forecaster.

5.3. The Parcel-Theory Assumptions Used in the DOD Skew-T Chart. Any thermodynamic diagram designed for use in atmospheric studies is merely a graphical means of presenting the parcel theory for such applications. However, there are actually a number of differences in the assumptions which have been incorporated into the various adiabatic diagrams used by meteorologists. Apart from the choice of physical constants, which has now been standardized by WMO [65], these differences have chiefly concerned the assumptions about what happens to the condensed water after saturation takes place and about the change in state due to freezing of the condensed water.

For the older-type adiabatic diagrams, the saturation adiabats at temperatures below 0°C were computed from vapor pressures over an ice surface. Evaluations of stability and parcel temperatures for lifting or heating effects on such diagrams will differ from results on the newer diagrams (such as the present DOD Skew-T Chart, the current Navy "Arowagram," and the U.S. Weather Bureau pseudo-adiabatic charts) based on vapor pressure over water at all temperatures. In some cases, the differences are considerable.

The assumption of vapor pressure over water at all temperatures is deemed somewhat more realistic in view of the predominance of supercooling in clouds at least down to -20°C.

The error due to the pseudo-adiabatic assumption (that all the condensation products immediately fall out) is small (<1°C) in case of a cloud which does not precipitate as long as the rise of the saturated parcel is not over 200 mb and no freezing takes place [54]. In real clouds, the latent heat of fusion (freezing), however, adds considerable buoyancy to the parcel at temperatures below -10°C (compared to the water pseudo-adiabatic assumption) [54]. Direct fallout of most of the condensed water as precipitation, of course, does occur from many clouds. In large cumulus and thunderstorms, much of the precipitation from one part of the cloud may be evaporated into another part of the cloud, causing a marked redistribution of the buoyant energy.

5.4. Identifying the Basic Types of Stability and Instability for Small Parcel Displacements in a Sounding Plotted on the Skew-T Chart. The stability of air parcels in a given layer of the atmosphere according to elementary parcel theory is indicated on any thermodynamic diagram by comparing the slope[13] of the T_v curve for the layer with

[13] The term "slope" when used in this manual in reference to the Skew-T Chart is the angle from the horizontal (i.e., isobars) counterclockwise to a segment of the *T* curve. In terms of stability, the smaller the counterclockwise angle from the horizontal, the greater the stability, or the less the instability. Frequently, it is convenient to refer to the "steepness" of a slope (lapse rate). This descriptive term is usually applied only to slope angles greater than 90 degrees. When one lapse rate is said to be "steeper" than another, this means that its slope angle is the greater.

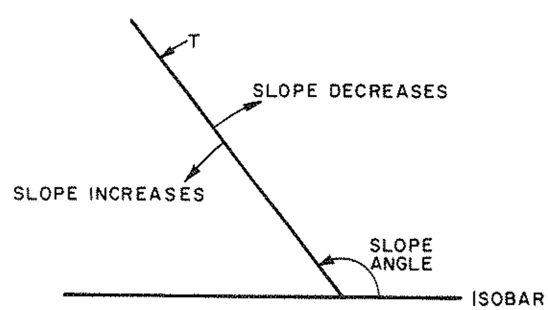

the slope of the dry or saturation adiabats. The dry adiabats are applicable to the comparison when the parcel is unsaturated; the saturation adiabats when the parcel is saturated.

In present forecasting practice, however, the ambient (free-air) T curve is almost always used in lieu of the more exact T_v curve in making these comparisons, thus eliminating the need for the laborious point-by-point computation of the T_v curve and permitting quick evaluation of the stability or instability. Under certain conditions, this substitution becomes a source of significant error in stability evaluations. A discussion of these errors is given in paragraph 5.8. In this manual, all the stability criteria are applied, unless otherwise specified, by use of the T curve in making slope comparisons with the adiabats. A detailed discussion of the exact (mathematical) form of the stability criteria according to parcel theory can be found in many standard textbooks on meteorology, e.g., [33].

Before describing the criteria used to judge the stability or instability of parcels with respect to their environment *at the time of the sounding*, it is well to note two underlying assumptions that have not been explicitly mentioned in most textbooks.

a. These criteria employ the observed lapse rate through a finite layer as the indicator of the stability of all the infinitesimal parcels in the layer. Thus, it has become customary in using these criteria to speak of the "stability of a *layer*," meaning that *all* the parcels in the layer are liable to the same effect from a vertical displacement because the lapse rate of the layer is constant. In this sense, a "layer" is defined as a slab of the atmosphere which has a uniform, constant lapse rate and is bounded by significant discontinuities in the lapse rate. However, in practice, "layers" are often referred to by arbitrary boundaries which may not coincide with the extent of the uniform lapse rate — the context of the reference will usually make clear what kind of bounds are being used. (For the formal classification of "layers" and "discontinuities," see Chapter 6.)

b. The theory of these criteria assumes that the parcels are subjected only to *small* vertical displacements such as those caused by very slow, general vertical motion embedded in a large-scale flow or by the usual small-scale eddy turbulence in the free air (away from surface friction and deep convection currents). In spite of this theoretical qualification, in practice the criteria apply well to a very large part of the atmosphere most of the time. Both the troposphere and stratosphere are predominately very stable, and their general circulation is prevailingly quasi-horizontal. The non-adiabatic processes and vertical motions which tend to alter the lapse rate (see pars. 5.10 through 5.17) operate relatively slowly, and the areas where at any moment these processes are causing change from stability to instability, or vice versa, cover only a small proportion of the total troposphere. Thus, instability tends to be localized, as in cumulus clouds or in frontal cloud-shields, and to be surrounded by much larger areas of compensating gentle subsidence (which usually increases stability). As a rule, the individual parcels within a widespread stable layer can be lifted or lowered a considerable distance as the whole layer is lifted or lowered, without greatly changing the general structure or identity of the layer. For these reasons the lapse-rate criteria for stability of parcels under small vertical displacements are generally representative over large areas and for periods of many hours if not longer.

For the analysis of stability with respect to the effects of *large* vertical displacements of single parcels (or of whole layers en masse), and to the effects of non-adiabatic heating or cooling, various criteria and procedures in addition to those described in this paragraph are required — these will be introduced in paragraphs 5.17 through 5.22.

5.5. Description of Stability Criteria. The stability of any given layer for small parcel displacements is classified as follows:

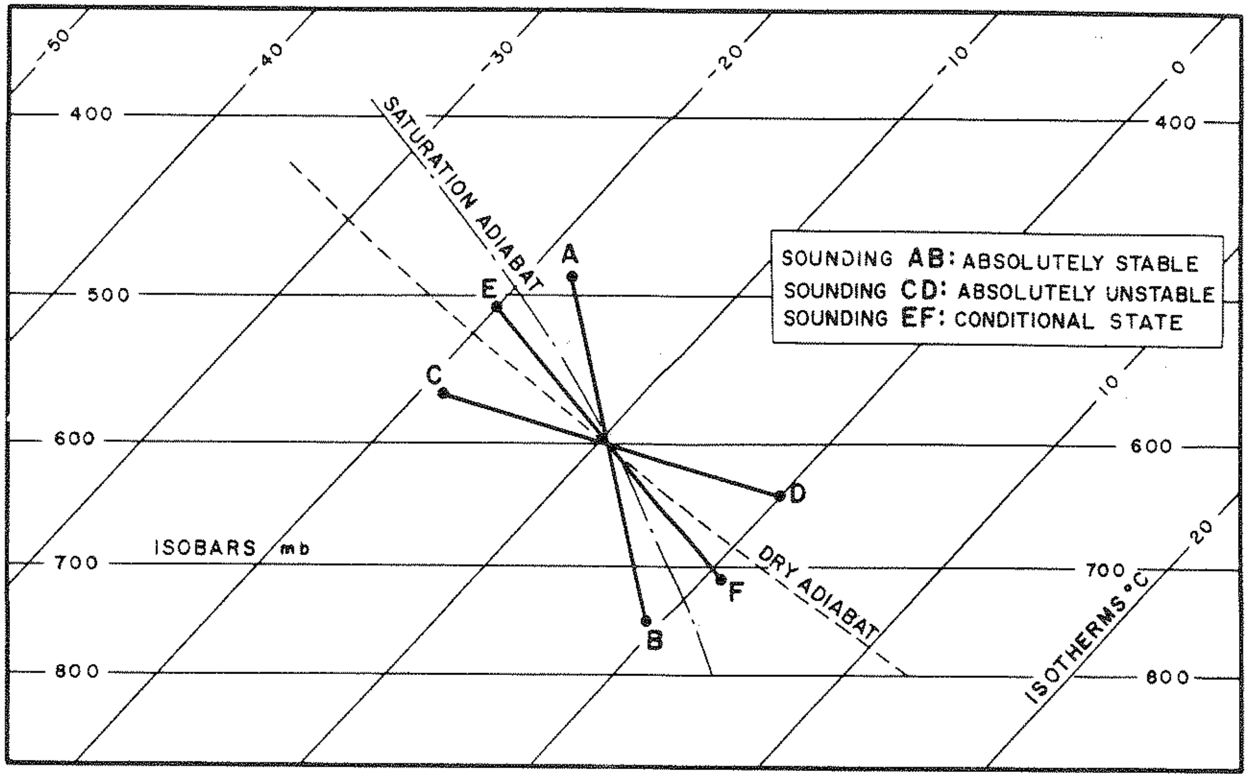

Figure 23. Stability Classifications.

$\Gamma = \frac{g}{c_p}$

a. *Absolutely Stable*. If the slope of the *T* curve is greater than the slope of the saturation adiabat (see Curve AB in Figure 23), the layer is *absolutely stable*; i.e., stable regardless of its moisture content. If a parcel at Point B in Figure 23 were displaced upward, its temperature change would follow either the saturation or the dry adiabat, depending on whether or not the parcel were saturated. In either case, however, the parcel would be colder than its new environment, and would tend to sink back to its original position. If either a saturated or unsaturated parcel were displaced downward from Point A, its temperature change would follow the dry adiabat. The parcel would then be warmer than its new environment and would tend to rise back to its original position. (Various sub-types of absolutely-stable lapse rates are mentioned in par. 6.2.)

b. *Absolutely Unstable*. If the slope of the *T* curve is greater than the slope of the dry adiabat (see Curve CD of Figure 23), the layer is *absolutely unstable*; i.e., unstable regardless of its moisture content. This condition is also referred to as a *superadiabatic lapse rate*. If a parcel at Point D in Figure 23 were displaced upward, its temperature change would follow either a saturation or a dry adiabat depending on whether or not the parcel were saturated. In either case, however, the parcel would then be warmer than its new environment, and would be accelerated upward. If the parcel at Point C were displaced downward, its temperature change would follow the dry adiabat. The parcel would then be colder than its environment and would be accelerated downward.

c. *Autoconvection Lapse Rate*. There are superadiabatic lapse rates where the temperature decrease with altitude is so great that the density of the air is either constant or increases with altitude. The density of air is constant with height when the lapse rate is equal to 3.42°C per 100 meters. This is known as the *autoconvection lapse rate* or the *autoconvection gradient*. When this lapse rate is reached or slightly exceeded, the denser air

$\Gamma \geq 3.5\,\Gamma_d$ $\Gamma_d = 9.8\ \frac{deg}{km}$

$\Gamma \geq 3.43\frac{°C}{100\ m}$

above will spontaneously sink into the less dense air below. This spontaneous overturning of the atmosphere is termed *autoconvection*, for it represents the self-convection of air without an external impulse being applied.

d. *Conditional State.* If the slope of the T curve is less than the slope of the dry adiabat, but greater than the slope of the saturation adiabat, as along Curve EF of Figure 23, such a layer is often called "conditionally stable," or "conditionally unstable," meaning that it is stable if unsaturated, unstable if saturated.[14] If a saturated parcel at Point F in Figure 23 were displaced upward, its temperature change would follow the saturation adiabat. The parcel would then be warmer than the surrounding air and would be accelerated upward; hence, the layer would be unstable. If the displaced parcel were unsaturated, however, its temperature change would follow the dry adiabat. In its new position, the parcel would be colder than its surroundings and would sink back to its original position; hence, the layer would be stable. In the case of downward displacement, the temperature change of both saturated and unsaturated parcels (under the pseudo-adiabatic assumption) would follow the dry adiabat. In its new position, the parcel would be warmer than its environment, and would tend to rise back to its original position. In other words, parcels in a conditional layer are actually stable for *all* downward displacements, whether initially saturated or unsaturated and regardless of moisture content. (In real clouds, evaporation of suspended water droplets will cause downward displacements to follow the saturation adiabat until the drops have evaporated, but if the layer has a lapse rate less steep than the saturation adiabatic, such parcels will be stable and tend to return upward.)

e. *Neutral Equilibrium.* If the T curve parallels an adjacent saturation adiabat, the layer is *in neutral equilibrium* for the upward displacement of *saturated* parcels; i.e., the upward displacement of saturated parcels will be neither aided nor hindered by the surrounding atmosphere. (However, for upward displacement of unsaturated parcels and downward pseudo-adiabatic displacement of all parcels, this curve is stable.) Similarly, if the T curve parallels an adjacent dry adiabat, the layer is *in neutral equilibrium* for the displacement of *unsaturated* parcels (but unstable for upward displacement of saturated parcels). These two conditions of equilibrium are frequently termed "Saturation Indifferent" and "Dry Indifferent," respectively.

5.6. Discussion of Superadiabatic Lapse Rates. Many investigations have shown that genuine superadiabatic lapse rates frequently occur within the lowest 1000 feet of the ground. However, when absolutely-unstable lapse rates are reported in the troposphere above the gradient-wind level, as shown between Points C and D of Figure 23, they often have been rejected as erroneous data [32]. This rejection arises from the assumption that some measurement defect or spurious effect, such as condensed water evaporating from either the radiosonde instrument housing or the thermistor, must be causing the excessive cooling. Presumably, this generally occurs while the instrument is emerging from the top of a cloud layer into the very dry air of a capping inversion. This is, in fact, where superadiabatic lapse rates are frequently reported. Admittedly, the resulting error is more likely with some makes of radiosonde than with others, and does account for some of the cases of superadiabatic lapse rates reported. However, there is now

[14] The expression "conditional instability" is frequently used by meteorologists to refer to both the unsaturated and the saturated condition. The context will usually make clear which sense is meant. Also, the term "conditional stability" is sometimes incorrectly used when "conditional equilibrium" or conditional instability" is meant; this confusion results from an effort to avoid the apparently illogical use of the word "instability" to describe a layer which is actually stable. For this reason the expression "conditional state" is preferable. Some writers denote "conditional (in)stability" as "selective (in)stability," which is equally ambiguous.

sufficient evidence to indicate that valid cases of superadiabatic lapse rates can occur through a fairly shallow layer sandwiched between stable layers in the troposphere [26] [32].

There are two processes which can explain the occurrence of such real superadiabatic lapse rates:

a. Sufficient destabilization due to rapid lifting at a saturated/dry-air interface within the lifted layer.

b. High rate of evaporation at the top of a cloud layer. The simultaneous occurrence of both processes is also likely.

Thus, when a superadiabatic lapse rate is included in a raob report, the possibility of it being a valid observation can no longer be ignored. A study of the synoptic conditions occurring in the area of the raob ascent to determine the causal process is preferable to a routine rejection of the report. When rapid lifting of tropospheric layers is likely, due to either the rapid movement of a cold front or orographic lifting, there is a rather high probability of finding a shallow layer with a transitory superadiabatic lapse rate. Altocumulus castellanus reports on the surface chart are often noted in the area of such activity. (See also par. 5.20.2 for further details on the effects of lifting on the lapse rate.)

5.7. Oscillation of a Parcel as a Function of Stability. It is a corollary of the classical parcel theory of stability that a parcel given a forced or buoyancy impulse may be assumed to oscillate about its EL rather than return to EL immediately. The period of such an oscillation is given by an equation analogous to that for simple harmonic oscillation of a pendulum, i.e., approximately:

$$2\pi/\text{period} = \sqrt{\frac{(\text{gravity})}{(\text{temperature})} \quad \text{x (“delta” lapse rate)}}$$

where "delta" lapse rate is the difference between the dry-adiabatic lapse rate and the actual lapse rate in the region of the oscillation. Actually, of course, in a stable layer the parcel's oscillation amplitude will be damped with time so that finally the parcel comes to rest at the EL. In an unstable layer, however, the oscillation period and amplitude in effect increase with time, and the period tends to approach asymptotically an equilibrium value at which the parcel oscillates between top and bottom of the unstable layer (i.e., continuous convectional overturning). The latter case is interesting because it seems to confirm the potentialities of empirical parcel-theory applications to atmospheric convection phenomena. Thus, Priestley [50] found a relation between the observed cumulus top-height oscillations and the environment lapse rate which agreed in a general way with the theory. Radar and photographic studies of cloud growth show that each cell builds up with a periodic pulsating motion.

5.8. Note on Errors Caused by Use of the Observed-Temperature *(T)* Curve for the Virtual-Temperature *(T_v)* Curve in Stability Determinations. The use of the T curve in lieu of the T_v curve for stability determinations (see par. 5.4) causes a certain amount of misrepresentation of the stability. The discrepancy will be greatest where a layer of high moisture content is adjacent to a dry one. Use of the T curve will affect stability determinations as follows:

a. If T_d (moisture content) *decreases* rapidly with height, using the T curve will indicate too much stability.[15]

[15] The moisture condition described here frequently occurs at the top of a stratus deck located just below a temperature inversion.

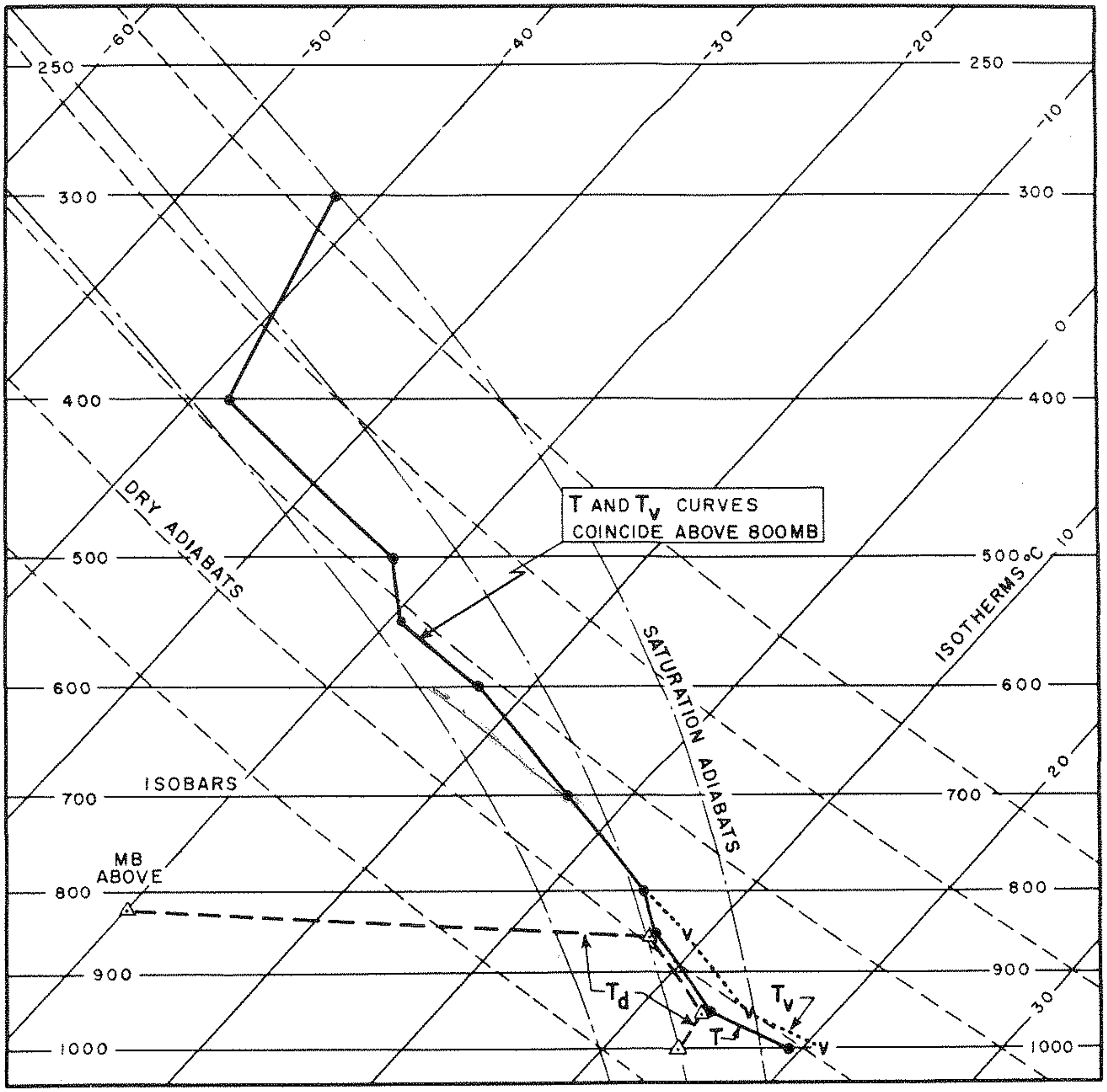

Figure 24. Sample Sounding for Stability Analysis.

b. If T_d *increases* rapidly with height, the T curve will indicate too much instability. This frequently occurs at the base of a warm front.

The example of a sounding on which the difference between the use of the T and T_v curves would introduce an appreciable error into the stability analysis of a layer is shown from 850 to 800 mb in Figure 24. Through this layer, the lapse rate of the T curve is more stable than the T_v curve indicates.

If T_v curves should actually be computed, and should it be desired to use them in moisture-stability analysis, then the sounding

T_v curve should be compared with *virtual saturation adiabats* rather than with the ordinary saturation adiabats. The virtual saturation adiabats are not available, but they would have a steeper (more unstable) lapse rate than the ordinary saturation adiabats. As an approximation, one can assume [49] that the virtual saturation adiabats starting at a condensation level computed using the T_v of the parcel will asymptotically approach at about -20°C the ordinary saturation adiabat for the same parcel but started at its condensation level computed using ordinary T and T_d .

The weight of the suspended water in a saturated parcel reduces the virtual temperature somewhat; in the hypothetical pseudo-adiabatic process this effect is eliminated by definition, but in the full adiabatic process, as might be approached in a real cloud, it might be important. We can define a *cloud virtual temperature* as the temperature at which dry air would have the same density as the cloud air (i.e., weight of moist cloud air plus water or ice particles). This cloud virtual temperature for an adiabatic parcel rise of over 100 mb can be approximately 1°C to 2°C colder than the temperature indicated by a similar rise under the pseudo-adiabatic assumption (as on the Skew-T Chart) [54].

5.9. An Example of Stability Determinations (for Small Parcel Displacements) on a Skew-T Chart. The plotted sounding shown in Figure 24 might represent conditions above a station some distance behind a cold front. The frontal zone is indicated by the stable layer just below 500 mb. The drying out above 850 mb is a result of subsidence in the cold air as it moves south. The T_v curve is shown as the dashed line from 1000 to 800 mb. Above 800 mb, it parallels the T curve. The stability of the sounding according to the principles of paragraph 5.5., is analyzed as follows:

a. *1000 to 950 mb.* The slopes (see Footnote 13) of the T and T_v curves are both greater than the slope of the dry adiabat. Therefore, this layer is absolutely unstable (in fact, superadiabatic); i.e., it is unstable regardless of its moisture content (actually, the T and T_d curves show the layer to be unsaturated).

b. *950 to 850 mb.* The slopes of the T and T_v curves are both less than the slope of the dry adiabats, but greater than that of the saturation adiabats. Therefore, this layer is in a conditional state. Since the T and T_d curves practically coincide, the layer is saturated. The slopes of both the T and T_v curves when compared with that of the saturation adiabats, show the layer to be unstable as long as it remains saturated.

c. *850 to 800 mb*. The slope of the T_v curve is greater than that of the saturation adiabats, and slightly less than that of the dry adiabats, indicating that this layer is also conditional. (The T and T_d curves indicate that the layer is definitely unsaturated.) A comparison of the T_v curve and the dry adiabats show the layer to be stable. The T curve indicates greater stability than the T_v curve.

d. *800 to 600 mb.* The layer is unsaturated, and the slope of the T curve is less than that of the dry adiabats; hence, the layer is stable.

e. *600 to 550 mb.* Through this unsaturated layer, the T curve is parallel to the dry adiabats; hence, the layer is in equilibrium for small upward and downward displacements of parcels within it. (The effect of large upward displacements that would saturate the parcel or bring it into the layer above 550 mb have to be considered by the procedures of par. 5.23.)

f. *550 to 500 mb*. The slope of the T curve is less than those of the dry or saturation adiabats. Hence, the layer is absolutely stable.

g. *500 to 400 mb.* This layer is in equilibrium since the *T* curve parallels the dry adiabats and the air is unsaturated. The remarks on the 600- to 550-mb layer apply here also.

h. *400 to 300 mb.* The air is absolutely stable above 400 mb.

5.10. Processes Which Change the Lapse Rate. It is not feasible to obtain an optimum, routinely-applied stability analysis of radiosonde ascents unless the processes that tend continually to change the lapse rate are well understood. Since their effects will be referred to throughout the rest of this manual, a general discussion of them is introduced at this point.

It is desirable for proper understanding to distinguish the four basic kinds of *physical* processes that can change the lapse rate at a point or in a given local vertical:

a. Non-adiabatic heating and cooling (due to radiation, conduction, evaporation, and condensation).

b. Solid (or non-shearing) advection of an air column with a lapse rate different from that already over the station.

c. "Differential (or shearing) advection" of temperature due to vertical wind-shear.

d. Vertical motion (orographic, convergence, divergence, and penetrative convection).

The combined effect of these processes may be visualized in the form of an equation, each term of which may be positive or negative:

The Local Change of the Lapse Rate with Time
= a (The Local Change with Height of the Additions or Subtractions of Heat per Unit Time)
+ b (The Advection of the Lapse Rate)
+ c (The Differential Advection of Temperature Due to Vertical Wind-Shear)
+ d (The Local Change of Temperature Due to Vertical Motion).

Figure 25 illustrates the effects of these four terms schematically. In addition, Attachment 2 contains a mathematical discussion of the above equation, which is not found in textbooks. In the following paragraphs, some comments are made on the synoptic importance of these processes, and on how they can be evaluated in practice. In actual synoptic situations, several of these processes are usually operating simultaneously at the same location, and it may be difficult or impossible to evaluate their effects separately. Empirical and subjective judging of the combined effects is often practiced.

5.11.0. Non-Adiabatic Heating and Cooling Effects. These are generally important only at the ground surface and within some clouds. The formation of low-level stability (or inversions) by nocturnal radiation, and of low-level instability by isolation, are discussed in paragraphs 5.11.1 and 5.11.2. Radiation in the free air and at cloud tops, however, is slow and its effect on the lapse rate is generally negligible for short-term forecasting. The release of the latent heat of condensation (and fusion) has important local effects readily observable whenever condensation takes place at sufficiently high temperature so that the resulting buoyant energy leads to deep convection. The latent heat is also an important source of kinetic energy in the stratiform-cloud shields formed by upward vertical motion organized on a large scale; but here the effect of the release of the latent heat on the lapse rate occurs evenly over thick layers and wide areas and is masked by the effects of the vertical motion on the temperature, so that it is not easily identifiable in the soundings. Evaporational-cooling and melting effects have a trivial direct effect on lapse rates except locally in heavy precipitation (see [64] and *AWSM 105-51/1*).

5.11.1. Instability from Surface Heating. The ground absorbs solar radiation causing the surface temperature to rise. This heats the surface air parcels by conduction. These heated parcels tend to organize into large "bubbles" that ascend by virtue of their buoyancy relative to the surrounding unheated or

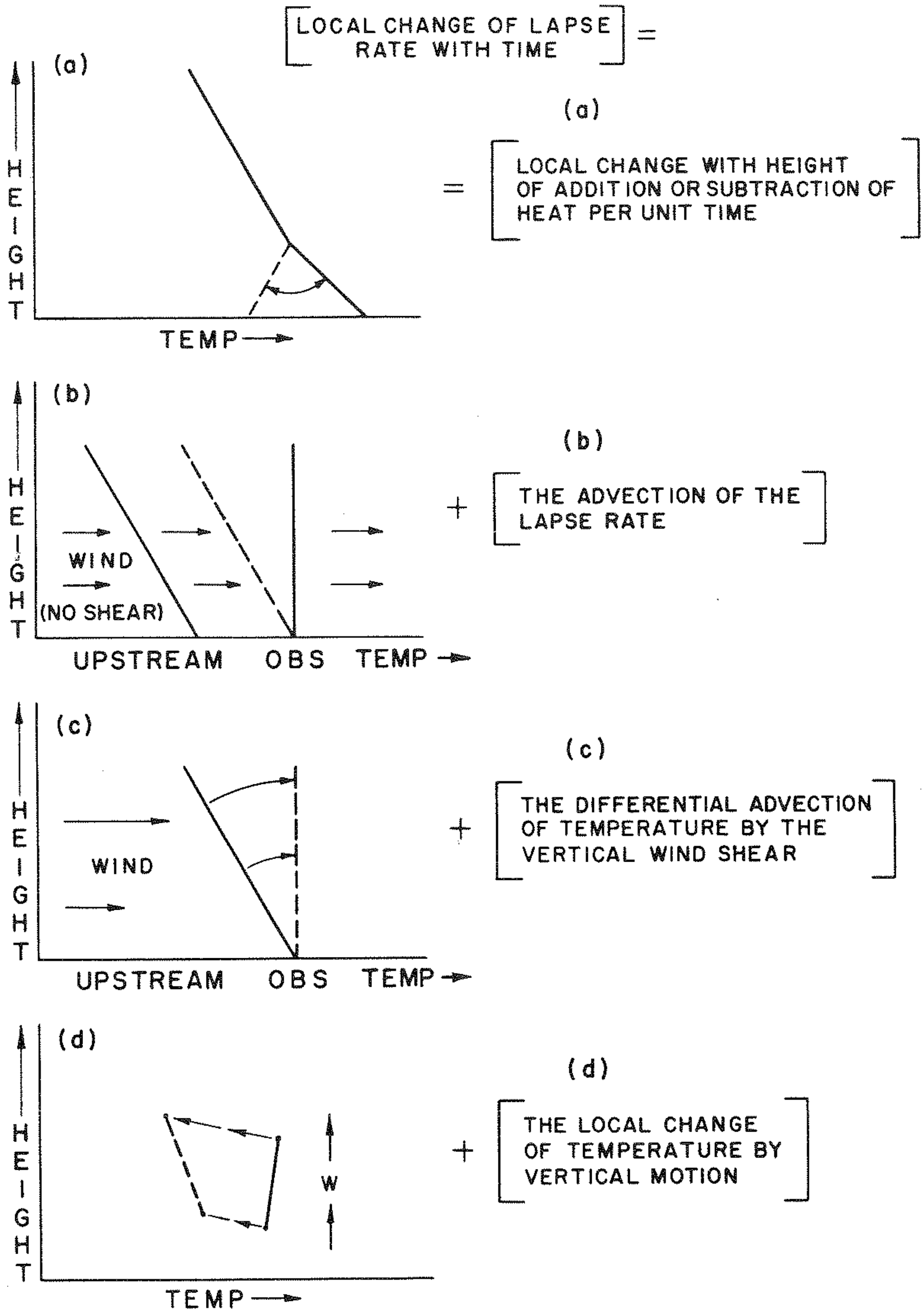

Figure 25. Schematic Illustration of the Four Effects Which Affect the Local Change of the Lapse Rate with Time.

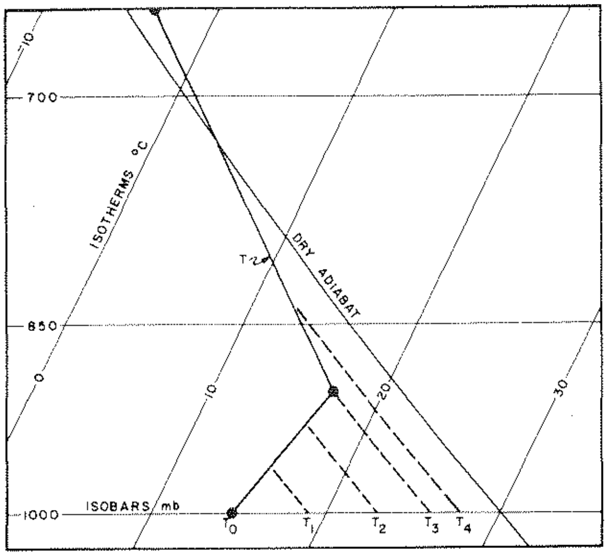

Figure 26. The Successive Changes of the Temperature Lapse Rate Due to Solar Heating of the Ground with Time (*t*).

less-heated parcels. If the lapse rate is already adiabatic (or superadiabatic), the "bubbles" rise rapidly until a stable region is reached which resists further rise. If the initial lapse rate is stable, then the rise of the surface-heated parcels is resisted from the start. Once some of the "bubbles" of heated parcels at the base of the stable region acquire sufficient buoyancy from a small excess of temperature over their neighboring parcels, or as soon as some of them are impelled upward by mechanical turbulence, their momentum causes them to penetrate some distance into the overlying stable region.

Through such penetrative convection (really a form of vertical motion whose effects on lapse rate will be discussed more generally in par 5.16), heated "bubbles" of air can successively rise and mix at higher and higher altitudes in the stable layers above, thereby slowly extending the dry-adiabatic lapse rate to greater altitudes and allowing the surface temperatures to rise, as shown in Figure 26.

Thus surface heating creates instability indirectly through the intermediate mechanism of vertical motion. However, the amount of heat absorbed and conducted to the air by the ground sets an upper limit for the magnitude of the penetrative-convection effect on the lapse rate. For this reason, when Sir Napier Shaw popularized the tephigram he attempted to induce forecasters to compute on the diagram the heat-energy input in ergs required to make stable surface layers unstable and clouds to form, etc. The energy in ergs expected from the surface heating could then be compared with the energy in ergs required for penetrative convection to a given depth, i.e., could be compared with the ergs equivalent of a negative energy area on the diagram. (Note: The energy equivalent in ergs for a unit area on a given thermodynamic diagram can be readily determined—see par. 4.25 for such evaluations on the DOD Skew-T Chart.) This approach has been found feasible and has been used successfully to some extent for maximum-temperature forecasting (USWB Forecasting Guide No.4). However, usually there are practical difficulties in obtaining the proper data on radiation properties of the ground (albedo, conductivity, wetness, etc.), which affect the proportion of the insolation that goes into heating the air.

Another way of judging the heat transferred from ground to air, one which obviates computations in energy units, has come into more general use by forecasters. This is based on the assumption that the rise of surface air temperature is a measure of the amount of energy taken up by the air from the ground. From Figure 26, it will be seen how the stable lapse rate or the so-called negative-energy area is wiped out or reduced by surface heating as the surface temperature rises. The amount of the negative area removed is proportional to the surface temperature rise. However, the *rate* of increase of the surface temperature depends also on the shape of the negative area and on the structure of the initial lapse rate. This use of the surface temperature also has the advantage that the progress of the heating effect can be followed continuously, whereas soundings are available only one to four times a day.

The case of air moving over warmer ground may be considered analogous to that of local surface heating, except that the upstream distribution of the ground-surface temperature then becomes the main factor in determining the amount of the change in surface air temperature. This is often called an "advection effect" in synoptic parlance, but from the physical point of view it is mainly a non-adiabatic heating effect.

5.11.2. Stability from Surface Cooling (and the Effect of Wind Stirring). The lapse rate that characteristically results from pure nocturnal-radiation effects in a calm air mass, is a shallow inversion based at the ground. The depth of the inversion layer increases as the duration of the cooling, and the steepness of the inversion (degree of negative lapse rate) increases as the degree of cooling. However, over a snow cover, long cooling (as during the Polar night) also tends to develop an isothermal layer above the inversion [63]. The effects of cooling of the ground (by radiation, or by passage of air over colder ground) on the lapse rate of the lower atmosphere are complicated by wind. Wind, by turbulent mixing of the air cooled at the ground with warmer air above, tends to establish a surface layer with an adiabatic lapse rate and a turbulence inversion above it, as described in Chapter 6. (Note: In this particular case, the wind does not change the overall stability, but merely shifts the inversion base to a higher level.) All sorts of intermediate conditions and combinations between the ground inversion and the turbulence inversion can occur, depending on the relative degrees of wind and cooling. The movement of air over cooler ground, of course, implies wind, and usually results in a turbulence layer and inversion. Further complications arise when saturation results from the surface cooling, leading to fog or stratus (see chapter 8 and AWSM 105-44). However, unlike the case of condensation in cumulus clouds, the latent heat released in fog or stratus is usually too small to increase greatly the depth of mixing. On the other hand, the formation of fog or stratus greatly reduces or stops the further radiational cooling of the ground, though there is some radiational cooling at the top of the fog or stratus which tends to promote instability (or lessen stability) below the top.

The use of the parcel-method analysis to estimate quantitatively the stabilization effect of surface cooling is greatly limited in practice by the deficiencies in the available means of estimating the radiation flux and the wind mixing, though these factors can often be successfully accounted by indirect empirical methods.

5.12. Advection Effects. Advection, both at the surface and aloft, has a strong influence on the lapse rate through a given region of the atmosphere. Before a forecast is made from a sounding, consideration should therefore be given to the lapse-rate changes which will result from the effects of advection during the forecast period.

The advection effects, as indicated in paragraph 5.10, may be visualized as two processes: a) the advection of air of a different lapse rate, and b) "differential advection" of temperature due to vertical wind shear. (Do not confuse these with the effect of "advection" of horizontally homogeneous air over warmer or colder ground, which is mostly a non-adiabatic heating or cooling effect; see pars. 5.11.1 and 5.11.2.)

The first effect is the easier to visualize. An air mass with a different lapse rate may move into the area of interest and the typical weather associated with the imported lapse rate also accompanies the air mass, often with little modification. This can happen even without vertical shear, as shown schematically in Figure 25b.

The second effect is less obvious and also more difficult to evaluate on synoptic charts. This effect is often present even when the lapse rate is uniform horizontally throughout the air mass (see Figure 25c). It is due to ageostrophic winds. For this reason it is useless to use the geostrophic wind in attempting to estimate the shearing advection effect, since in a regime of geostrophic winds (at all heights) all shears are parallel to the isotherms and the shearing motion does not change the lapse rate. It is the vertical shear of the ageostrophic-wind components that accomplishes advectional change of the lapse

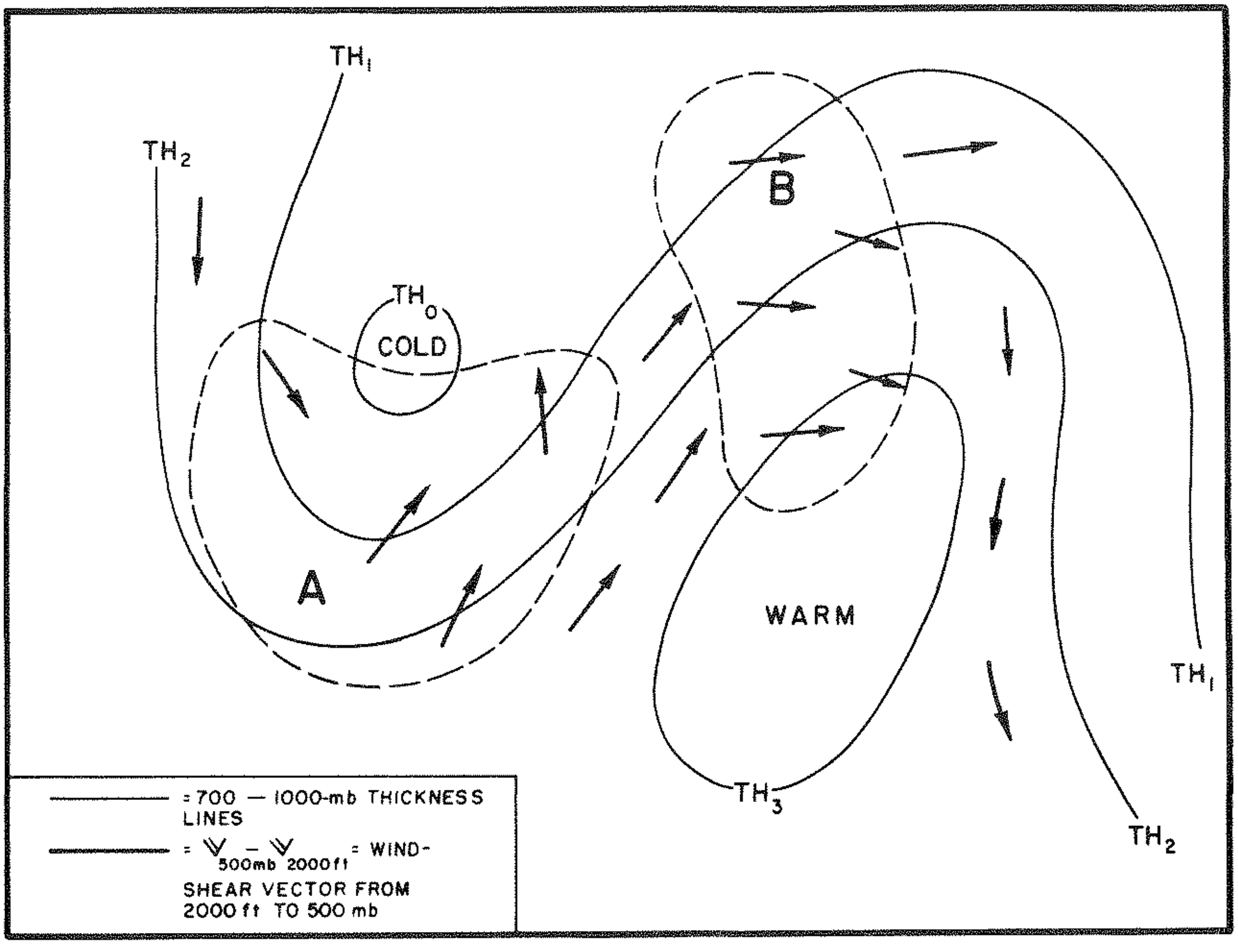

Figure 27. The Effect of Shearing Motion on the Lapse Rate. Stabilization of the lapse rate occurs where the shear vector crosses the thickness lines towards lower thickness: $\left(\frac{\partial V}{\partial Z} \cdot \nabla T < 0\right)$, as in Area A; destabilization occurs where the shear vector crosses thickness lines towards higher thickness: $\left(\frac{\partial V}{\partial Z} \cdot \nabla T > 0\right)$, as in Area B.

rate, and this shear must have a component normal to the isotherms to give any change of the lapse rate. So in practice, we should estimate the temperature advections at the two levels concerned by using actual winds and not the geostrophic winds. The rule is simply: *Where more rapid cooling is indicated at the upper than at the lower level, stability is decreasing, and vice versa.*

There are regions on some upper-air charts where the ageostrophic-wind components are so strong that the influence of the "differential advection" can be assessed directly by inspection. But most of the time, the actual flow cannot be clearly distinguished from the geostrophic wind, and then the lapse-rate change due to shear cannot be reasonably judged.

One way of judging the shear effect would be to plot the actual wind-shear vector of the layer from 2000 feet above the surface to 500 mb on a chart which contains the 1000- to 500-mb thickness analysis; wherever the shear vectors are directed towards warmer regions, a decrease of stability should be taking place, and vice versa. If the winds were geostrophic at all levels in the layer the shear vectors would blow along the thickness lines and no stability change would be taking place. Unfortunately, no experience with this approach is available. The principle is illustrated in Figure 27.

In actual practice, many forecasters estimate the total advective change of stability on a given sounding by estimating the temperature advection at several levels in the troposphere using the actual winds and isotherms. This procedure takes into account the combined lapse-rate advection and shear effects, if both are present.

5.13. Preliminary Remarks on the Effects of Vertical Motion. The vertical motions which affect the lapse rate may be of any scale or type, from small-scale turbulence to the large-scale mean vertical-motion field associated with macro-synoptic features. As different principles apply to the vertical motion of different scales or types, it is customary to consider the vertical motions of different scales as somewhat distinct phenomena. Accordingly, we will discuss separately in the next few paragraphs: Ascent and subsidence of whole layers, horizontal divergence and convergence on the meso- and macroscale, and penetrative convection. The lifting effects of mountains and fronts involve combinations of these phenomena.

The lapse-rate changes of a layer during ascent or descent are solely a linear function of the change in thickness of the layer resulting from such vertical motion (see Figure 28). For a simple approach to assessing the effects of vertical motion on a layer, it is customary in textbooks to assume no horizontal divergence and, of course, the conservation of mass. However, the assumption of no divergence over any considerable depth and extent is realized in the atmosphere only where there is neither development nor change in the pressure field. Therefore, the attempt to assess the effects of ascent or subsidence under that assumption is so artificial as to greatly limit its practical application. Divergence and large-scale vertical motion are so intimately associated in the atmosphere that a general discussion of their combined effects on the lapse rate will be given in paragraphs 5.14.0 through 5.14.6. In that discussion the no-divergence case is included as a special case.

5.14.0. Effects of Convergence and Divergence. The divergence (convergence) is, of course, not necessarily zero in the atmosphere, for in developing pressure systems there must be a more or less marked field of divergence. What are the complications that the divergence introduces in assessing the effects of vertical motion on the lapse rate? The answer is unfortunately not simple, because it depends on the relative magnitudes of the divergence and the rate of ascent or descent.

Let us consider a thin layer defined by a pressure interval, Δp, and the area, A, of its projection on the horizontal plane. Then, for any transformation of the layer under the conservation of mass, the product of Δp and A does not change: $\Delta p_1 A_1 = \Delta p_2 A_2$, where subscript 1 refers to the initial state and subscript 2 to the final state. (This is the equation of continuity.)

By the hydrostatic equation, $\Delta p = -\rho g h$, where ρ is density, g is gravity, and h is the thickness of a layer (in feet or meters). Substituting for Δp and dropping g (which is essentially a constant for our purposes), we may write the equation in ratio form as:

$$\left(\frac{\rho_1}{\rho_2}\right)\left(\frac{h_1}{h_2}\right) = \frac{A_2}{A_1}$$

When convergence (negative divergence) occurs, A_2/A_1 is $<$ 1, and when divergence

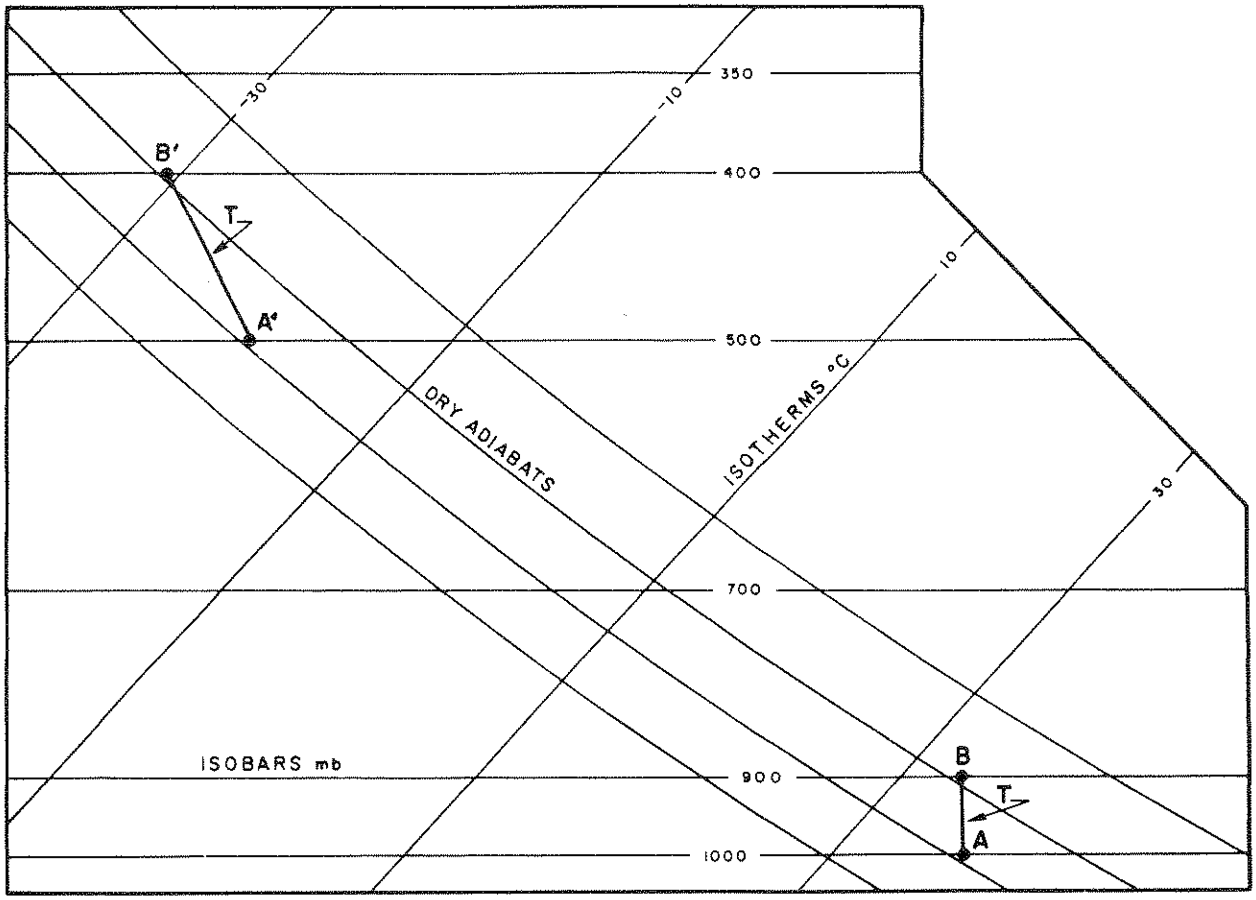

Figure 28. Lapse-Rate Changes Caused by Lifting or Subsidence of a Dry Layer.

occurs it is >1.[16] There are innumerable combinations of the three parameters, ρ, h, and A, that satisfy the above relationship. Before proceeding to the most general case, it is of interest to discuss several "special" cases where one of these parameters remains constant.

5.14.1. Cases Without Vertical Shrinking or Stretching. For example, assume that $h_2 = h_1$ (no vertical stretching or shrinking occurs) and that there is convergence to the extent that $A_2/A_1 = 0.9$. Then, $\rho_1/\rho_2 = 0.9$ also. Since ρ increases from the initial to the final state, there is descending motion to obtain the density increase. Similarly, if $A_2/A_1 = 1.1$, the area increases from the initial to final state; i.e., divergence exists, ρ decreases and there is ascending motion. Thus, convergence or divergence can be associated with vertical motion without resulting in any change of lapse rate provided only the thickness of the layer remains constant.

[16] Physically, divergence has time as one of its dimensions so the actual amount of divergence depends on how long it continues. In the simple demonstration here we are concerned only with its sign.

5.14.2 Cases With Convergence but Without Vertical Motion. Alternatively, let us assume that $\rho_1 = \rho_2$; i.e., there is no vertical motion, but $A_2/A_1 = 0.9$; i.e., there is convergence. Then $h_1/h_2 = 0.9$ and the thickness increases, since the final state, h_2, must be larger. Also, the lapse rate is changed in the same sense as in the case of ascent without divergence (see par. 5.14.4); that is, the lapse rate tends to approach the dry (or saturation) adiabats.

5.14.3. Cases With Divergence but Without Vertical Motion. If $\rho_1 = \rho_2$; i.e., there is no vertical motion, but $A_2/A_1 = 1.1$; i.e., divergence is occurring, then $h_1/h_2 = 1.1$ also, which means a thickness decrease. Hence, the lapse rate changes in the same sense as for descent without divergence (see par. 5.14.4), that is, the lapse rate tends to depart further from adiabatic.

5.14.4. The No-Divergence (No-Convergence) Case. If there is no divergence or convergence, ρ and h vary according to:

$$\left(\frac{\rho_1}{\rho_2}\right)\left(\frac{h_1}{h_2}\right) = \frac{A_2}{A_1} = 1 \text{ ; or } \frac{\rho_1}{\rho_2} = \frac{h_2}{h_1}$$

That is, without convergence or divergence (meaning A does not change), the density and thickness of a layer vary inversely with one another.

If the layer ascends $\rho_2 < \rho_1$, since the density decreases with height in the atmosphere; then from the last equation it follows that $h_2 > h_1$; i.e., the layer stretches vertically. For an entirely dry-adiabatic (or entirely saturation-adiabatic) process, the lapse rate will, as a result of vertical stretching, tend to approach the dry (or saturation) adiabatic (respectively).[17] On the other hand, if, again without divergence, the layer descends, $\rho_2 > \rho_1$, and $h_2 < h_1$; i.e., the layer shrinks vertically. In this case, the lapse rate tends to depart further from the adiabatic.[17]

5.14.5. In the Lower Atmosphere. Thus, the effects on the lapse rate of ascent and descent without divergence are the same as those of convergence and divergence without vertical motion. This fact has a practical significance in the *lower* atmosphere, where, because of the constraining boundary at the earth's surface, divergence must always accompany descent and convergence must always accompany ascent. Therefore, in this region it is customary to regard the effects on the lapse rate of divergence-combined-with-descent (or of convergence-combined-with-ascent) to be of the same kind, additive, and for practical purposes, inseparable.

5.14.6. In the Upper Levels. This is not so for the middle and higher levels where the continuity equation can be satisfied by any of the possible categories of combinations of ρ , h , and A, shown in Table 1. This table includes as categories 7-12 the special arbitrary cases, four of which (categories 9-12) were discussed in paragraphs 5.14.1 through 5.14.4, where one of the parameters is held constant: $\rho_1 = \rho_2$, $h_1 = h_2$, or $A_1 = A_2$.

[17] These effects of ascent and descent on the lapse rate for the no-divergence or no-convergence assumption are the "rules" often stated in textbooks. Though their limitations are often overlooked, these "rules" are widely used by forecasters. They are generally valid only for qualitative use and for the lower troposphere -- up to 700 mb and sometimes to 500 mb. Nor are they safely applicable to very thick layers or for very large displacements, in view of the fact that vertical motion and divergence usually vary markedly with height and time.

Categories 2 through 5, however, do not occur in the lower atmosphere, where the ground forms a fixed boundary surface. It is obvious that in the upper levels there is no *a priori* basis for assessing which of the categories 1, 2, 3, 7, and 9 occurs, assuming one can determine that divergence is present, nor which of the categories 4, 5, 6, 8, and 10 occurs if convergence is present. This is a problem that in practice has to be approached empirically.

TABLE 1

Category Number	Divergence	Vertical Motion	Thickness	Change In Lapse Rate (If Initially Stable)
1.	Divergence	Descent	Shrinks	More Stable
2.	Divergence	Ascent	Shrinks	More Stable
3.	Divergence	Ascent	Stretches	Less Stable
4.	Convergence	Descent	Shrinks	More Stable
5.	Convergence	Descent	Stretches	Less Stable
6.	Convergence	Ascent	Stretches	Less Stable
7.	Divergence	None	Shrinks	More Stable
8.	Convergence	None	Stretches	Less Stable
9.	Divergence	Ascent	No Change	No Change
10.	Convergence	Descent	No Change	No Change
11.	None	Ascent	Stretches	Less Stable
12.	None	Descent	Shrinks	More Stable

5.15. How to Assess the Vertical-Motion Field in Practice. The determination of the distribution, sign, and magnitude of the vertical motion aloft poses some difficulties in routine synoptic practice. The NWP vertical-motion charts (both the synoptic and prognostic) for the layer 850 mb to 500 mb now being transmitted by facsimile from the National Meteorological Center are probably the best answer for the region they cover and the detachments that receive them. (These charts should improve in accuracy and coverage over the next several years.)

There are also several other less satisfactory techniques. One of these is by inspection of the vorticity advection on vorticity charts, such as transmitted on facsimile for the 500-mb surface over the United States. The principles to be followed in this are well discussed by Cressman [20]; note that the inference of the vertical motion requires that care be taken to consider the local-change term in the vorticity equation when the vorticity gradients are large. Examples of the inference of vertical motion from vorticity advection at 300 mb are shown in Section 4.2 of *AWS TR 105-130*.

If vorticity charts are not available, it is possible to judge the approximate vorticity advection by inspection of the contour and isotach charts (see *AWSM 105-50/1A*). But here, there is difficulty in inferring the sign of the vertical motion except near the ground.

Without vertical-motion or vorticity charts it is necessary, therefore, to use empirical models such as those of Figures 29 and 30, as well as the well-known Bjerknes-Holmboe model [15] for the relation of the vertical-wind profile to the convergence-divergence pattern (that determines how troughs and ridges move), and the Endlich jet-stream

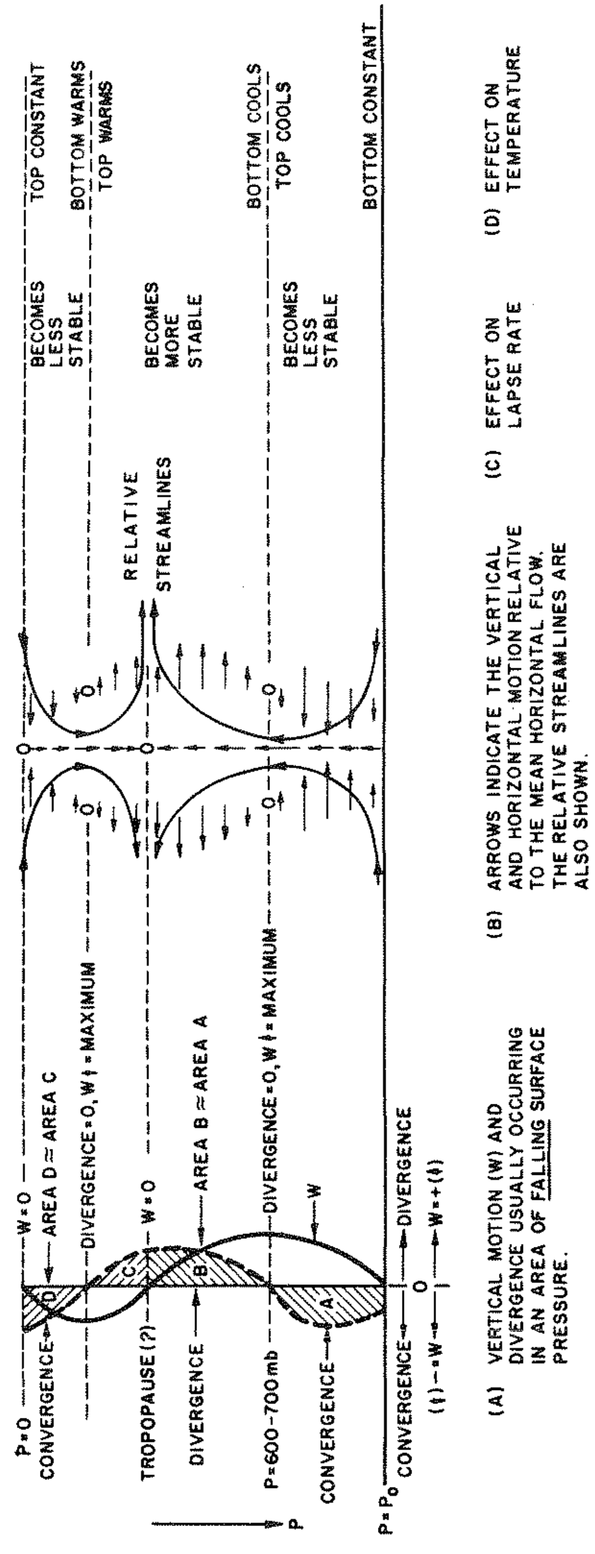

Figure 29. Effect of Divergence and Vertical Motion Upon the Lapse Rate Above an Area of *Falling* Surface Pressure.

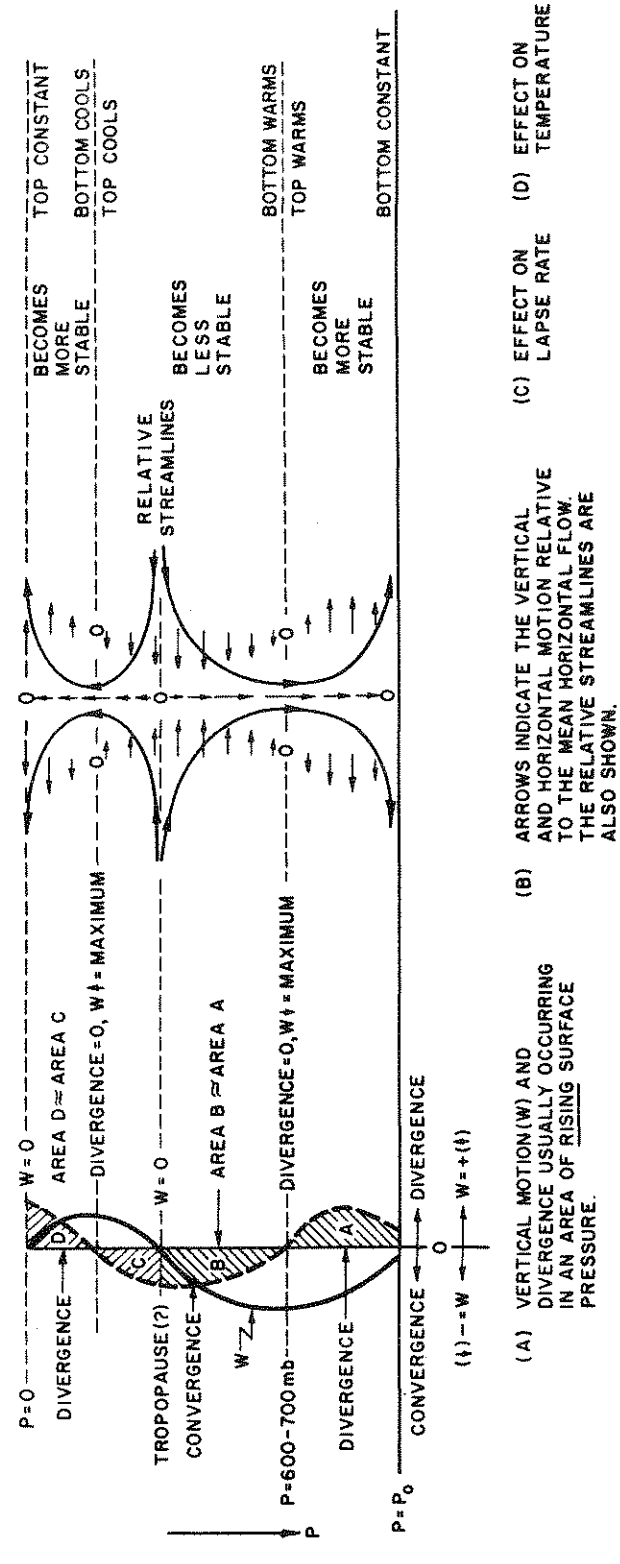

Figure 30. Effect of Divergence and Vertical Motion Upon the Lapse Rate Above an Area of *Rising* Surface Pressure.

model [24] . The associated surface-reported weather distribution is also often indicative of whether the motion is generally upward or downward.

Figure 29 illustrates the typical distribution of vertical motion, divergence, and lapse-rate change in an area of falling surface pressure, and Figure 30, in an area of rising surface pressure. We see that in the typical case the rise or fall of surface pressure is due to a small net difference in several large-magnitude convergence and divergence regions in the vertical column above the ground. Even in areas without marked surface-pressure tendency, there may be layers aloft with divergence and convergence, but if so, the magnitudes are usually small and they fully compensate one another. Observe in Figures 29 and 30 these rules: *Where the upward motion increases (or downward motion decreases) with height, the lapse rate (if initially stable) tends to become less stable; and where upward motion decreases (or downward motion increases) with height, the lapse rate tends to become more stable.*

Finally, there are the so-called "objective" measures of the divergence and vertical motion computed from a triangle of rawin soundings [11] [22] [28]. These are too sensitive to errors in the rawin equipment to be very accurate, and the usual station spacing is so coarse that the divergence areas of small lateral extent are smoothed out or missed as much as they are on vertical-motion or vorticity charts.

5.16. Penetrative Convection. This is a form of vertical motion in the atmosphere consisting of either random or organized local vertical currents having cross-sections of the order of a few feet to a few miles.[18] Most of these vertical motions, especially in the lower atmosphere, are due to *thermal convection* initially created by the effect of heating or cooling (e.g., as described in par. 5.11.1). (The heating or cooling may be non-adiabatic or adiabatic.) The buoyancy forces (see par. 5.1) acting on the parcels in the unstable column or layer lead not only to neighboring up and down currents within the layer but also to ones which (aided by turbulence from shear or friction) penetrate into adjacent more stable layers (above or below). The effect is called *penetrative convection* and is one of the chief processes which tend to change the lapse rate of stable layers towards a less stable or the unstable state. When condensation takes place in the convection column (usually this is an adiabatic heating) additional buoyant energy is provided by the latent heat released, and the penetrative effect is greatly augmented. Besides surface heating (non-adiabatic), convergence and adiabatic ascent also frequently create instability through penetrative convection, especially at the higher levels.

The speed with which the penetrative convection changes the lapse rate varies greatly according to the duration of the convection, the resistance (stability) of the layers affected, the size spectrum and pattern of convection cells, etc. The rate of change is also modified by mixing between the "thermals" or clouds and their environment, as well as by any compensating subsidence which may be spread over a much larger area of the environment than that affected by the updrafts. Ultimately, whole layers can be rendered completely unstable by widespread continued penetrative convection, as frequently happens from thermal convection in the lowest layers near strongly-heated ground or in layers lifted by a front.

5.17. Stability-Instability Criteria for Large Vertical Displacements. The stability criteria of paragraph 5.5 for small parcel displacements, while generally applicable and widely used, are not indicative of what might happen when layers or parcels are

[18] The term "convection" in synoptic practice usually deals explicitly with only the larger vertical currents associated with cumulus clouds, with "thermals," " bumpiness," "turbulence affecting aircraft," etc.

given larger vertical displacements, such as would cause whole layers to change their type of stability over a broad area, or would cause parcels to cool adiabatically to saturation and to penetrate deeply into layers having different stability (i.e., "stability" according to the criteria of par. 5.5). As a result, a number of procedures have been proposed to apply the parcel theory to this problem of large vertical displacements. However, for some reason, more attention has been given to the effects of large displacements from lifting than to those from heating.

Two different approaches to the lifting problem have been developed and appear in most textbooks. The first one involves the concept of *latent instability*, and aims to predict what happens when a parcel is lifted mechanically (as by a front, mountain, or convergence); the other approach involves the concept of *potential instability*, (or *convective instability*) in which the effect of bodily lifting any layer (or the whole atmosphere!) is considered. It will be shown in the next few paragraphs that these two concepts lead to rather different results — see paragraph 5.22 for a comparison summary.

The practical value of the procedures developed from these approaches now seems to be along different lines than originally envisaged by their authors. Most textbooks still present these methods as their originators did, rather than in the light of present-day practice and experience. Unfortunately, the reasoning behind these procedures was never carefully nor fully explored by the proponents of the procedures. Nor have other theoretical meteorologists felt the parcel approach to the problem sufficiently interesting or promising to give it a more thorough and comprehensive formal development. As a result, these procedures have been developed or modified mostly by empirical "trial and error" in forecasting offices to the point where the rational basis for them has become generally obscure. This makes it difficult to give a logical and systematic presentation of the state of this "art."

5.18.0. Latent Instability. Although the analysis for latent instability has not been widely practiced outside of India and its value is controversial, many publications and meteorology courses have represented it otherwise. A discussion of it here is desirable if only to clear up the confusion and misunderstanding.

Normand [46] suggested that for estimating the effects of lifting parcels of a deep layer *which is in the conditional state*, it should be useful to classify the soundings into types. First, he distinguished soundings in which lifting would cause at least some parcels to become unstable (warmer than the environment) from those soundings in which lifting could not result in any parcels becoming unstable. The first type he called *latent instability*. The second type has no latent instability and he designated it as the *stable type* of the conditional state.

Normand then noted that the cases of latent instability fall into two sub-types, one of which should lead to no more than shallow clouds (if any), and the other to thick clouds, showers, or thunderstorms. The first sub-type he called the *pseudo-latent type* (which other writers have called "pseudo-lability" or "pseudo-instability"), and the second sub-type he called the *real-latent type.*

Using the ideas of Sir Napier Shaw, Normand visualized the effect of lifting on these types of conditional soundings in terms of energy. That is, he compared the latent energy of the water vapor in the parcels to be lifted with the kinetic energy needed to lift the parcels high enough to release their latent energy through condensation and any resulting free convection.

Referring to Figure 31, Part A illustrates a sounding of the stable type, i.e., no latent instability. The curve of the ascent of the lifted parcel (the surface parcel in this example), nowhere crosses the environment curve and the Area N is proportional to the energy that has to be provided to lift the parcel. The parcel consumes kinetic energy

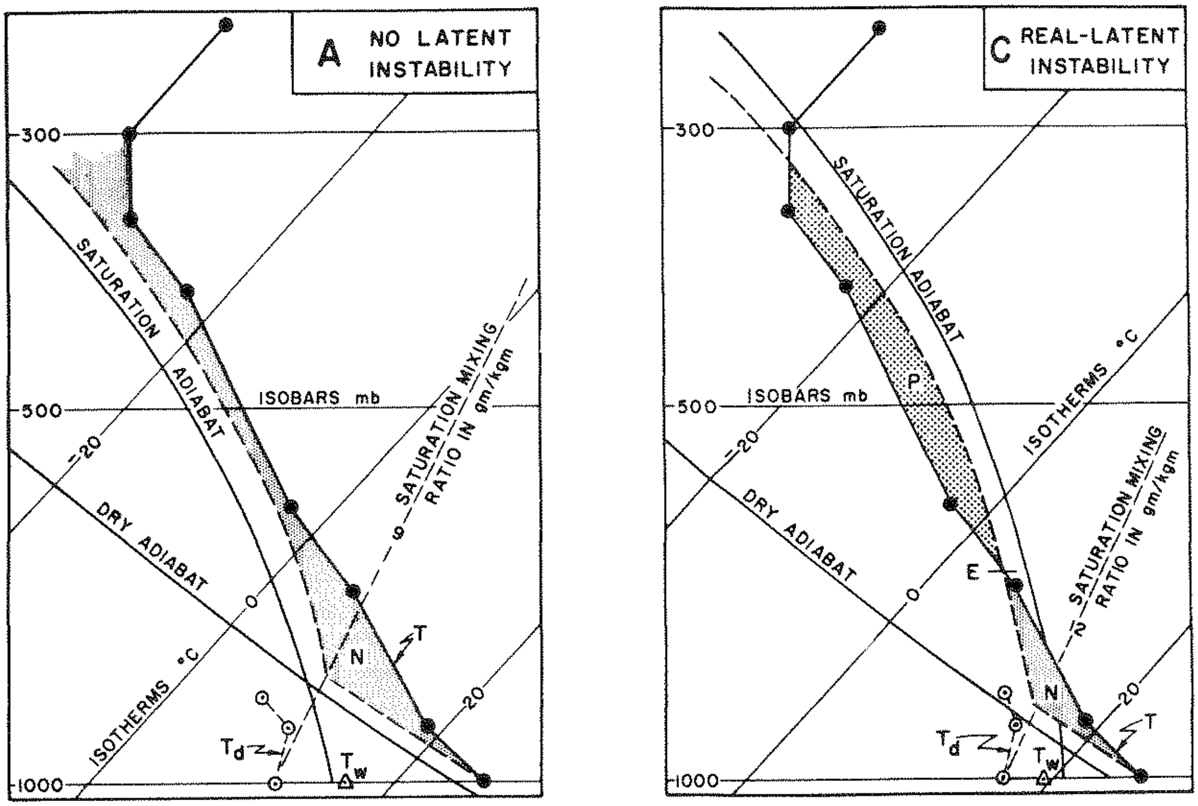

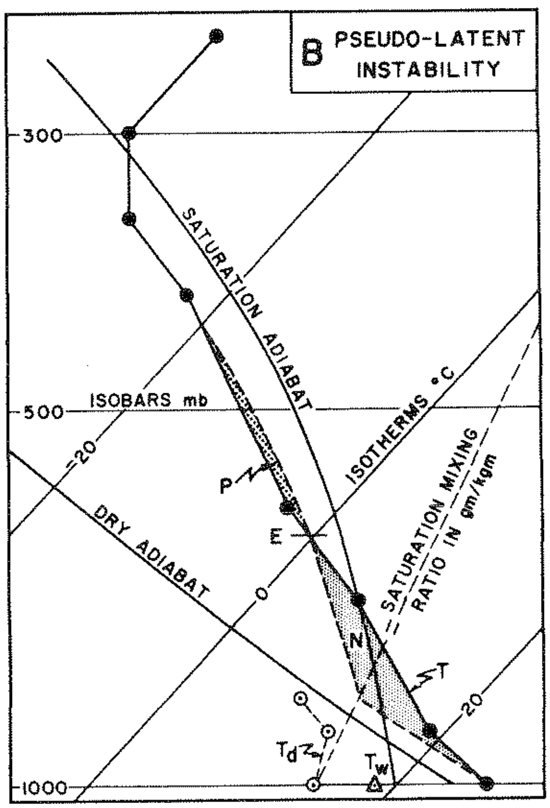

Figure 31. Three Types of Conditional Equilibrium for a Lifting Process. It is assumed that it is the surface parcel that is lifted. Part A shows the stable type with no latent instability; Part B shows a case of pseudo-latent instability; Part C shows a case of real-latent instability. Notice that the temperature lapse-rate curves *(T)* in all three parts of the figure are the same, and to obtain the types of conditional equilibrium one needs only to vary the moisture content of the lifted surface parcel.

(from the lifting mechanism) all the way up and the Area N is therefore called the *negative energy area* (see par. 4.23). There is no positive energy area in this case. In Part B of Figure 31, above Point E the curve of the temperature of the lifted surface parcel is warmer than the environment and, as explained in paragraph 5.1, the parcel will rise freely from the buoyancy provided by the released latent-heat energy of the water vapor condensed. Outside sources of energy (i.e., the lifting force) were consumed up to Point E, proportional to the negative Area N; above Point E an excess of latent-heat energy is released and the Area P, therefore called the *positive energy area*, is proportional to its amount. Since the P-area is smaller than the N-area, more energy was used to lift the parcel to Point E than was released for free convection after it reached Point E. Thus, Normand reasoned that this type of sounding would give little or no weather from lifting and therefore should be called "pseudo-latent." Part C of Figure 31 shows a sounding with a much larger positive area than negative area, meaning that much more energy could be released above Point E than was consumed to lift the surface parcel to Point E. This is Normand's "real-latent instability" type.

5.18.1 Validity of Assumption. There are implicit in Normand's ideas certain assumptions which are not valid. The hypothesis that the *relative* size of the positive and the negative areas should be a criterion for the intensity of the convection weather from lifting was purely intuitive as well as a gross oversimplification. Experience has shown that the actual sizes of the negative area and of the positive area are more important for the forecasting of cumulus clouds and showers than is the difference in size between the positive and negative areas [49] . This is because the negative area in every case must first be wiped out before any convection weather can begin, and the negative area may be too large for the available lifting to overcome regardless of the size of the positive area. Also, even a pseudo-latent sounding can sometimes produce very severe weather, such as when both the negative and the positive areas are narrow and deep and there is marked convergence. Strictly speaking, the positive area evaluates only that part of the latent energy which contributes to buoyancy for *free convection*. Normand's criteria fail to account for the additional latent energy released by both the lifting and convergence processes, which often make the difference between weak cumulus development and severe storms. The magnitude of the lifting may also be the critical factor; e.g., even with a small positive area, a sufficiently large lift might cause severe weather. In this connection, note that Normand's criteria imply that the lifting always stops once the CCL or LFC is reached, which is of course arbitrary and unrealistic. Marshall [39] has shown from simple parcel theory how greatly a small amount of lifting could augment the convection in cumulus clouds already existing. In actual clouds, the effect of this energy contribution from lifting is probably often manifested by a greater amount of "overshooting" above the EL than would occur if there were no lifting or convergence, e.g., as in a pure air-mass-heating cumulus.

5.18.2. Procedure for Finding Whether Any Latent Instability is Present. Normand discovered a simple procedure to determine whether a sounding is of the stable type or has some latent instability (of either type). For this procedure it is necessary that the T_w curve for the sounding be plotted on the adiabatic diagram along with the T curve. Figure 32 shows an example.

Step 1. In Figure 32, select the saturation adiabat (γ_s) that is tangent to the T curve, as shown at Point Q.

Step 2. Plot the curve of the wet-bulb temperature (T_w) on the sounding as described in paragraph 4.9. Latently-unstable conditions are indicated for those portions of the sounding where the T_w curve lies to the right of the tangent saturation adiabat (γ_s), and which are below the altitude where γ_s is tangent to the T curve. In Figure 32, latent instability is indicated for the layer below 860 mb.

General use of the above procedure undoubtedly has been discouraged by the fact that now only dew-point temperatures are transmitted in upper-air reports, so that the T_w curve has to be computed by the forecaster. (Note from the T_d curve in Figure 32 that there is no way in which the T_d curve can be used to determine at a glance the layers with latent instability.)

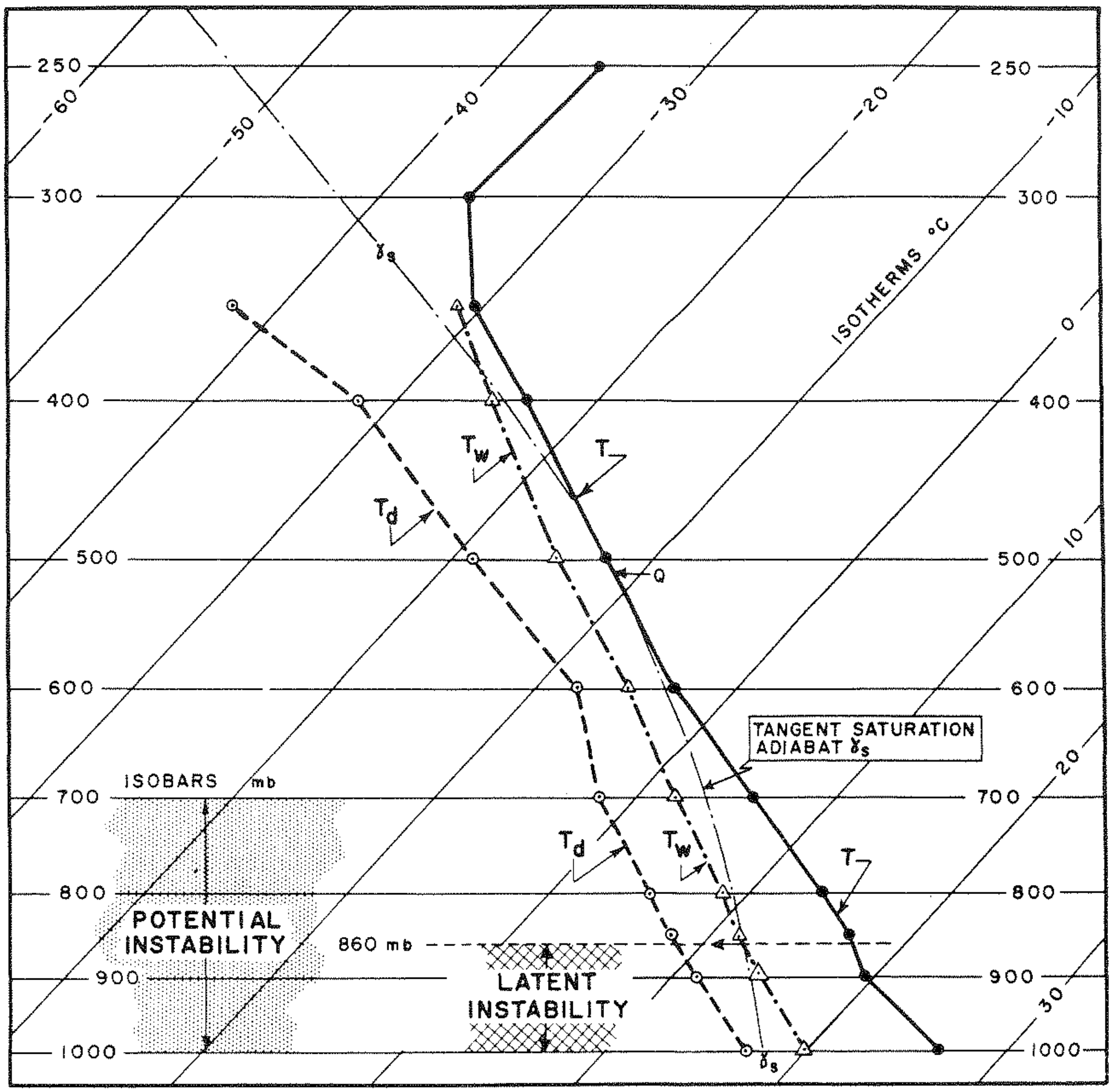

Figure 32. The Determination of the Latent-Instability Layer(s) of a Sounding. The potential-instability layer(s) are also shown for comparison.

5.18.3. The Value of the Distinction Between Pseudo- and Real-Latent Instability.

According to Normand, merely determining which layers have some latent instability does not answer the more important question (to him) as to whether the latent instability is of the pseudo- or real type. The only way to determine this is to analyze on an adiabatic diagram the negative and positive areas for lifting of each of those parcels which are shown by the T_w curve to have latent instability. The sizes and shapes of the negative and positive areas will often differ considerably for different parcels within this layer; without "testing" each parcel in this way one cannot be certain which ones have what type of latent instability. Obviously the labor of making this evaluation for many parcels and soundings requires much more time than most practicing forecasters can spare for it. Normand and his disciples have not been able to develop any objective procedure to simplify and shorten this procedure — if indeed it is even possible. However, their papers indicate that they consider the surface parcel usually to be sufficiently representative of the whole latently-unstable layer whenever the T_w or T_d curves show that the moisture content decreases regularly but not too rapidly with height in the lowest 100 mb. Furthermore, they generally assume that latent instability is most likely in the surface and lower tropospheric layers, where the moisture content is usually highest. In India, the only region where the criteria for the type of latent instability have been extensively applied, this is probably true; and it also has been the practice there to consider the surface and lower layers as the ones that will always be lifted. In middle latitudes these assumptions seem unnecessarily restrictive, because moisture contents increasing or varying irregularly with height and lifting of upper layers as well as surface layers are frequently observed. Very few reports have appeared on systematic attempts to apply latent-instability-criteria evaluations to the variety of conditions found in middle latitudes. Since the moisture content normally decreases with height, Normand's method of locating the layer(s) with latent instability tends to favor the surface layers and often misses higher layers that have strong potential instability (see par. 5.19.0) releasable with a large but expected lift. It has been suggested that where a temperature sounding plotted on a Skew-T Chart has several pronounced and thick projections of the lapse rate to the left, and/or the moisture curve has several such projections to the right, a separate tangent saturation adiabat should be drawn for each projection or distinctive segment of the temperature curve. In this way, secondary layers of latent instability are revealed which may also be released if there is (as often happens) more convergence in their region than in the lower region of the primary latent instability.

5.18.4. Utility of Latent-Instability Analysis in General. In the absence of some guidance on how to decide in an economical way which parcel(s) and layer(s) should be tested for latent instability, practicing forecasters have not been inclined to experiment further with the latent-instability concept. In addition, the weaknesses (discussed above in par. 5.18.1) in the assumptions underlying Normand's criteria for latent instability, give reason to doubt that any effort to apply these criteria in practice would be worthwhile.

Nevertheless, the examination of the negative and positive areas for heating *and/or* lifting of the surface or other selected parcel, is a procedure (first advocated by Shaw) which many forecasters find useful in various ways, but entirely without reference to Normand's criteria. Some empirical relations of the energy areas to convective weather have been reported in the literature, but these relations have to be worked out for each local region. "Modifications" of the sounding curve in the lower layers are often made from experience to obtain more representative surface temperature and moisture values for analysis and forecasting of lifting and heating effects (see Chapter 8). These same considerations should be applied to the soundings when analyzing them for latent instability.

Since the value of analyzing for pseudo- versus real-latent instability is questioned, one may ask: Is it still useful to examine soundings with the aid of the T_w curve to determine merely whether latent instability *of any sort* is present? Because the layer(s) with latent instability contain the parcels most liable to cloud formation (not necessarily the unstable or thick clouds) upon uniform lifting of the whole air column, the procedure for identifying these layers might be useful in routine forecasting. (In this connection, mention should be made of a procedure sometimes used in India and British countries for plotting on the diagram the curve of lifting saturation temperature for each significant point of the lower levels of the sounding — variously called an "ST-gram," "estegram," or "Normand curve." This curve shows which levels will have cloud first.) In any case, the

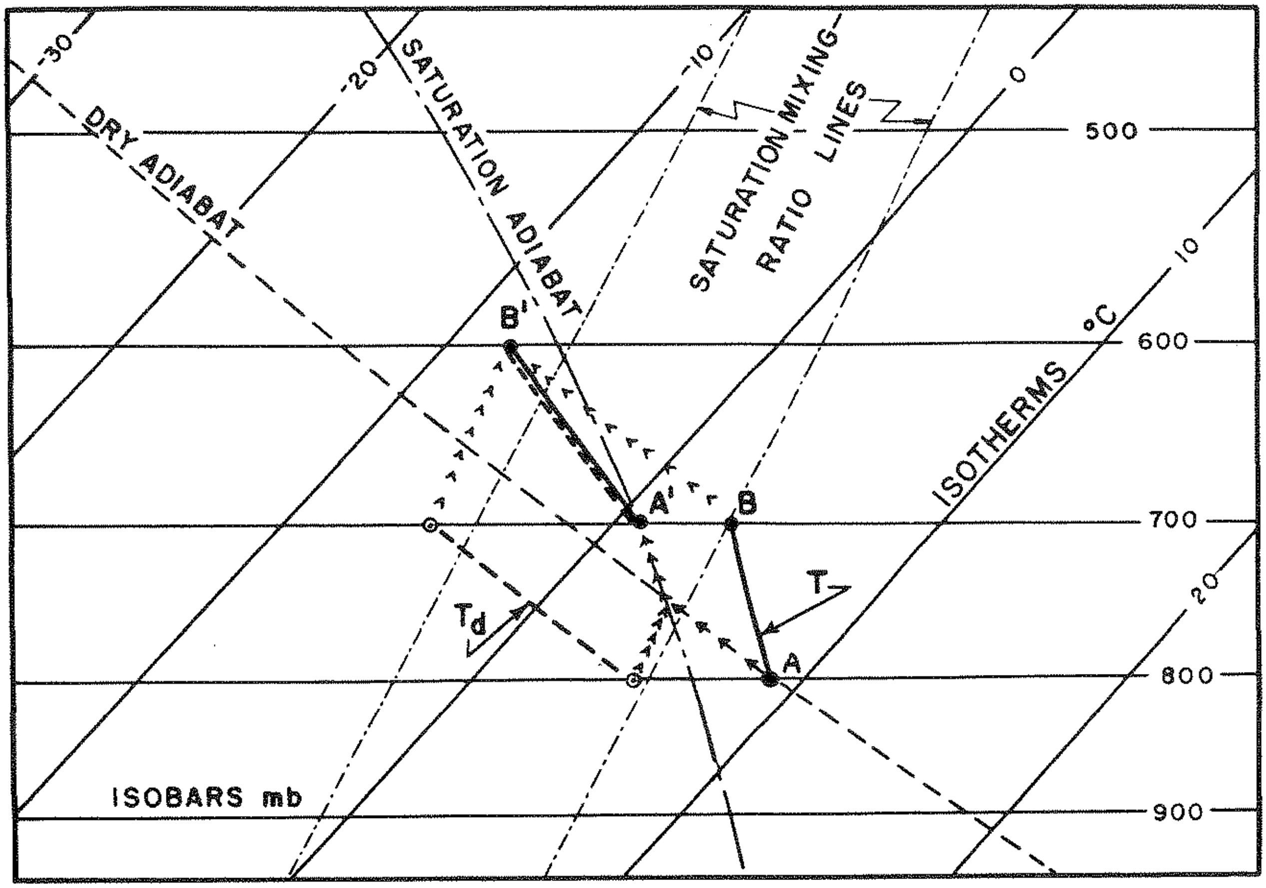

Figure 33. Example of a Stable Layer with Potential Instability.

latent-instability concept should be thought of mainly in this way, rather than as a criterion for "instability" in the usual sense of that term.

5.19. Potential Instability. In the early 1930's, when forecasters were trying to explain as much weather as possible in terms of fronts, Rossby [52] introduced the concept of a criterion for the instability or stability of a layer resulting when it is lifted as a whole, as at a front or mountain. He called the instability released in this way "convective instability," an unfortunate term because it implies that convection does not result from any other type of instability or lifting. Later, Hewson [31] proposed this should be more properly called "potential instability," a more appropriate and less ambiguous term that is gradually coming into wider use than "convective instability." However, other meteorologists sometimes carelessly use the term "convective instability" to mean absolute instability or even "conditional instability". Hence, some confusion is possible with Rossby's term.

The criteria which Rossby introduced were based on the lapse rate of equivalent potential temperature (see par 4.12). This was a convenient unit in the 1930's when it was customary to plot soundings on a Rossby diagram, which has θ_E as one of its coordinates. As the routine use of Rossby diagrams was never universal (and in time was abandoned entirely) it was pointed out by Petterssen that one could apply Rossby's criteria on any diagram containing the saturation adiabats, which are also lines of constant θ_E (as well as of wet-bulb potential temperature), provided that the

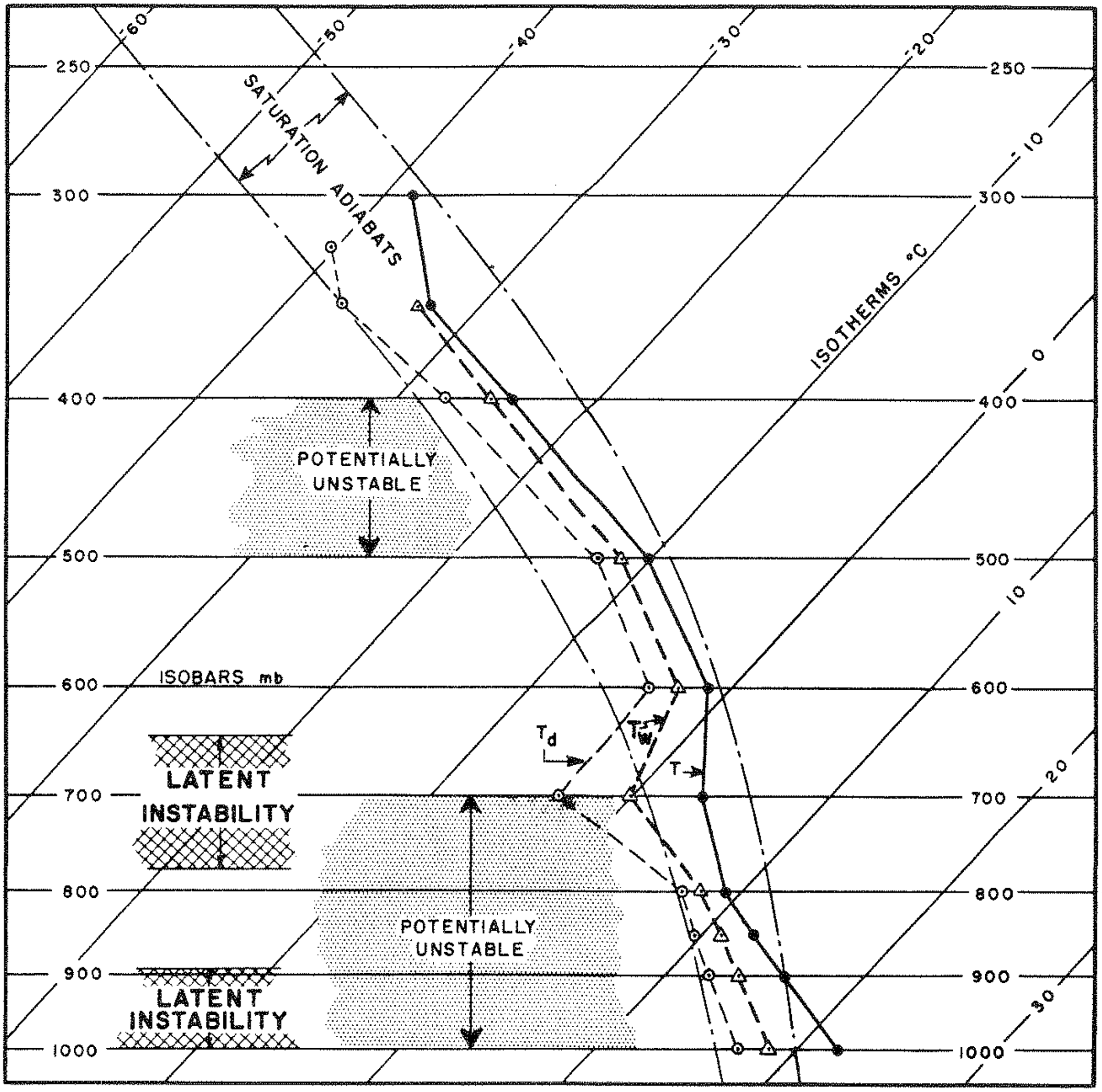

Figure 34. Example of Potentially Unstable Layers, Comparing Use of T_w and T_d Curves for Diagnosis.

T_w curve of the sounding is plotted (see par. 4.9). The Rossby criteria then become:

a. Layers in which the wet-bulb lapse rate is greater than the saturation adiabatic are *potentially unstable*.

b. Layers in which the wet-bulb lapse rate is less than the saturation adiabatic are *potentially stable*. In other words, the slopes of the T_w curve and the saturation adiabats are compared.

Illustrated in Figure 33 is an analysis on a Skew-T Chart to show how a stable layer having potential instability, as indicated by the T_w curve becomes unstable when lifted enough. (Note that this demonstration is made by parcel procedures; the use of the potential-instability concept is sometimes referred to as "the layer method" as though it was not derived from the parcel theory, which is a misconception.)

In Figure 33, the unsaturated layer with lapse rate AB is stable in its original position between 700 and 800 mb. However, if the layer were lifted 100 mb, its new lapse rate would be A'B'. (Paths of the parcels from Points A and B are indicated by arrowheads.) The layer is now saturated and its stability is then found by comparing the slope (see Footnote 13) of A'B' with that of the saturation adiabats. Since the slope of A'B' is greater than that of the saturation adiabats, the layer is now unstable. Thus, the original layer AB is potentially unstable, the instability being releasable by a lifting of 100 mb or more.

Potentially-stable layers are all those layers of the sounding which will not become unstable by any amount of lifting.

In Figure 34 is an example of potentially unstable layers identified by the T_w curve, and with the T_d curves added to show what extent one may substitute the latter for the T_w curve to get an approximate idea of where there is potential instability. In layers of marked departure of T_w lapse rate from the saturation adiabats, the T_d curve will usually show the same sign of departure, though the exact top and bottom limits of the potentially unstable layers may not always be determinable from the T_d curve. When the T_w curve is more nearly parallel to the saturation adiabats, the T_d curve becomes quite undependable as an indication of potential instability and the T_w curve must be used.

5.20.0. Effects of Lifting Potentially Unstable and Stable Layers. The idea of potential instability and stability appears to be very simple and the criteria for them are certainly very easy to use. But the relation of these states to the resulting weather is very complex and not well understood. The "classic" example of the release of potential instability causing severe convection weather (deep cumulus, thunderstorms, hail, and showers) is the lifting of an air mass having a small T_w lapse-rate slope in a strong "dry" inversion or having a rapid drying out above a surface moist layer. There are, however, many other layers with less-marked potential instability (steeper T_w lapse-rate slopes), and it is always a question what kind of weather their lifting will produce. This question has not been given any formal theoretical analysis; but a few inferences can easily be made.

For example, a shallow potentially-unstable layer with deep layers of potentially-stable air both above and below, when lifted to saturation may produce any of the following: A solid stratiform deck of cloud, only scattered shallow cumulus, cumulus and altostratus mixed, or deep cumulus penetrating into the higher stable layers with or without precipitation. Which of these possibilities will actually occur presumably depends on a variety of factors, such as the amount of lifting beyond that just sufficient to start condensation, the steepness of the lapse rate of wet-bulb temperature, the degree of stability of the adjacent layers, the speed and spatial uniformity of the lifting, etc. For many practical purposes there may be little difference in the clouds and weather that result from lifting a shallow potentially-stable layer as compared to those from lifting a shallow potentially-unstable layer. Therefore, there are probably many cases of potential instability in which the "instability" aspect is of trivial significance, especially in winter.

5.20.1. Does the Whole Layer Become Unstable? When the layer or layers of potential instability are deep, it may be desirable to examine the effect of the lifting on representative parcels at several heights in the layer to see whether the condensation will start first at the top, or the middle, or the bottom of the layer. One can find cases where considerable more lifting is required to saturate the bottom than the top, or vice versa, and the question then arises: If the lifting expected will not be sufficient to saturate the whole layer, will the convection started in the first-saturated part spread rapidly through the remainder of the layer anyway? It is often assumed that the whole layer will become unstable upon saturation of any part of it, but this presumably cannot happen until the lapse rate of the unsaturated part of the layer becomes conditional[19] (if it were not already conditional before lifting — see Figures 35a and 35b). It could also happen that potentially-stable layers adjacent to the potentially-unstable layer saturate first, with the possibility of starting a premature convection in the potentially-unstable layer by mixing and penetration across the boundary. Likewise, surface-heating convection may penetrate into a low-lying potentially-unstable layer while it is being lifted, resulting in local releases of its instability before the layer lifting alone would do so.

For example, on the sounding shown in Figure 35a, an absolutely-stable lapse rate AB exists through the potentially-unstable layer between 800 and 900 mb, where both the dew point and wet bulb decrease rapidly with height. If this layer were lifted by 50 mb, its lapse rate would appear as A'B', and the layer would become saturated and unstable from 850 to about 820 mb. The upper, unsaturated portion of the layer, however, would remain absolutely stable, and the potential instability being released would be confined mostly to the saturated portion of the layer. Under such conditions, the total potential instability of the layer would not be realized until the entire layer had been lifted to saturation. For the

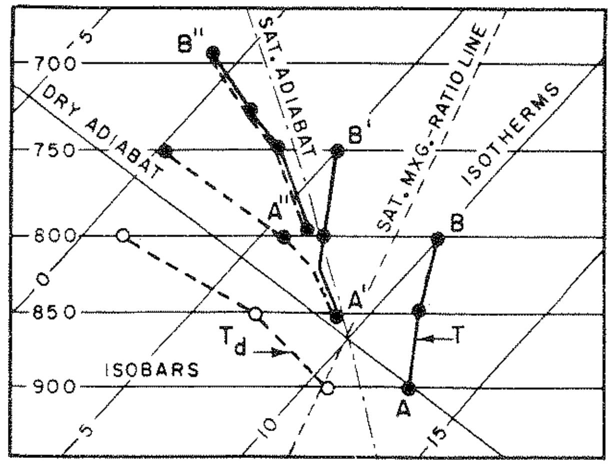

Figure 35a. Effect of Lifting an Absolutely-Stable Layer AB on the Release of Its Potential Instability.

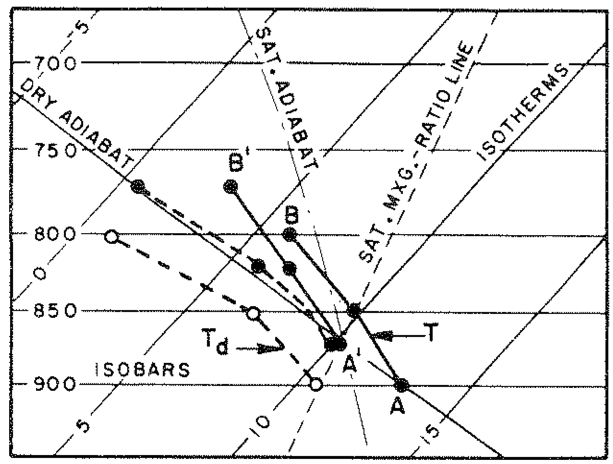

Figure 35b. Effect of Lifting a Conditionally-Unstable Layer on the Release of Its Potential Instability.

example in Figure 35a, this would require lifting by an additional 55 mb, after which the resultant lapse rate would then be A''B''.

If, on the other hand, the original temperature lapse rate of the same layer were in a conditional state as shown by the sounding AB of Figure 35b, lifting through only 30 mb would result in lapse rate A'B', enough to saturate the bottom portion of the layer from

---

[19] Note that the lifting of an absolutely-stable layer having potential instability must always first convert the layer to the conditional state (Figure 35a) before the instability can be released.

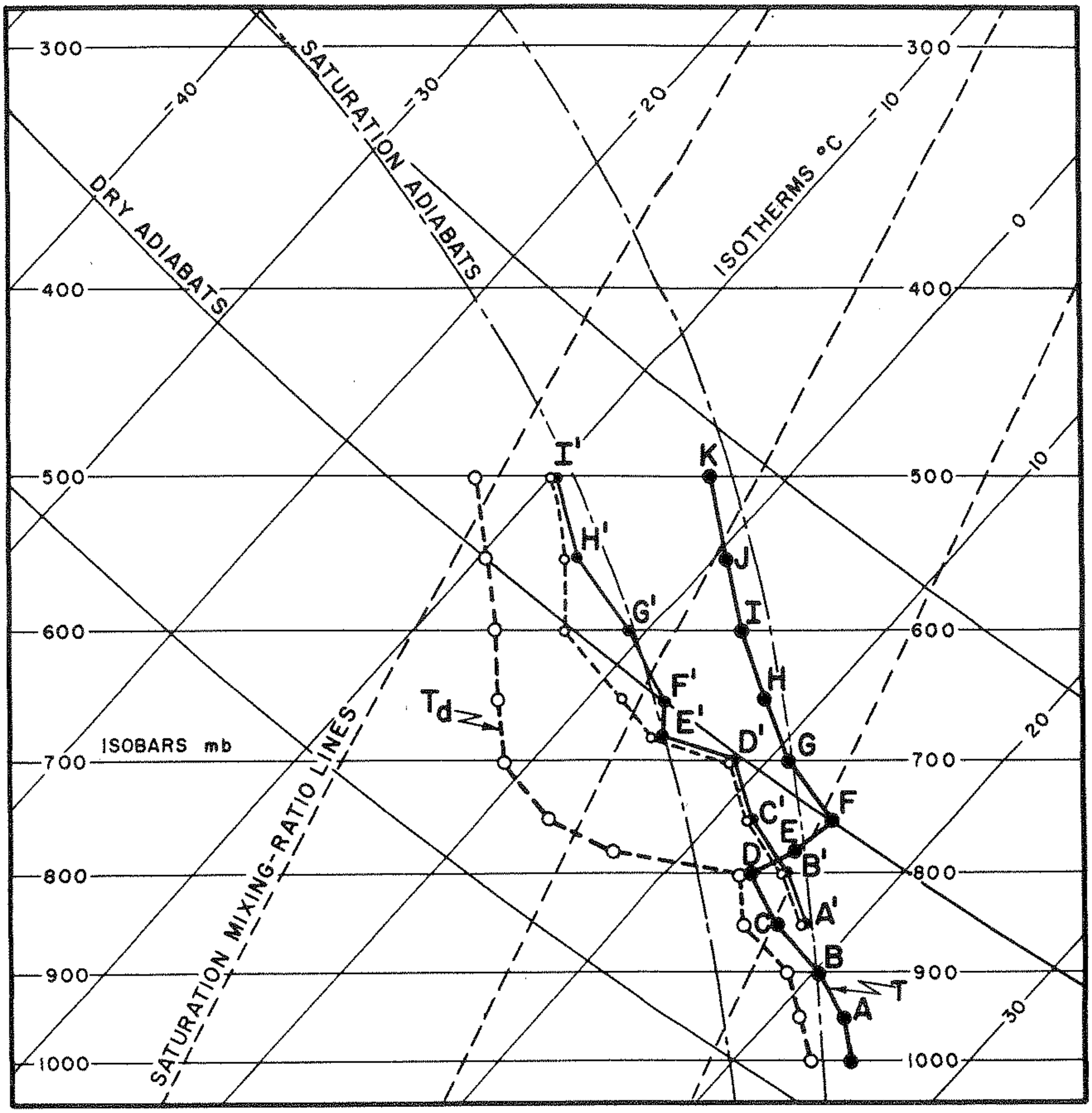

Figure 36. Superadiabatic Lapse Rate (D'E') Resulting from Lifting an Air Mass 100 mb.

about 870 to about 850 mb. The resultant upward acceleration and convection of the saturated portion would then tend to push rapidly upward into the upper, still unsaturated remainder of the layer without further lifting.

If, however, the dew-point *depression* or wet-bulb *depression* decreases with height through a potentially-unstable layer, such as the 1000- to 800-mb layer shown in Figure 34, lifting will then release the potential instability first at the *top* of the layer. As the lifting continues, the height of the release of potential instability will progress downward through the layer; but the total potential instability of the original layer will not be realized until the entire layer has been lifted to saturation.

5.20.2. Superadiabatic Lapse Rates from Layer Lifting. In evaluating on a diagram the effect of lifting of potentially-unstable layers, one sometimes finds cases where a superadiabatic lapse rate appears to result, as illustrated in Figure 36.

A superadiabatic lapse rate (i.e., slope less than the dry adiabats) can result from the lifting of a layer through which the moisture content decreases sharply with height, as in "dry-type inversions" (subsidence, trade wind, etc.).

In Figure 36 the T and T_d curves which include such a layer are shown before and after the sounding is lifted 100 mb. The layer AB is lifted to A'B', the layer BC is lifted to B'C', etc. After each layer is lifted 100 mb, as might be caused by the advance of a fast-moving cold front, a superadiabatic lapse rate results in the layer D'E'. The validity of such lapse rates is discussed in paragraph 5.6.

5.20.3 Effects of Divergence. Divergence has no effect on the potential instability of an unsaturated layer, since the potential wet-bulb temperature is conservative for a dry-adiabatic process. However, the effect of divergence on the temperature lapse rate during a lifting process may speed up or slow down the rate of the lifting, and thus has a bearing on how soon the potential instability might be released. Note also that there may be *potentially-stable* layers that if lifted enough, could become unstable with or without saturation under the combination of convergence or divergence with vertical stretching (see par. 5.14.6).

5.20.4. How Much Lift is Needed for Release of Instability? The practical use of potential instability requires that the layer or layers identified as having it be examined to see how much lift is needed for its release. This can be done by choosing in each such layer the parcel with the highest relative humidity (the one where $T - T_d$ is least) and lifting it to saturation on the Skew-T Chart. Perhaps half of the potentially-unstable layers one sees are hardly susceptible to release by the lifts that could be expected. This is why the stability indexes based on the potential-instability concept (see par. 5.24.0, and Chapter 8) are not useful unless combined with other factors or considerations.

5.20.5. Lifting of Potentially-Stable Layers. The saturation of a *potentially-stable* layer upon lifting may begin at any part of the layer. One can predict the location and final extent of the resulting cloud only by "testing" parcels in different parts of the layer to see which one becomes saturated first by the amount of lifting expected. In addition, potentially-stable layers may be penetrated by clouds formed in the release of potential instability of the layers beneath.

5.21. Processes Which Change the Potential Instability. In general, those processes which increase the moisture content (wet-bulb or dew-point temperature) of the lower levels, and/or decrease the moisture content at higher levels tend to create or increase potential instability. All the effects that change the lapse rate, as discussed in paragraph 5.14.6, can indirectly change the vertical distribution of potential stability and instability, through their effects on evaporation and diffusion of moisture.

5.22. Relation Between Potential and Latent Instability. It is evident from the literature that many meteorologists confuse potential with latent instability, or incorrectly assume that they measure essentially the same thing. The relation between latent instability and potential instability is neither simple nor definite. For example, the following cases may be cited: Layers with latent instability (stability) often overlap or partly coincide with those of potential instability (stability); only the bottom parts of layers of potential instability generally have latent instability; in layers where both types of instability occur, the latent instability is usually of the real-latent type; potentially-stable layers often have latent instability. See Figures 32 and 34 for illustrations of some of these cases.

The basic reason for this lack of close correspondence between latent and potential instability is that the former requires a high relative humidity and assumes the conditional state, whereas the latter does not depend directly on the relative humidity and is independent of the initial lapse rate. It is obvious, therefore, that potential instability is not a substitute for latent instability or vice versa. The main value of potential instability is as an indicator of possible convective overturning from either layer ascent or convergence.

5.23. Slice Method. The assumption in the parcel theory that the parcel moves up or down without disturbing the environment is obviously unrealistic. As the parcel moves, the environment must readjust to some extent flowing into the space evacuated by the parcel and giving way in front of it, causing the distribution of temperature and density in the environment to change slightly. This effect may be considered trivial on the scale of parcels; but when we try to apply the parcel method to convection columns of the size of large cumulus and thunderstorms, the effect greatly limits the practical application. A step towards improving on the parcel theory in this respect, was introduced by J. Bjerknes [14] who considered theoretically the effect of neighboring up and down currents in a horizontal (isobarically bounded) "slice" of the atmosphere on the parcel-stability criteria. Petterssen [48] and Beers [13] developed actual procedures for applying this concept in practice. These procedures are rather cumbersome and time-consuming, even with use of Beers special nomograms. Although several experiments [8] [13] seemed to indicate these procedures give some improvement in thunderstorm forecasting over parcel methods, other studies cast considerable doubt on this conclusion and suggest that the apparent improvement was due to other factors previously overlooked [36]. In any case, the procedures have not been adopted routinely and therefore will not be described here.

The Bjerknes-Petterssen slice approach is incomplete because the effects of mixing, entrainment, and shear across the cloud boundaries are not considered. However, for cumulus forecasting the effects of entrainment and wind shear could probably be estimated empirically, using as a qualitative guide the extensive research literature on cumulus dynamics.

There is a difficulty in choosing a suitable convection model for a valid slice theory. The nature of the compensating subsidence in the environment of a convection updraft is not definitely known. The descent may be largely concentrated close to the boundary of the updraft (the Bjerknes assumption), or spread over a wide area extending far from the updraft, or in case of a cumuliform cloud take place partly inside the cloud (as often actually observed). All three processes probably occur in varying degrees and combinations from case to case.

Petterssen, et al, [49] experimented with an application of his slice method to the analysis of soundings for estimating the amount of cloudiness (sky cover) and the height of cloud tops. In light of later studies [36] it seems doubtful that a better prediction of the cloud tops is given by Petterssen's procedure than by parcel procedures. Nor has it been demonstrated that the cloudiness is satisfactorily predictable by this approach although the slice reasoning seems to account for the statistical fact that in air-mass convection situations, the probability is about 85% that the cloud cover will not exceed four octas.

Cressman [21] derived an interesting and apparently significant extension of Petterssen's analysis to show the effect of horizontal divergence on the cloudiness. When the ratio $(\gamma - \gamma_s) / (\gamma_d - \gamma)$ is small, the effect of the divergence (convergence) on the cloudiness is large; and, when this ratio is large, the effect of the divergence (convergence) is small. (γ is the sounding lapse rate, γ_d, the dry adiabatic, and γ_s, the saturation adiabatic lapse rate.) This would seem to explain the fact that in the oceanic tropics where the lapse rate in the lower troposphere is always close to the saturation adiabatic, the cloudiness may be little or much, depending largely on the presence of general subsidence or convergence.

The slice-method procedures so far developed do not greatly alter the results of the parcel methods and the apparent differences may easily be due to other factors overlooked. The effect on stability criteria by using these slice-method procedures instead of the parcel procedures is to indicate somewhat less instability (or more stability) in that region of the positive area lying above the height where the sounding curve becomes parallel to the saturation adiabats, and somewhat more instability (or less stability) below that height [48] [49]. In empirical forecasting procedures this difference is usually of little or no consequence for the relationships of stability criteria to weather, although the numbers obtained will be different.

The slice method requires a more complete development before its theoretical advantages can be realized in practice.

5.24.0. The Stability Indexes. The overall stability or instability of a sounding is sometimes conveniently expressed in the form of a single numerical value called a *stability index*. Such indexes have been introduced mainly as aids in connection with particular forecasting techniques or studies. Most of the indexes take the form of a difference in T, T_d, $(T - T_d)$, T_w, $(T - T_w)$, θ, θ_E, θ_w, $(T - \theta_w)$, q, w, pressure, height, etc., between two arbitrarily chosen surfaces (or heights), such as 850 mb and 500 mb, 1000 mb and 700 mb, etc. The indexes of this type have the advantage of ease of computation, flexible choice of the layer most pertinent to the particular problem or area, and a numerical form convenient for ready use in objective studies. On the other hand, details of the lapse-rate structure important to the problem at hand may be smoothed out or completely missed in these indexes, unless the index is carefully chosen and evaluated by statistical studies on many cases. Also, these indexes are generally useful only when combined, either objectively or subjectively, with other data and synoptic considerations [3] [61]. Used alone, they are less useful than the standard stability analyses of the complete sounding by the parcel method described in the preceeding paragraphs of this chapter; in fact, used alone, a stability index is apt to be almost worthless. The greatest value of an index lies in alerting the forecaster to those soundings, routes, or areas, which should be more closely examined by other procedures. One way to apply a stability index for this purpose is to construct a "stability chart" on which the index values for soundings over a large area are plotted and isoplethed (see *AWS TR 200*; also [2] [3] [4] [59]). Such charts offer several possible advantages:

a. Incorrect or unrepresentative indexes may be spotted.

b. Location and movements of stable and unstable air masses can be visualized.

c. Systematic local or regional effects (e.g., orographic) may be discovered.

d. Patterns can be related quickly to other synoptic charts, and some correlations of index values with other parameters may be suggested (for further investigation by objective studies).

However, experience has shown that an index or critical index value which is significant in one region (or season) may not be in another [4] [61]. Hence, the stability chart should be more of an experimental or investigative tool than a routine one, unless extensive

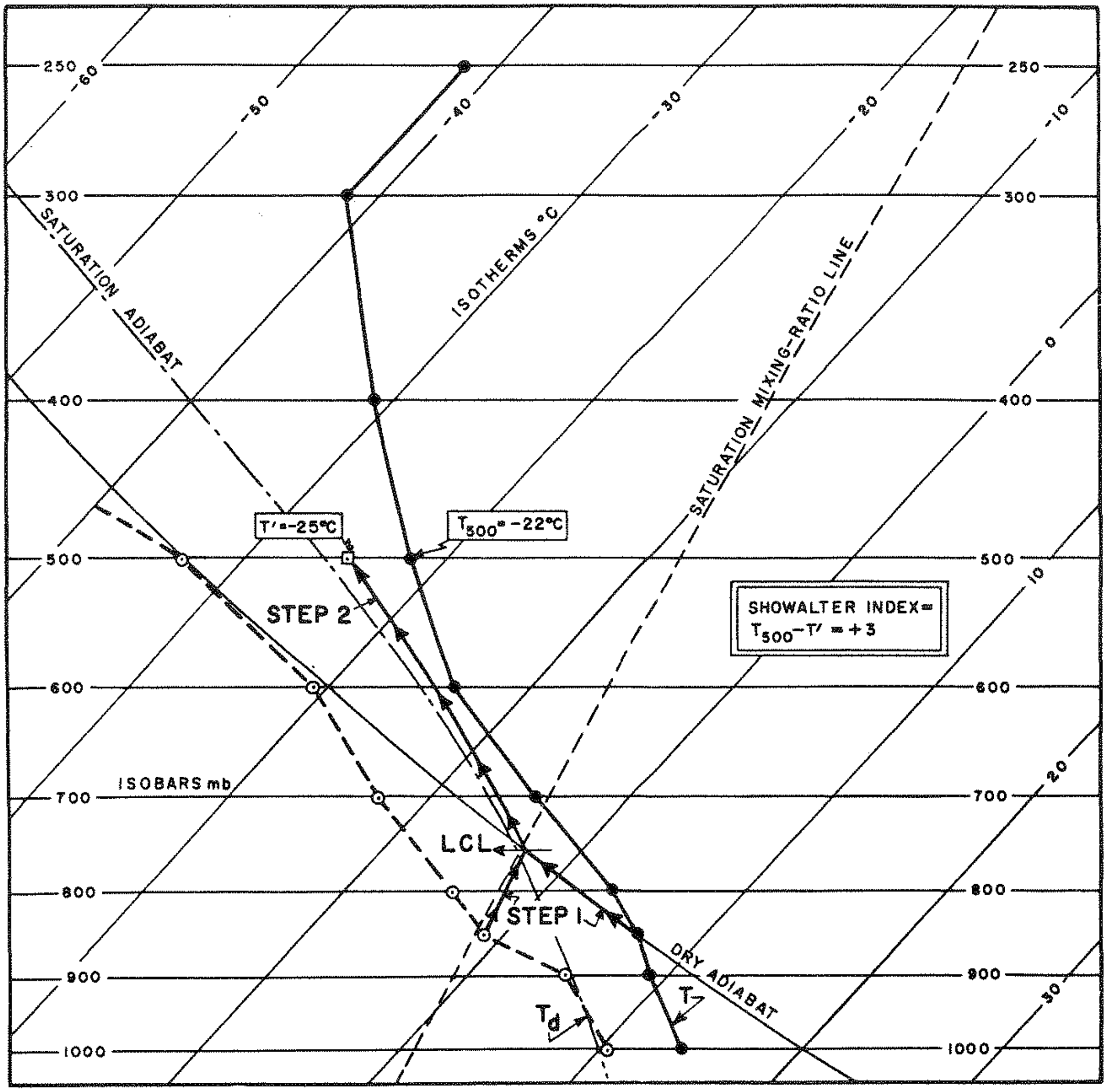

Figure 37. Computation of the Showalter Stability Index.

correlation studies have selected an index significant for the extended general application [4] [61], and the critical index values for various weather conditions have been determined.

The Showalter, Fawbush-Miller, and Lifted Indexes described below are all based on the potential-instability concept; but many forecasters have applied them to the forecasting of showers in general, from heating as well as from lifting. The fact that the results of such "across-the-board" applications seem to be useful (when combined with other parameters) indicates that these indexes to a considerable extent also reflect conditions affecting the formation of showers from surface heating. This is presumably because the θ_E or θ_w lapse rate used in these indexes is partly a function of the ordinary-temperature lapse rate, and hence is partly indicative of the stability criteria for surface-parcel heating.

5.24.1. The Showalter Index. The procedure for computing the Showalter Stability Index (SI) is illustrated in Figure 37.

Step 1. From the 850-mb temperature (T), draw a line parallel to the dry adiabats upward to the LCL (see par. 4.20). (Mountain stations should start with some higher constant-pressure-surface temperature chosen according to circumstances. Such a procedure is incorporated into the instructions given in FMH No. 3 *(Circular P)* for computing the stability indexes that are transmitted as part of the radiosonde reports from U.S. and Alaskan stations these indexes also appear on the stability index charts transmitted by facsimile from the NMC.)

Step 2. From the LCL, draw a line parallel to the saturation adiabats upward to 500 mb. Let the temperature at this intersection point at 500 mb be called T'.

Step 3. Algebraically subtract T' from the 500-mb temperature. The value of the remainder (including its algebraic sign) is the value of the Showalter Index. (In Figure 37, $T' = -25°C$, $T = -22°C$; the Showalter Index is therefore +3.) This Index is positive when T' lies to the left of the T curve. Positive Index values imply greater stability of the sounding.

For forecasting purposes in the United States, Showalter [58] groups the range of index values as follows:

a. When the Index is +3 or less, showers are probable and some thunderstorms may be expected in the area.

b. The chance of thunderstorms increases rapidly for Index values in the range +1 to -2.

c. Index values of -3 or less are associated with severe thunderstorms.

d. When the value of the Index is below -6, the forecaster should consider the possibility of tornado occurrence. However, the forecasting value of all index categories must, in each case, be evaluated in the light of other synoptic conditions.

5.24.2. The Lifted Index. The arbitrary choice of 850 mb in the Showalter Index makes it difficult to use on a detailed synoptic time and space basis when, as often happens, there is an inversion or rapid drop in moisture which passes through the 850-mb surface between stations or between two successive sounding times. To avoid this difficulty, Galway of the U. S. Weather Bureau SELS Center [2] devised the "Lifted Index" (LI), a modification of the Showalter Index. To evaluate the LI, the mean mixing ratio in the lower 3000 feet of the sounding is determined by equal-area averaging. Then the mean potential temperature in the lower 3000 feet at the time of convection is determined by forecasting the afternoon maximum temperature and assuming that a dry-adiabatic lapse rate will prevail through this 3000-foot layer (if significant heating, or cooling, is not expected during the afternoon, the mean temperature of the lower 3000 feet as shown on the sounding is used). From these mean values the LCL is located (see par. 4.20). Then the saturation adiabat through this LCL is extended upward to 500 mb. The 500-mb temperature thus determined is assumed to be the updraft temperature within the cloud if one develops. The algebraic difference between the environment temperature and the updraft temperature (observed minus computed) at 500 mb defines the LI. LI values are usually algebraically less than SI values.

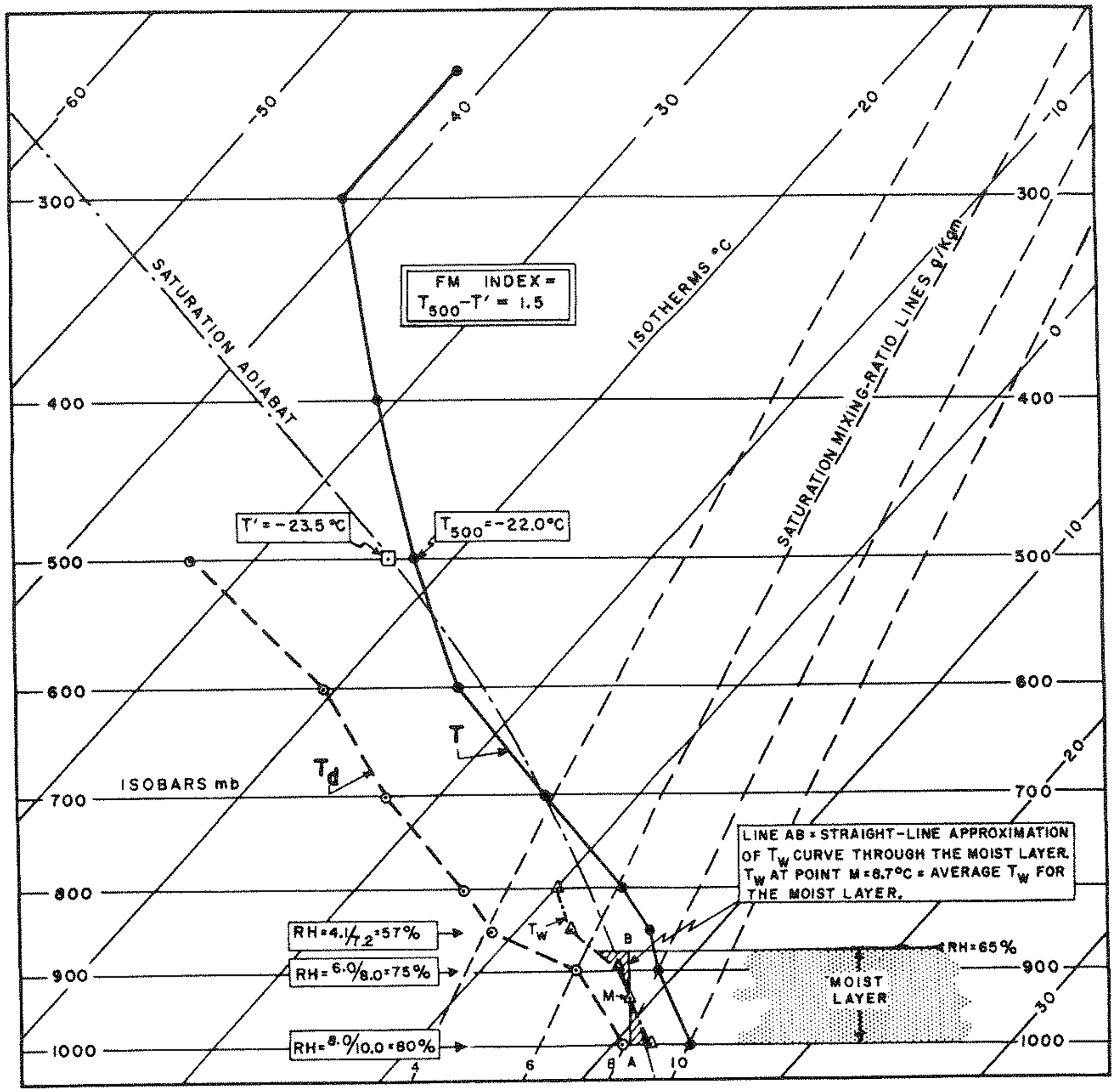

Figure 38. Computation of the Fawbush-Miller Stability Index (FMI).

5.24.3. The Fawbush-Miller Stability Index (FMI). This index involves consideration of a surface "moist layer." This "moist layer" is defined as a surface stratum whose upper limit is the pressure surface where the relative humidity first becomes less than 65%. If its vertical extent exceeds 6000 feet, only the lowest 150-mb layer is used to determine the mean wet-bulb temperature of the "moist layer." (Soundings sometime contain shallow dry layers within this defined "moist layer;" e.g., in the lowest 30 mb, or in the top layers of a surface inversion. In such a case, the assumption is made that the normal convective mixing of moisture will wipe out such shallow dry layers, and they are therefore ignored in identifying the "moist layer.")

The procedure for computing the FM Stability Index is illustrated in Figure 38:

Step 1. Compute the relative humidity (see par. 4.4) for enough points in the lower part of the sounding to identify the "moist layer." In the sounding shown in Figure 38, the "moist layer" extends to approximately 875 mb, since the 65% relative-humidity value is about half-way between 900 mb (where RH = 75%) and 850 mb (where RH = 57%).

Step 2. Plot the T_w curve (see par. 4.9) for the "moist layer." Draw a straight-line approximation of the T_w curve through this layer. The approximation will be sufficiently accurate, if the area between the straight line and the T_w curve is the same on each side of the straight line (equal-area averaging). The isotherm value at the mid-point, M, of this straight-line approximation of the T_w curve is the average T_w for the layer (in Figure 38, the "moist layer" average T_w = 8.7°C).

Step 3. From Point M of the straight-line approximation of Step 2, proceed upward parallel to the saturation adiabats to 500 mb. Subtract the isotherm value (T') at this new position from the observed 500-mb temperature indicated by the T curve. The value of the remainder (including its algebraic sign) is the numerical value of the FM Stability Index (in Figure 38, the FM Stability Index = +1 1/2). Positive values of the FM Index indicate stability; minus values, instability.

Fawbush and Miller classify the relative stability of soundings as follows:

a. FM Index greater than +1: Relatively stable.

b. FM Index between 0 and -2: Slightly unstable.

c. FM Index between -2 and -6: Moderately unstable.

d. FM Index lower than -6: Strongly unstable.

The values of the FMI and the SI are usually quite similar. Occasionally, however, significant differences from the Showalter Stability Index result when the moisture value at 850 mb is not representative of the layer below that pressure as when a subsidence inversion is located just below 850 mb. Since the FMI considers more information about the moisture values, it appears to be more representative than the Showalter Stability Index. However, computation of the Showalter Stability Index is much easier, and in many cases is of comparable utility.

5.24.4. The Martin Index (MI). A stability index devised by Delance Martin, is claimed to be more "sensitive" to the low-level moisture than either the Showalter or FM Indexes [35]. It is evaluated on the Skew-T Chart as follows: Draw the saturation adiabat intersecting the temperature-sounding curve at 500 mb past the height of maximum mixing ratio. Find the intersection of this line with the saturation mixing-ratio line through the maximum mixing-ratio value in the sounding. From this intersection, draw a dry adiabat to intersect the 850-mb line. Algebraically subtract the sounding temperature at 850 mb from the temperature at the latter intersection. The resulting number (including its algebraic sign) is the Martin Index. With a marked low-level turbulence or subsidence inversion, the reference height is taken as the height of the base of the inversion instead of 850 mb.

Chapter 6

ANALYSIS OF DISCONTINUITIES AND STABLE LAYERS IN RAOBS

6.1. Introduction. The prevailing condition of the atmosphere is stable, with stratification into distinct layers. The mean lapse rate, above the surface layer affected by nocturnal radiation inversions and daytime surface heating, is near the saturation adiabatic up to the mid-troposphere, above which the mean lapse rate becomes increasingly stable with altitude. A typical sounding in any region and season will be stable over the greater part of its height and the stable parts will be divided into layers of different degree of stability.

For various reasons the analysis of the stability features of soundings is as important for forecasting as the analysis of the instability features. Although much of the weather that is of operational concern is associated with instability, the forecasting of instability weather generally is made from a currently stable condition and certain features of the stable structure are critical for the possibility of instability developing. Moreover, certain cloud, fog, and visibility conditions are associated with absolute stability. Stable layers are significant as indications of the kind of flow (smooth versus turbulent), of the possibilities for vertical and lateral mixing, and hence for the diffusion and transport of heat, moisture, aerosols, and momentum.

Two properties of the stability are of interest: The degree of stability (as indicated by the lapse rate) and the discontinuities of the lapse rate which mark the boundaries of each layer (so-called "laminar") of different stability.

6.2. Classification of Stable Layers. The types of stability have been described in Chapter 5. Stable layers of two kinds were defined: *absolutely stable* and *conditional.* The absolutely stable layers can be subdivided into three well-recognized types: *inversion*[20], *isothermal*[21], and *stable-lapse*[22] *layers.*

It has been customary to attempt to identify and describe these layers in terms of a single physical process supposedly the cause. The results of this must be rather arbitrary in many cases, because in Nature several of the causes are often operating simultaneously. Moveover, for many of the stable layers the recognition of the cause cannot be made with any assurance from the soundings alone.

[20] The free-air temperature normally decreases with altitude in the troposphere. However, frequently soundings show shallow layers where a reversal of the normal lapse rate occurs and the temperature increases with altitude or "inverts." These layers are called "inversions," or more specifically, *temperature inversions*. The prime characteristic of the inversion is the great stability of the air within the inversion layer.

[21] A layer through which the temperature does not change with height.

[22] Any stable layer in which the temperature decreases with height (excludes isothermals and inversions).

The analysis of the stable layers cannot be made independently of their boundary discontinuities (see par. 6.3) even though forecasters freely shift their attention from layer to discontinuity and vice versa as the situation and problem at hand may dictate. Whether one prefers to think of an "inversion" as a layer or as a discontinuity (strictly speaking, the base or top of the inversion) depends on the context and is mainly a difference in emphasis.

6.3. Synoptic Discontinuities. The usually-recognized "synoptic discontinuities" are: *fronts, bases of subsidence and turbulence inversions, and tropopauses*. These are considered "important discontinuities" in routine analysis and forecasting. Their location and identification are only partly made from raob soundings, however, and their importance likewise is judged largely by other factors.

6.4. The "Unexplained Discontinuities." One sees in the soundings many prominent discontinuities (as well as many lesser ones) that are ignored in conventional analysis, because their significance has not been obvious and no acceptable models for their interpretation have been developed. With the present spacing of sounding stations and existing coding procedures, it is difficult to trace any time and space continuity that may exist in many of the discontinuities observed in the transmitted soundings, unless they are obviously accounted for by fronts or other familiar features on synoptic charts.

These "unexplained discontinuities," especially when they are widespread or persistent, may often be of practical importance because of their effect on turbulent diffusion and cloud formation, not to mention errors in analysis resulting from confusing them with fronts, etc.

The fact that many of the unexplained discontinuities seen in the regularly transmitted soundings probably have a synoptic-scale extent and history, is brought out by research studies [23] using a special detailed evaluation and analysis of the raobs. These studies also indicate there are many smaller discontinuities of similar nature which are "smoothed out" by the standard evaluation and coding procedures for raobs. An example of one of these detailed raob analyses will be instructive [23]. Figure 39 shows on a single adiabatic diagram a group of such detailed soundings for 1500Z, 29 March 1956. The great detail in these soundings was obtained by recomputing the evaluations from the original recorder records with less smoothing and retaining additional significant points that would be taken out by the coding procedure. The comparison of the soundings, which lie along a northwest-southeast line from Bismarck to Cape Hatteras, is effected by an extension of the hypothesis, first suggested by Palmén, that individual tropopauses are conservative along potential temperature surfaces [7]. The application of this hypothesis to other non-frontal discontinuities than tropopauses was given considerable justification by the experience with isentropic-chart analysis carried on routinely in the United States during 1938-1942; these charts seemed to show a marked tendency for the air flow and the stratification of the atmosphere to parallel isentropic surfaces, as predicted on theoretical grounds by Shaw and Rossby [45].

Note in Figure 39 that several prominent discontinuities in the troposphere conserve a similar shape and intensity from station to station while sloping through a great range in height. Relating them to the isentropes (dry adiabats) on the diagram, one can readily see that each of these discontinuities lies within small limits along a particular isentrope. The isentropic cross-section for the same soundings shown in Figure 40, reveals this tendency more clearly. The thin, solid lines on the cross-sections are isolines of potential temperature drawn for each whole °K. Packing of the isentropes on a vertical cross-section indicates layers of the atmosphere which are very stable (the greater the packing, the greater the stability). The great spatial extent of many of these stable layers ("laminars"), each associated with essentially the same "bundle" of isentropes, is evident in this figure. The accuracy and

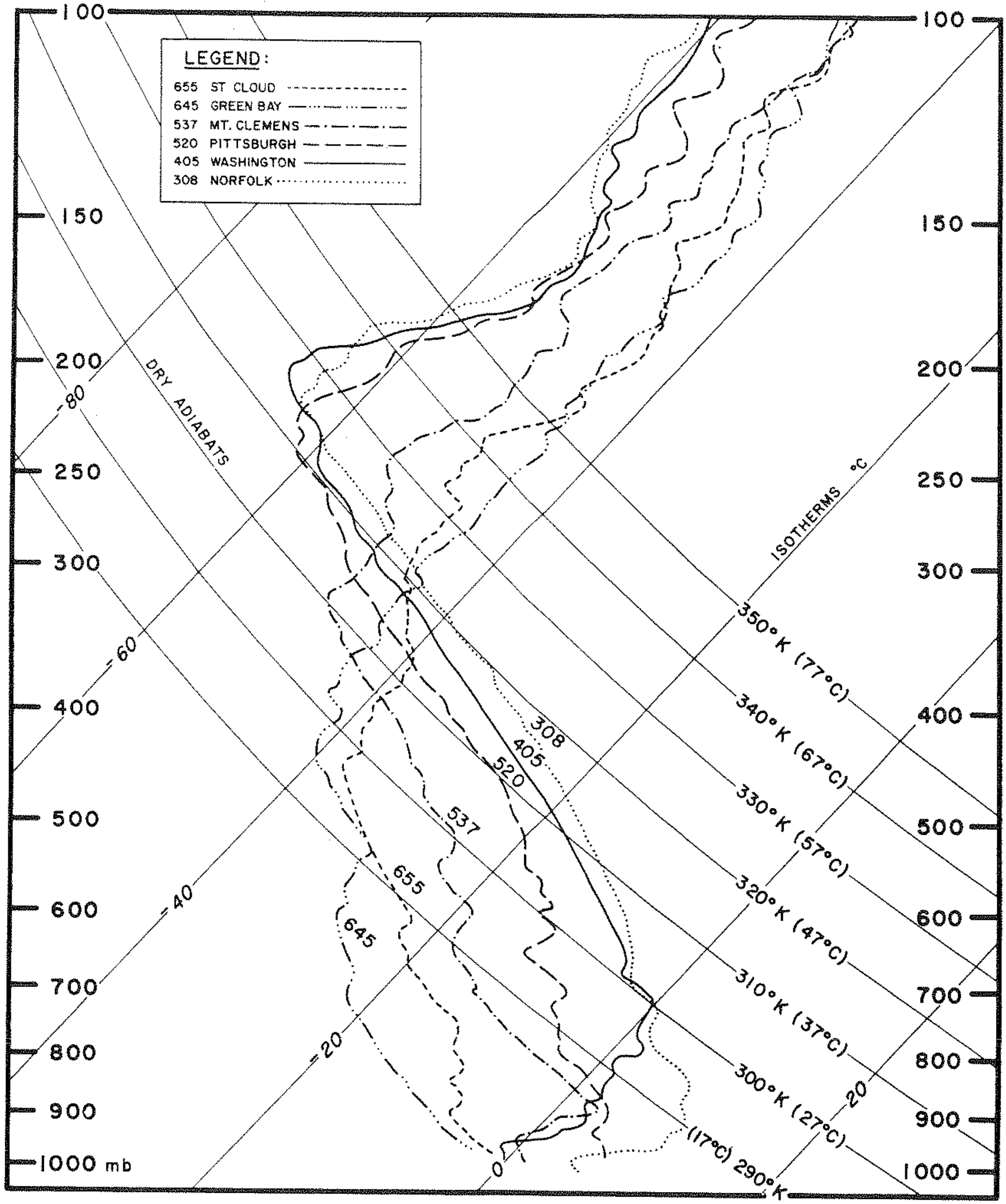

Figure 39. Sounding Curves for Six Stations Along a Line from Bismarck to Cape Hatteras, 1500Z, 29 March 1956 (Danielson [23]).

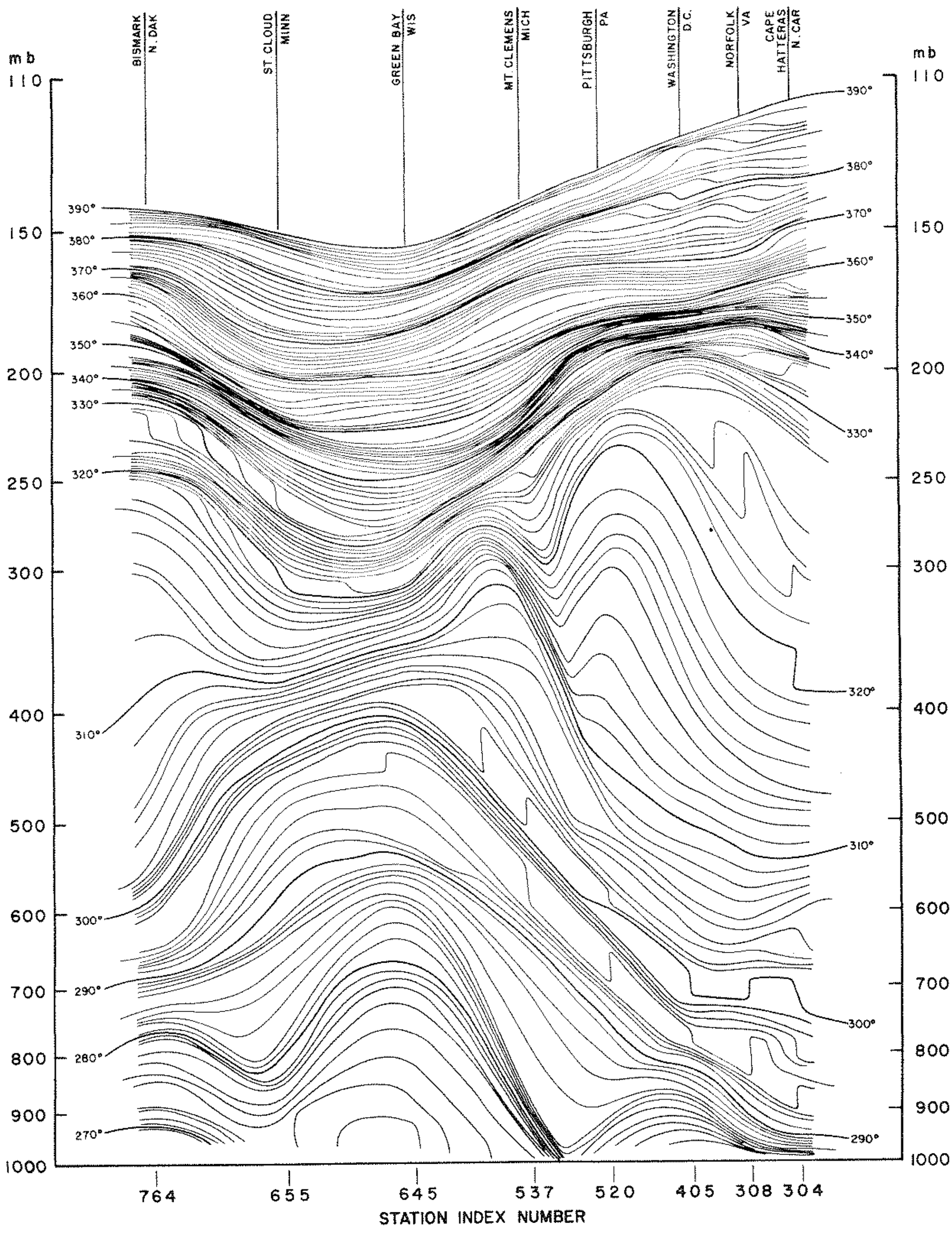

Figure 40. Isentropic Vertical Cross-Section from Bismarck to Cape Hatteras, 1500Z, 29 March 1956. The potential temperature isotherms are drawn for each °K (Danielson [23]).

spacing of the isentropes on this cross-section anaylsis have been corroborated by the constant-pressure and isentropic charts, trajectory analysis, and use of thermal-wind relationships. Another interesting feature is the continuity of some tropopause "leaves" with discontinuities reaching far down into the troposphere (see par. 6.10.0).

6.5. Radiation Inversions and Layers. Nocturnal and polar radiation inversions are formed when the lowest layers of the atmosphere are cooled by contact with the radiationally-cooled earth's surface (see par. 5.11.2). The depth and lapse rate of the cooled layer will depend on the wind speed, amount of cloud, type of surface, and number of hours of darkness, as well as on the initial temperature difference between the air mass and ground [63]. An example of a sounding showing a nocturnal radiation inversion with calm conditions is seen in Figure 41. Wind tends to convert this structure to that of a turbulence inversion (see par. 6.7) which has its base at some level above the ground. All transitions between the two states are commonly observed. Often only a stable ground layer without inversion is found under nocturnal radiation conditions, a "radiation layer" which might be a pre-inversion stage but more probably is a light wind effect.

6.6. Subsidence Inversions and Layers. A subsidence layer is one which has undergone a general sinking. In the lower and middle troposphere, the sinking is manifested by vertical shrinking associated with horizontal divergence, as discussed in paragraph 5.14.6. Since widespread subsidence is directly involved in the creation and maintenance of high-pressure areas, subsidence layers in some degree are evident in nearly all anticyclones at some stage of their development. These layers are apt to be deep and pronounced in the so-called "warm highs," both in the tropics and mid-latitudes, in the polar high-pressure caps, and in rapidly equatorward-moving polar air masses ("cold highs").

The most striking feature of a well-developed subsidence layer is the inversion at its base with a strong upward decrease of moisture

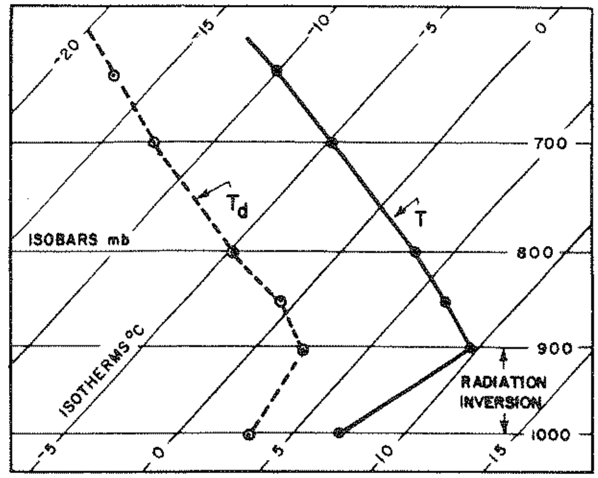

Figure 41. Nocturnal Radiation Inversion (1000 to 900 mb).

through the inversion ("dry inversion") and often continuing a great distance above it, as illustrated in both Figures 42 and 43. Above the discontinuity at the base of the layer (whether an inversion or merely a stabilization) is usually found a rather deep layer of stable, dry air. These features and the location of the sounding station within a high-pressure system are usually sufficient to identify a marked subsidence layer, provided the possibility of confusion with an overlying cold or warm front is carefully eliminated. (The katafront type of cold front can easily be confused with a subsidence inversion; see par. 6.9.1.)

The subsidence layer associated with a subtropical high cell (example in Figure 42) is usually deep and persistent, and over a given portion of the cell, especially in the central and western parts, the height of the inversion base is usually nearly constant. However, the height over a particular point does vary with time, due to the passage of migratory troughs, easterly waves, and the movement of the parent high cell. The subtropical inversion lowers and becomes very strong over the cold waters off the west coast of the continents. In the tropics these inversions are generally known as "trade-wind inversions." However, the term "trade-wind inversion" is also often used colloquially to indicate merely a stable layer associated with a rapid falling off of

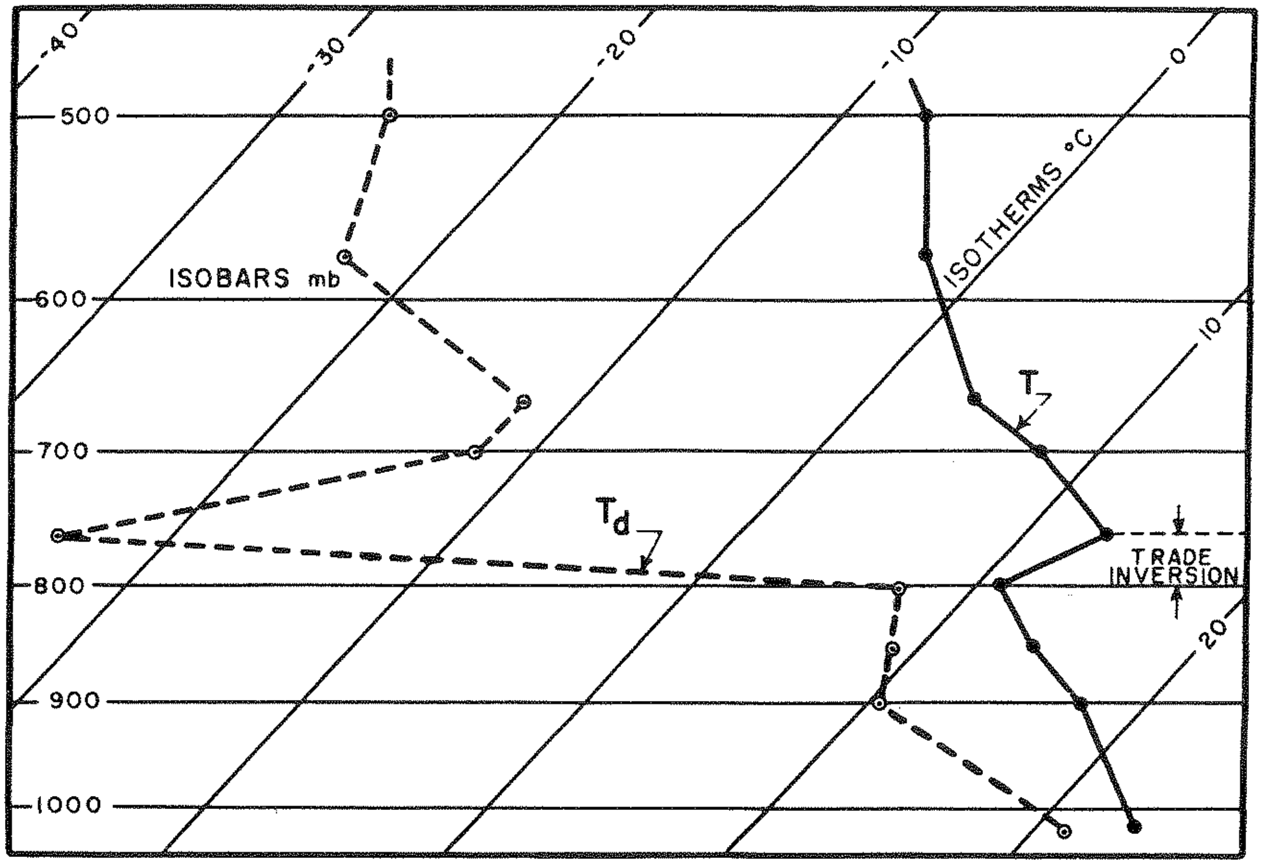

Figure 42. Subsidence ("Trade-Wind") Inversion Over San Juan, Puerto Rico.

moisture with height, rather than actual temperature inversion. The California coastal inversion is an example of a "trade-wind inversion" which persists for long periods in the summer and is removed only by a marked change in the prevailing pressure pattern. Unless the troughs and lows can be forecast, continuity and climatology are the best tools for forecasting the height of subsidence inversions in subtropical highs. (Sources of data on the subtropical inversion are given in [6] [51] and *AWSM 105-48*.)

Figure 43 is an example of a subsidence layer and inversion in a southward moving fresh polar air mass. The surface cold front passed 40 hours previously and is identified in the sounding by the inversion at about 650 mb (see par. 6.9.1).

A subsidence-inversion surface in a large high in the middle latitudes which is undergoing conversion from the cold to the warm type is often dome shaped, though the inversion tends to be stronger and lower on the eastern side. Such a subsidence inversion is usually highest over the center of the surface anallobaric (pressure-rise) field. As the high passes over a given station, the inversion base will first be observed to rise and then lower [44].

If it lowers too near the ground, as often happens near the periphery of a high, the inversion is likely to be modified or masked by frontal precipitation and by such surface effects as mixing (turbulence), convection, or radiation. Therefore, in the peripheral region it may be especially difficult to distinguish the subsidence inversion from frontal and turbulence inversions (see pars. 6.7 and 6.9.1).

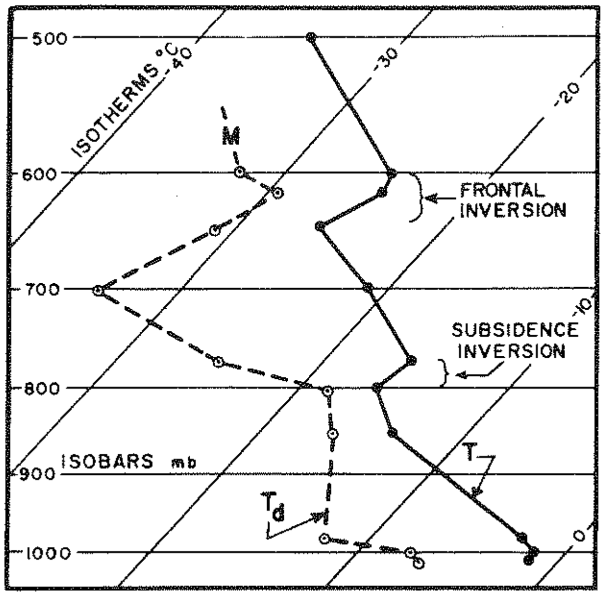

Figure 43. Subsidence Inversion in Polar Air Over Sault Ste. Marie, Michigan.

6.7. Turbulence Inversions and Layers. The movement of air over an uneven surface causes turbulence and vertical mixing. This mixing, in turn, causes the temperature lapse rate through the mixed layer to change toward the dry adiabatic (or saturation adiabatic if the moisture content and depth of the layer are great enough for the MCL to be reached - see par. 4.21). For an initially stable lapse rate, this means a decrease in temperature at the top of the mixed layer and a temperature increase at its base (i.e., at the surface).

The process is illustrated in Figure 44, which shows how a sounding would be affected by surface-frictional turbulent mixing in the simplest case (no cloud formation, no convergence, evaporation, radiation, nor advection effects).

On this sounding, the layer from the surface to 850 mb has been thoroughly mixed by low-level mechanical turbulence. As a result, the temperature lapse rate through the layer becomes dry-adiabatic, and an inversion developes at the top of the mixed layer[23] The turbulent mixing also acts to bring the moisture content to a constant value throughout the entire layer. This, in turn, means that the T_d curve for the unsaturated layer becomes parallel to the saturation mixing-ratio lines, that is, the mixing ratio of the turbulently-mixed layer becomes constant with height. The relative humidity is decreased at the bottom and increased at the top of the layer.

The lag in the moisture element on the radiosonde (see pars. 7.5.0 through 7.5.3 and [17]) causes the moisture reported at the top of the mixed layer to be somewhat too low and therefore the plotted T_d curve in such a layer may never actually become completely parallel to the saturation mixing-ratio lines.

If the original moisture content of the mixed layer is sufficiently high and the mixing deep enough, saturation will be reached in the upper portions of the mixed layer. The effect of this process on a sounding is shown in Figure 45. Here the 900- to 850-mb layer becomes saturated as a result of the turbulent mixing of the layer between the surface (1000 mb) and 850 mb.

From a systematic point of view, the decision as to the future formation of a turbulence inversion would revolve around an estimate of the depth of the layer that will mix. The depth estimate depends basically on the expected wind speed, roughness of the underlying terrain, and the original lapse rate in the lower layers. If the overall initial or expected lapse rate indicates only slight stability, turbulent

[23] If the turbulence causing such an inversion is due solely to the roughness of the ground or water surface, the inversion will not be higher than a few thousand feet above the earth's surface. When surface heating becomes an additional factor the inversion may be much higher. High inversions are not known to occur solely as result of turbulence within the "free air," but undoubtedly turbulence helps to accentuate or diffuse some inversions and discontiuities already formed aloft by other processes.

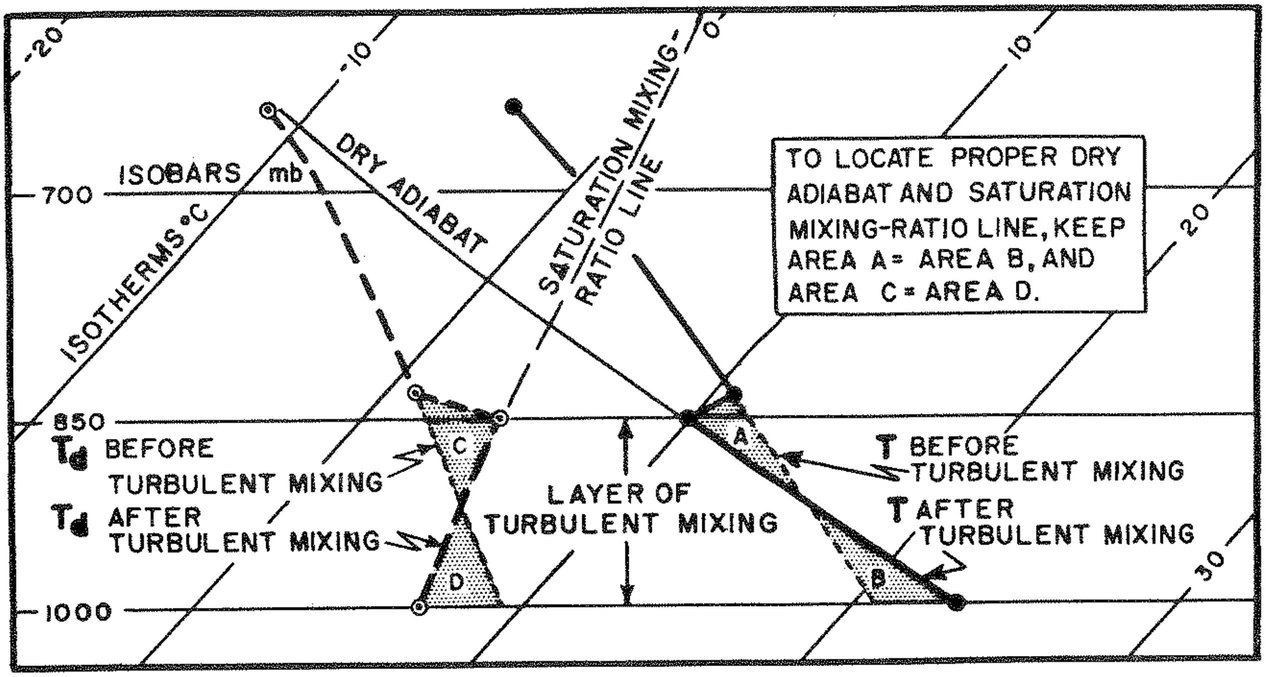

Figure 44. Formation of a Turbulence Inversion.

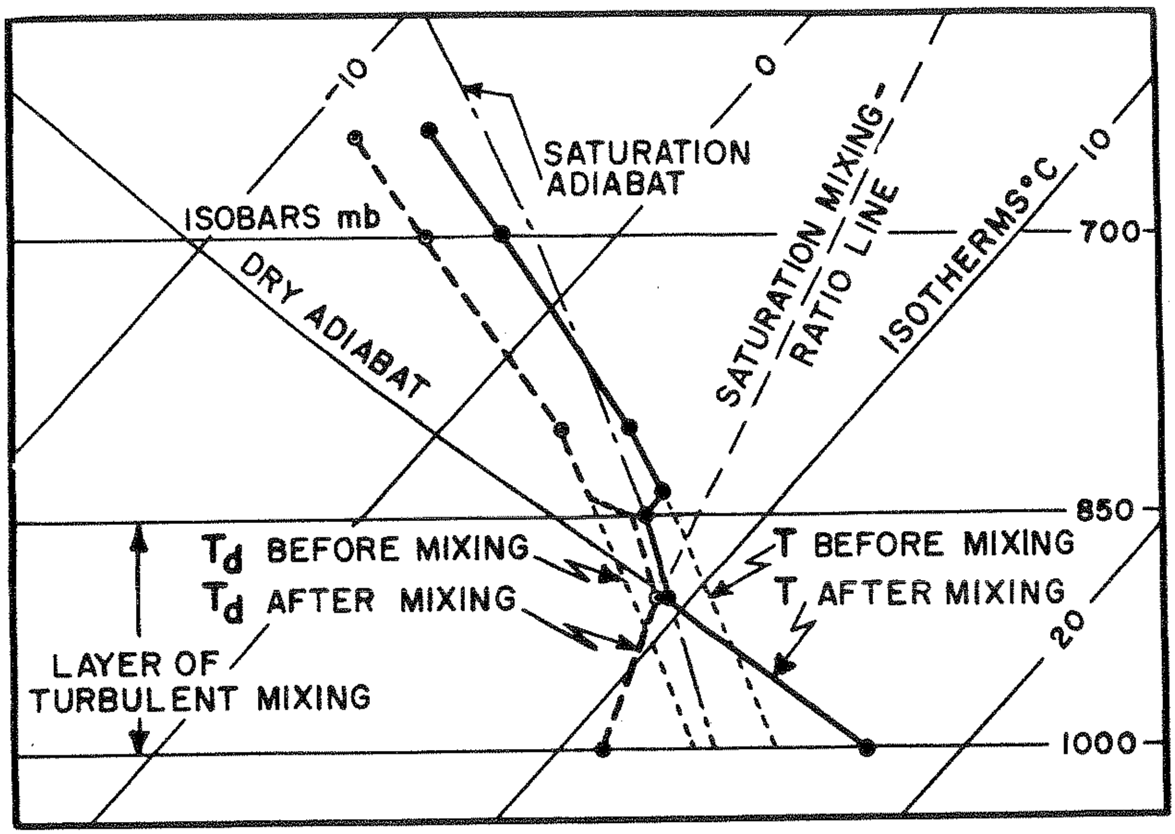

Figure 45. Saturation of a Layer by Turbulent Mixing.

mixing may easily extend to great heights without forming a marked inversion. There are often complicating factors. For example, vigorous cloud formation, convergence, upslope lifting, or additional convection from surface heating, tend to make a deeper mixed layer. On the other hand, divergence or continued radiation cooling tend to make a shallower mixed layer.

In face of these complications, experience is probably the best basis for predicting the depth of the turbulent mixing at any particular station; in this connection it is important to visualize the depth as a function of time, there being an ultimate maximum depth which is approached asymptotically as long as the constellation of factors continues unchanged. Once a first approximation to the expected depth has been estimated, the equal-area method can be used to find the appropriate dry-adiabat and saturation mixing-ratio line. This procedure is illustrated in Figure 44. If these two lines intersect within the layer as shown in Figure 45, the portion of the layer above the intersection is saturated with a lapse rate equal to the saturation adiabatic lapse rate.

The complications mentioned above are due to the fact that turbulent mixing generally occurs in conjunction with various other important atmospheric processes. Typical synoptic combinations are cited by Petterssen [47]. In the common case of warm air moving over cold ground, the mean temperature of the mixed layer gradually decreases and the inversion intensifies and lowers. In cold air moving over a warm surface, the temperature of the mixed layer gradually increases, the inversion weakens and rises, and ultimately may be eliminated.

6.8. Convection Inversions. Often when the troposphere is generally stable with a conditional lapse rate, vigorous dry or moist convection from surface heating or low-level convergence extends well up into the stable region with widespread and continued overshooting (see par. 5.1). The overshooting produces either a slight inversion or more generally a shallow very stable layer just above or at the top of the convection layer [16]. This effect is difficult to distinguish from effects of subsidence, and in the tropics sometimes the results become identical with low tropopauses [29].

6.9.0. Frontal Surfaces and Zones. The front separates two different air masses [27]. Each air mass has characteristics which were acquired in its source region, but which have been modified through changes caused by vertical motions, surface temperature influences, addition of moisture from evaporation of precipitation falling through the cold air mass, etc.

Frontal zones are often difficult to identify on a plotted sounding. The reasons for this will be brought out in the discussions to follow.

6.9.1. Temperature Characteristics of Frontal Zones. The *T* curve on the plotted sounding is the basic reference for locating frontal zones aloft. If the front were a sharp discontinuity, the *T* curve should show a clear-cut inversion separating the lapse rates typical of the cold and warm air masses. On the sounding shown in Figure 46, such a frontal inversion is indicated between 700 and 650 mb. However, a shallow isothermal or relatively stable layer (horizontal zone) is the more usual indication of a well-defined front. Frequently, the frontal boundary is so weak, distorted, or confused with other discontinuities, that frontal identification is very uncertain. Some of the conditions responsible for this difficulty are:

a. An air mass is rarely entirely without some internal stratification due to subsidence, shear, turbulence, and advection. This "layering" within an air mass shows up as irregulatities in the temperature sounding (see par. 6.4). The sounding shown in Figure 47 illustrates such minor stratification within an air mass. These effects may combine with others (see below) to create a lapse-rate discontinuity which resembles that of a frontal zone.

b. Vertical motions within the two air masses distort the original temperature contrast across the front, especially in the case of cold fronts. The vertical motion in the air

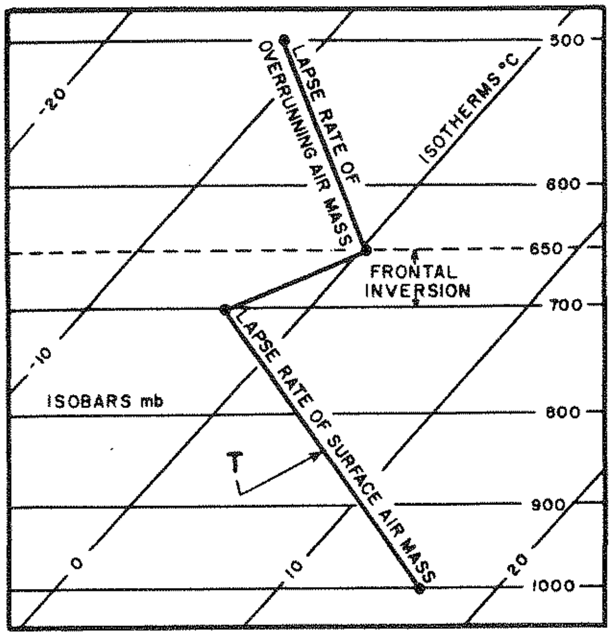

Figure 46. Frontal Inversion.

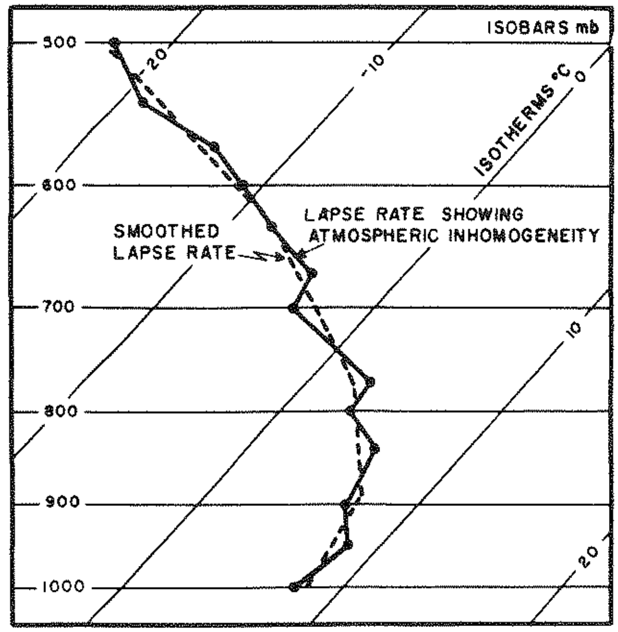

Figure 47. Effect of Atmospheric Inhomogeneity on an Otherwise Smooth Lapse Rate [55] .

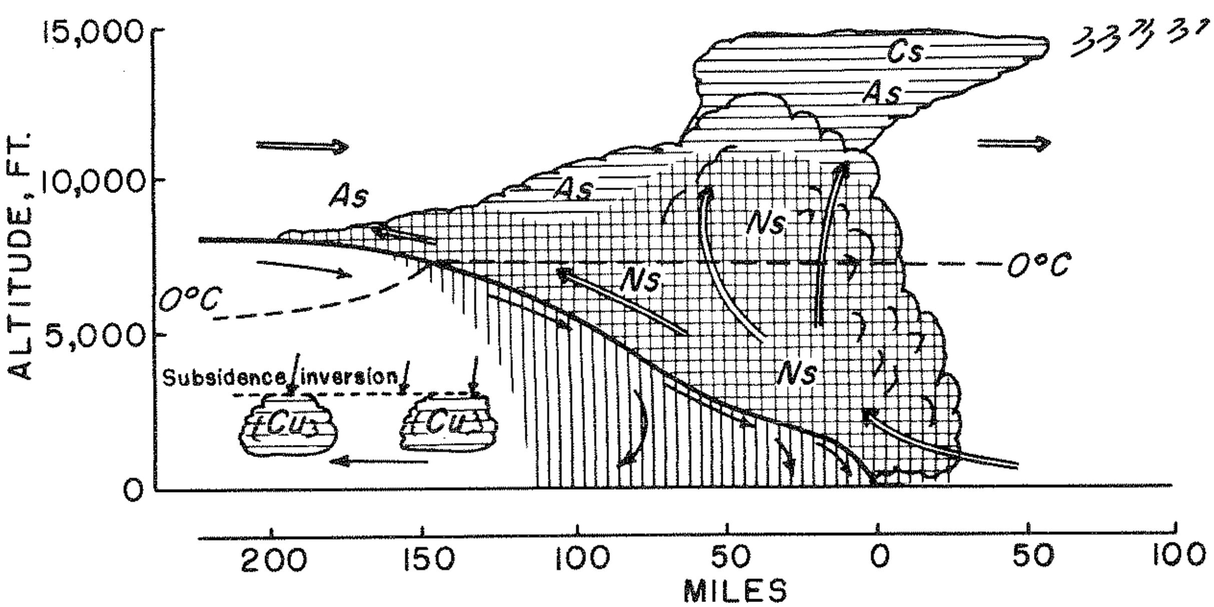

Figure 48a. Vertical Motion and Clouds Associated with an "Anafront" [25].

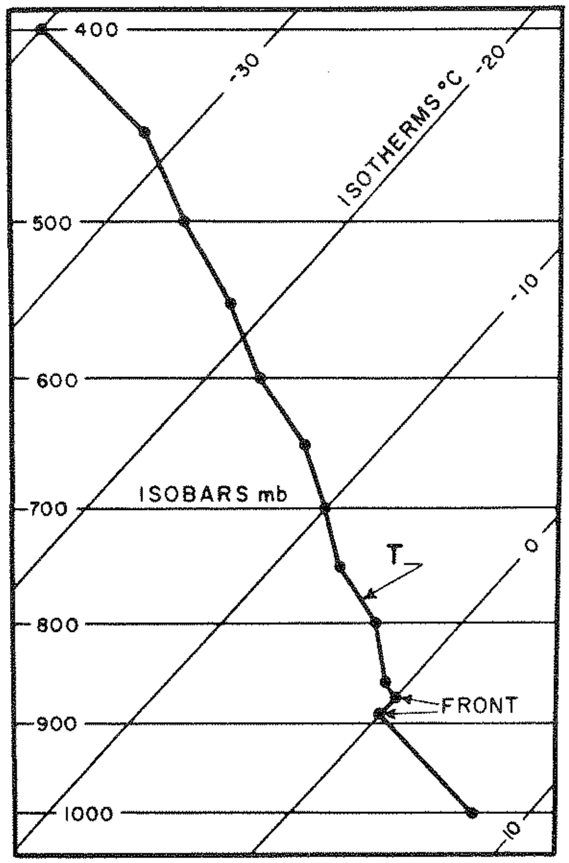

Figure 48b. Temperature Sounding Through an "Anafront."

masses associated with Bergeron's [12] two common types of cold fronts (see also par. 6.9.5) is shown in Figures 48a and 49a. An "anafront," a cold front which produces a widespread band of weather (see Figure 48a), is associated with downslope motion (subsidence and divergence) of the cold air and widespread upslope motion in the overrunning warm air. This process serves to decrease the temperature contrast across the front, thus weakening the frontal discontinuity. However, when condensation (warming) takes place in the warm air mass and there is evaporation of rain falling (cooling) through the cold air, the contrast across the front is likely to be maintained or increased. A "katafront," a cold front which is characterized by a narrow weather band (see Figure 49a), is associated with downslope motion in the warm air over the higher reaches of the frontal surface. The descending warm air mass is warmed adiabatically, and the temperature contrast across the front is increased, thus strengthening the frontal discontinuity. Examples of temperature soundings taken through an anafront and through a katafront are shown in Figures 48b and 49b, respectively.

c. The usual subsidence within the southward-moving cold air often creates one or more inversions or discontinuities in lapse rate *below* the frontal inversion (see in Figure 43, the 800- to 770-mb layer). These lower discontinuities can be mistaken for a true frontal zone; also, they may be so close to the frontal zone that only one deep inversion or stable layer is evident. An example of a sounding indicating a frontal layer and a subsidence layer in close proximity is shown in Figure 50. On this sounding, a subsidence layer from 870 to 820 mb is stronger than the frontal layer from 740 to 680 mb. The low T_d values of the 870- to 820-mb layer identify this layer as one caused by subsidence. However, if precipitation were to fall through the layer from above, thus raising the dew point, there might be little or no clear indication of the subsidence origin of the layer.

d. The boundaries of a frontal zone are frequently indistinct because the zone merges gradually into the adjacent air masses. In such cases the T curve changes gradually from a quasi-isothermal lapse rate in the frontal zone to the characteristic lapse rates of the air masses. To determine with assurance which significant point of discontinuity in lapse rate mark the limits of the frontal zones then becomes difficult or impossible. An example of a sounding taken through an indistinct frontal zone is shown in Figure 51. On this sounding, the frontal zone is most clearly evident in the 830- to 780-mb layer, but the exact frontal-zone boundaries (especially the top) are indistinct. In such cases [27], wind and humidity data, or possibly a temperature comparison with a previous sounding or with a sounding from a nearby station, may help to resolve the problem (see pars. 6.9.2 and 6.9.3). (In practice, the location of fronts should rest more on the analyses of the horizontal-temperature field on the

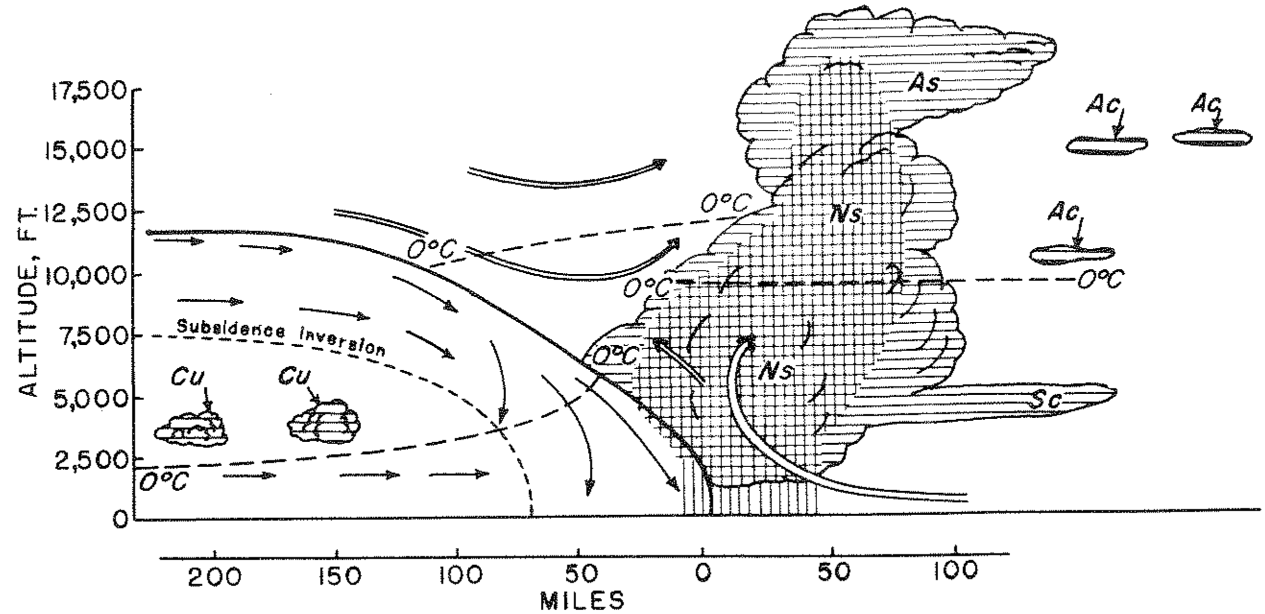

Figure 49a. Vertical Motion and Clouds Associated with a "Katafront" [25].

surface and upper-air charts.) For example, on the sounding shown in Figure 51, the height of the top of the frontal zone could be estimated as most probably 700 mb, although the 640- to 700-mb layer also shows evidence of a temperature gradient from colder air below to warmer air above. If the height of the frontal-zone boundary in question is more clearly defined on a sounding taken at some other not too distant station, the analyst may use the concept of quasi-constant potential temperature along the frontal surface, except in the lower layers; i.e., he may expect the frontal-zone boundaries to be located at or near the same potential-temperature value at both stations.

The lower frontal-zone boundary on the sounding of Figure 51 shows the influence of surface effects; nocturnal radiation had produced a surface inversion, which was being wiped out in the 850- to 1000-mb layer. The remains of the radiation inversion persist and mask the bottom of the frontal zone. Here again, a subjective if not arbitrary judgment is required — the analyst must select the significant point which he believes is most representative of the change from pure air-mass to transition-zone lapse rate. In this case, 860 mb is probably the best estimate because this level separates two layers having

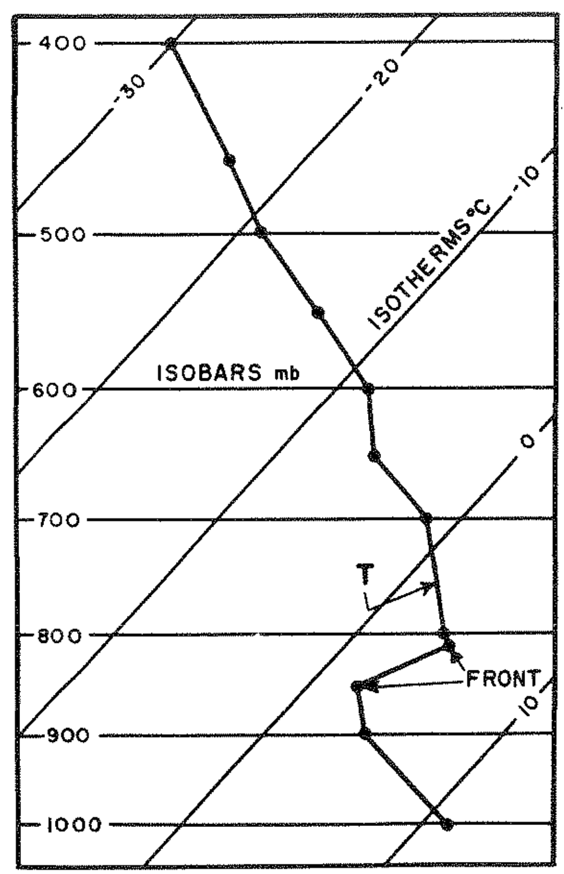

Figure 49b. Temperature Sounding Through a "Katafront."

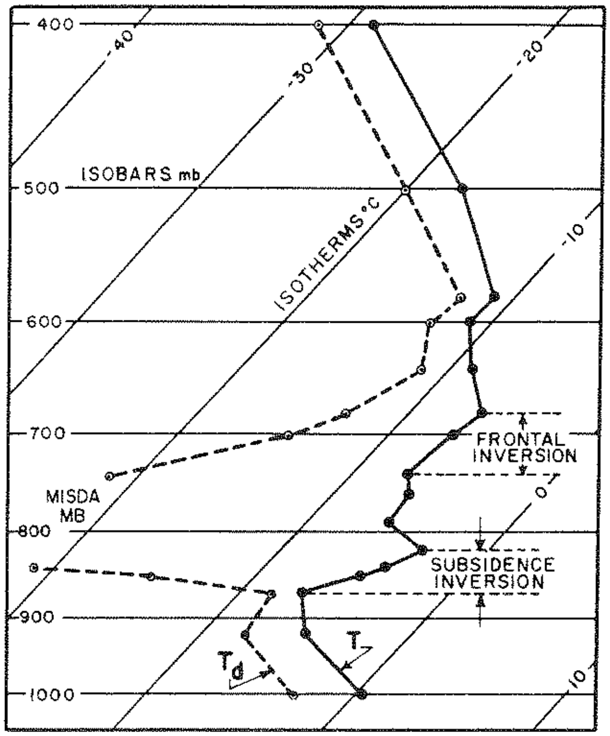

Figure 50. Frontal and Subsidence Inversions.

semi-constant lapse rates, viz., the layers from 950 to 860 mb, and from 860 to 780 mb.

6.9.2. Humidity Characteristics of Frontal Zones. The relative-humidity curve through a front would, of course, show a saturation or near-saturation where there is a frontal-cloud layer (see Chapter 7), but otherwise there may be no consistent indication of the front in the relative humidity. The mixing ratio, T_d, or T_w curve, however, often has a characteristic behavior. In an ideal case, the T_d curve through the frontal zone will show an inversion or sharp change associated with that of the T curve. On the sounding shown in Figure 52, a dew-point inversion (i.e., increase) is evident between 870 and 790 mb. In this particular case the T_d curve would be a primary aid in locating the frontal zone, since the T curve below 900 mb has been affected by nocturnal radiation to an extent that the location of the frontal inversion on this curve is obscured. Such a marked distribution of humidity through fronts is not regularly observed, however, because of the following effects:

a. The humidity element of the radiosonde is inaccurate in many respects [17] (see also, *AWSM 105-39*, *AWSM 105-48*, and Chapter 7).

b. The warm air mass may have been dried out, either by subsidence along the frontal slope (see Figure 49a), or by a trajectory past an upstream ridge. The cold air may then show T_d values higher than those of the warm air.

c. The underlying cold air often acquires moisture rapidly through evaporation from a water surface, such as the Great Lakes, and also through evaporation from wet ground or of rain falling from the warm air mass above.

However, these effects usually do not obscure all the more marked differences between frontal inversions and subsidence inversions (see Figure 50).

Sawyer [56], in a study of humidity data obtained on 23 Meteorological Research Flights through fronts over England, found that usually a characteristic tongue of relatively dry air was associated with many of the frontal zones. The dry zone extended downward in the vicinity of the fronts and was tilted in the same direction as the front. An example of this phenomenon is shown in Figure 53, which represents a cross-section of a front observed on one of the flights. The dry zone is indicated by the dew-point-depression maximum just above 600 mb.

The dry zone was less well developed with cold fronts than with warm fronts, and extended down to an average pressure of 700 mb in cold fronts and to 800 mb in warm fronts. In about half of the fronts, the driest air was found within the frontal transition zone itself, but there were also occasions when dry air was found on both the cold and the warm sides of the transition zone. Striking changes of frost point were observed as the aircraft entered the dry zone; about half of the flights showed a sharp transition from moist to dry

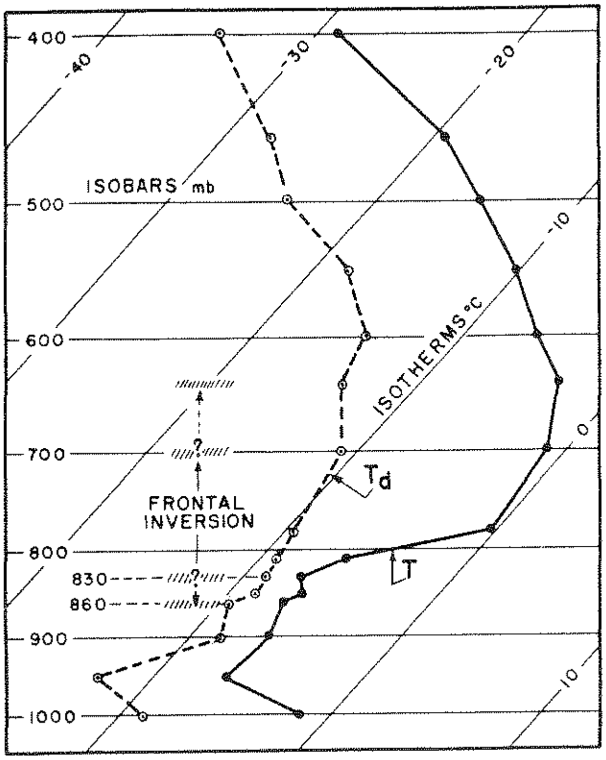

Figure 51. Sounding Showing Indistinct Frontal-Zone Boundaries.

air, with an average frost-point change of about 37°F in 35 miles horizontal distance. Some of the sharpest changes were more than 40°F in 20 miles.

6.9.3. Wind Variations Through Frontal Zones. Because the analysis of the vertical-wind profile through the front is an important and often necessary adjunct to raob analysis in locating fronts, it is desirable to discuss the subject here.

The classical picture of the variation of the wind along a vertical through a frontal zone is shown in Figure 54. Through a cold front, the wind backs with height; through a warm front, the wind veers with height. On the Skew-T Chart shown in Figure 55, the plotted upper winds (above the surface layer) which show the greatest variation are those for the 800- to 650-mb layer. This indication coincides closely with the frontal indications of the T and T_d curves. Since the wind veers with height through the layer, the front would be of the warm type.

6.9.4. Thermal-Wind Indications of Frontal Zones. The magnitude of the thermal wind for a layer indicates the strength of the horizontal gradient of the mean temperature of the layer. Since a frontal zone defines a layer of maximum horizontal thermal gradient, it also represents a zone of maximum thermal wind. Furthermore, since the thermal wind blows parallel to the mean-temperature isotherms for the layer (with cold air to the left), the direction of the thermal wind vector will be roughly representative of the directional orientation of the front. The winds-aloft for the sounding shown in Figure 55 are seen plotted as a hodograph in Figure 56. The thermal wind is indicated by the shear vector connecting the wind vectors for the base and top of each layer.

The maximum thermal wind is found between 700 and 650 mb, supporting the previous frontal indications described in paragraph 6.9.3, above. The direction of the thermal wind vectors from 800 to 650 mb is roughly north-south; the frontal zone could thus be assumed to be oriented along a generally north-south line.

6.9.5. Wind Distribution as an Indicator of the Dynamical Characteristics of Cold Fronts. Sansom [53], in an investigation of cold fronts over the British Isles, found a definite relationship between the variation of wind with height through a cold frontal zone and the weather characteristics associated with the front at the surface. He classified most of the cold fronts into Bergeron's two types (the lapse-rate indications for which were noted in par. 6.9.1), and listed the definitive upper-wind characteristics of each.

a. *Anafronts* are associated with widespread, heavy rain at the time of frontal passage, and with steady rain continuing for some time behind the front. The cloudiness resembles that of a warm front in reverse and clears slowly after frontal passage. Upper-wind variations through an anafront are as follows:

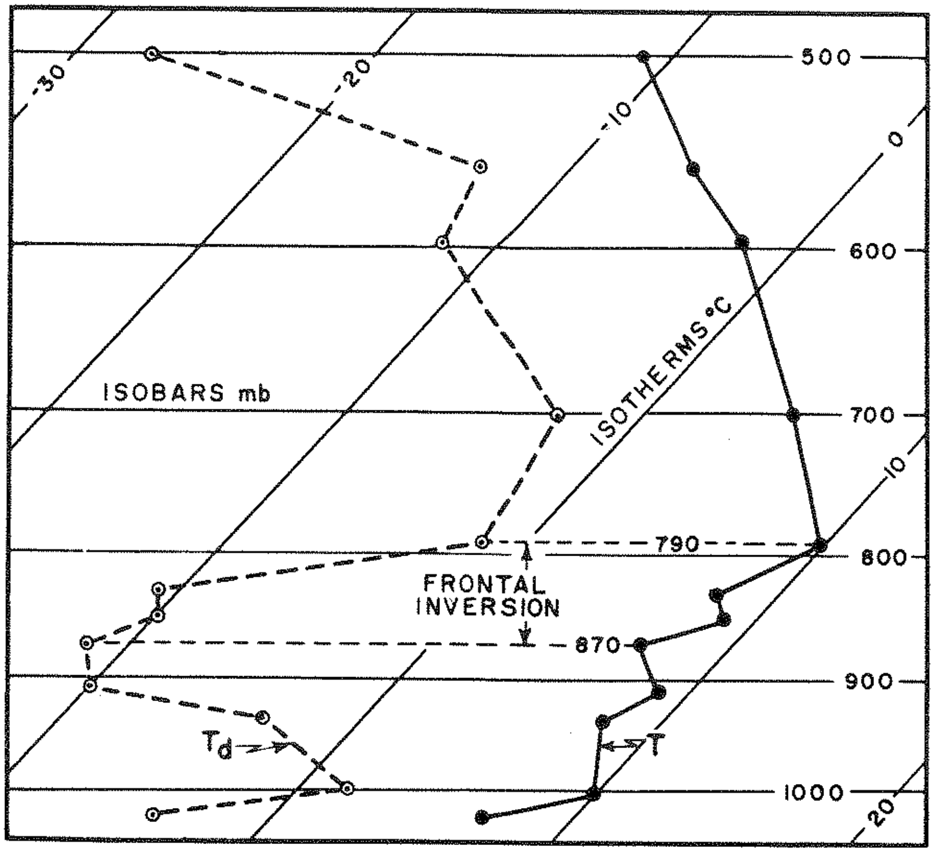

Figure 52. Frontal-Zone Indications from the Dew-Point Curve.

(1) Rapid backing of the wind with height (about 65 degrees between 950 and 400 mb); at 500 mb, the wind direction is inclined at a small angle (about 15 degrees) to the front.

(2) The wind component normal to the front decreases slightly with height, while the component parallel to the front increases rapidly. The mean speed of the front exceeds the wind component normal to the fronts, although the excess is insignificant below 800 mb.

(3) The thermal wind between 950 and 400 mb is almost parallel to the front.

b. *Katafronts* are associated with light, short-period precipitation and rapid clearing after frontal passage. The upper-wind variation through a katafront is as follows:

(1) Slight backing of the wind with height (about 20 degrees between 950 and 400 mb); at 500 mb, the wind direction is inclined at an average angle of about 42 degrees to the front.

(2) The wind components normal and parallel to the front both increase with height.

The wind component normal to the front exceeds the mean speed of the front at all levels above the lowest layers.

(3) The thermal wind between 950 and 400 mb is inclined at an average angle of about 30 degrees to the front.

The cold fronts which Sansom listed as "unclassified" were found to have upper-wind characteristics intermediate between those of anafront and katafronts. The wind component normal to the unclassified front was almost constant with height.

Sansom also investigated the vertical variation of the wind 50 to 150 miles ahead of the cold front; i.e., in the warm sector. He found little change of wind direction with height, but the angle between the warm-sector winds aloft and the surface fronts differed for anafronts

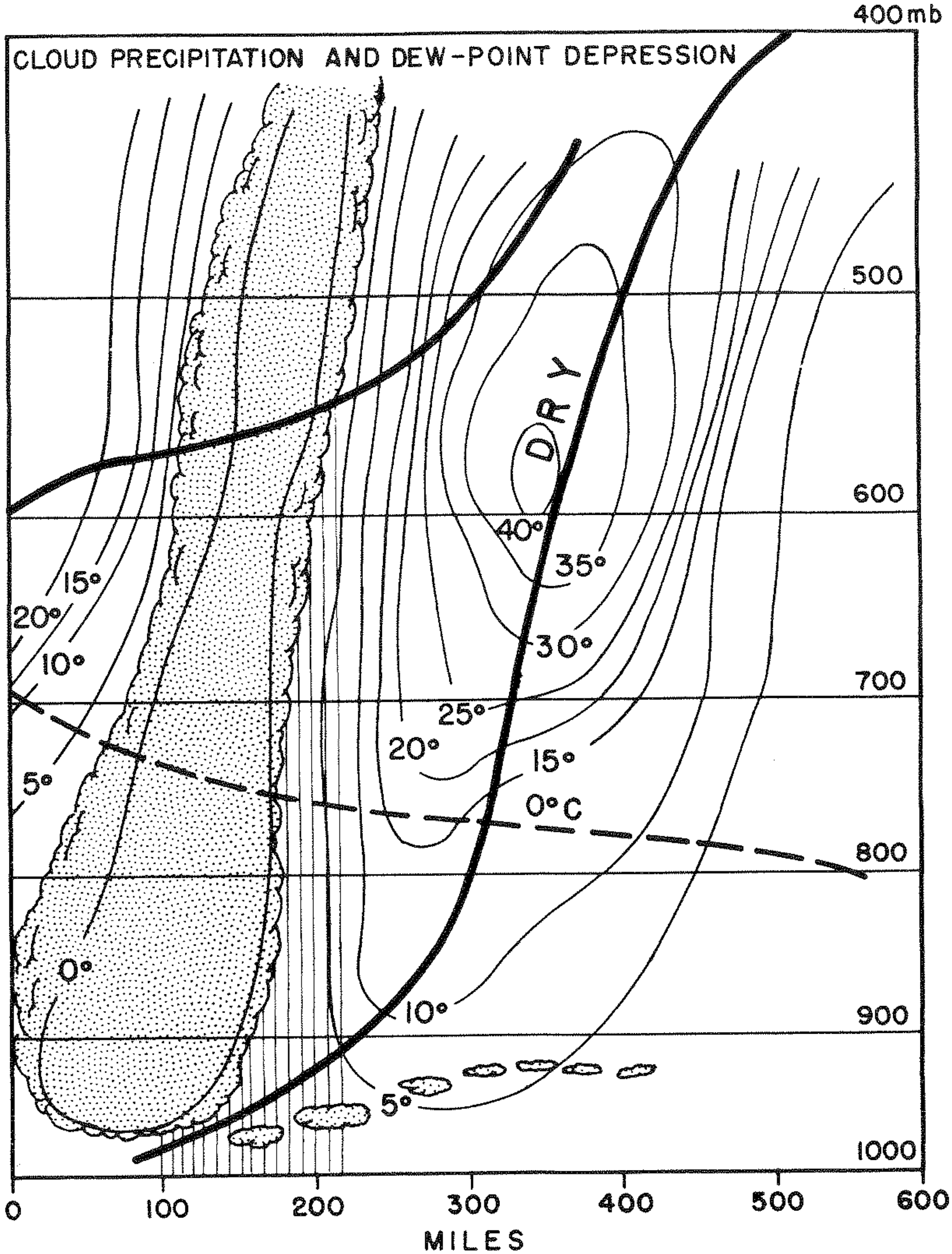

Figure 53. Vertical Cross-Section (Sawyer [56]) Indicating the Dry Tongue in a Warm-Frontal Zone. Cross-section is approximately normal to the front. Thick solid lines are boundaries of the frontal zone. Thin solid lines are isopleths of dew-point depression in °C. Shaded area indicates main features of the frontal cloud. Vertical hatching indicates precipitation outside of the cloud.

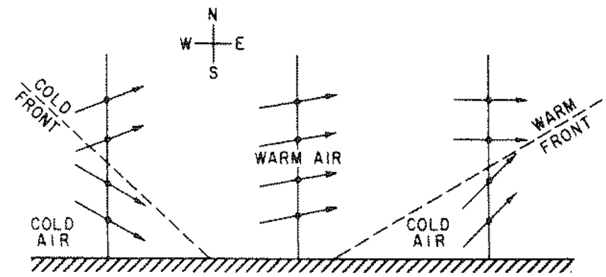

Figure 54. Vertical Distributions of Wind Direction in the Vicinity of Frontal Surfaces

and katafronts. The average angles between the surface fronts and the associated warm-sector winds at 700 and 500 mb are shown in Table 2.

TABLE 2

Angle between the Cold Front at the Surface and the Wind Direction in the Warm Sector.

	Anafront	Katafront
700 mb	18°	35°
500 mb	17°	35°

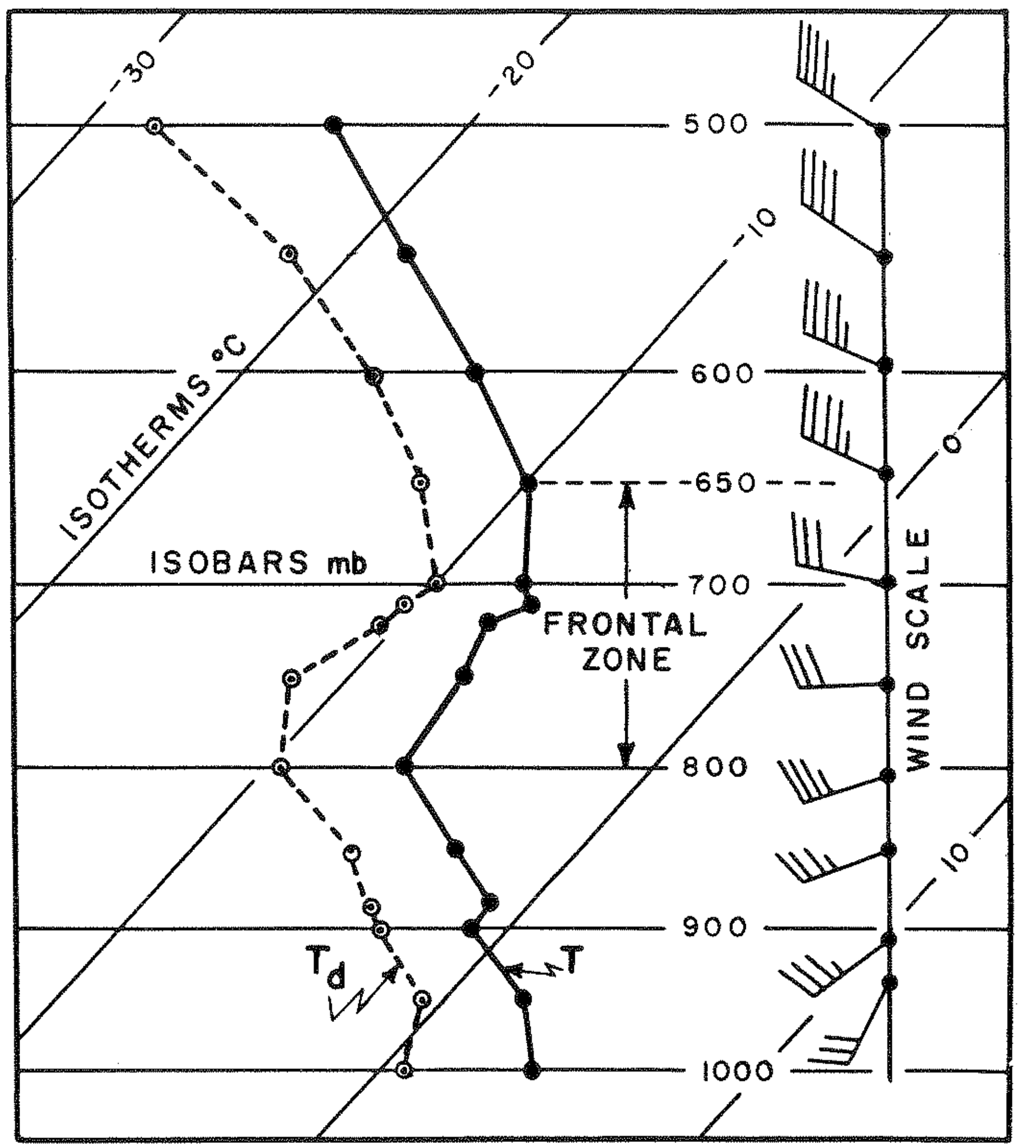

Figure 55. Distribution of Wind and Temperature Through a Frontal Zone.

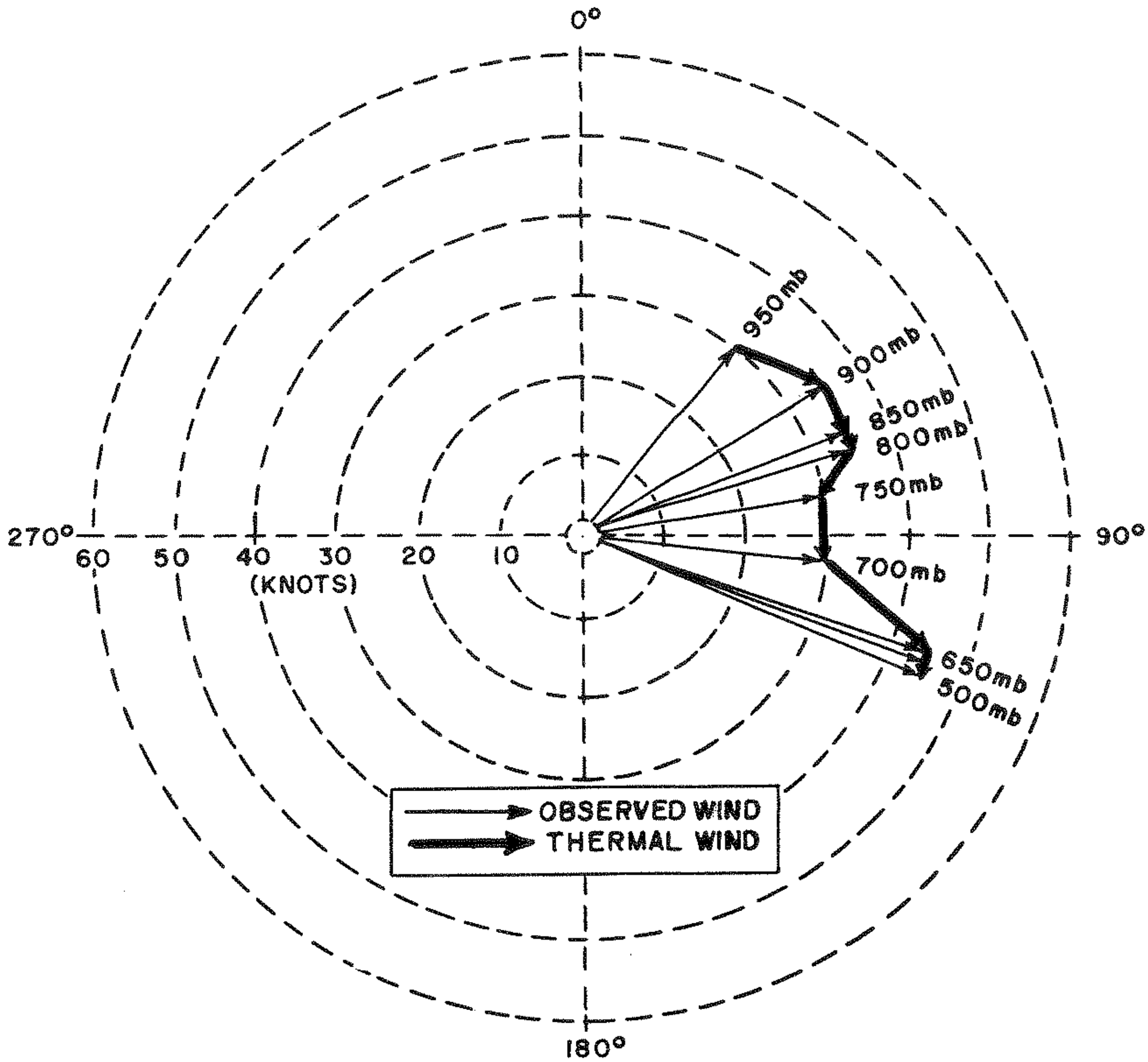

Figure 56. Hodograph of Observed and Thermal Winds for Sounding of Figure 55.

6.10.0. Tropopauses. Although the concept of a tropopause has been generally accepted for many years, there is still no agreement on how to apply the concept to synoptic analysis. Historically, the word was coined when the stratosphere was discovered, to describe the apparent "boundary" which separated the troposphere from the stratosphere. The scattered early soundings led meteorologists to believe that the tropopause was a single unbroken discontinuity surface, but later observations suggested that probably it is a varying transitional zone, often with several layers separated by overlapping discontinuities ("multiple tropopauses"). In any case, until recently it was generally assumed that the tropopause largely suppresses transfer of heat, air, or water vapor between the troposphere and stratosphere. However, with the large number of soundings now reaching the stratosphere each day, it becomes possible to see [7] [23] that through the tropopause "breaks" quasi-horizontal air flow passes freely between the troposphere and stratosphere. An example can be seen in Figure 40.

There are many soundings on which the locating of a generally acceptable tropopause is very easy. These cases include those where a single strong inversion or marked stabilization of the lapse rate occurs. However, there are many other soundings where it is quite difficult to determine where the troposphere ends and the stratosphere begins. In these cases, the lapse rate may just gradually become more stable without any prominent sudden stabilization of the lapse rate with height, or there may be more than one point of stabilization; then it becomes a controversial problem to decide which point should locate the tropopause. The variation in structure in the tropopause region has led to many different ideas on how to define and analyze a tropopause. It has also been proposed to analyze a "tropopause layer" which would arbitrarily include the zone encompassing the various tropopauses occurring over a given area at a given time [1]; but this does not appear to be of practical value in operational forecasting. The conflict between the definitions officially advocated or used in different countries was finally compromised by the WMO who have standardized an arbitrary definition of the tropopause for operational use in internationally-exchanged uper-air sounding reports.

The present WMO definition does not attempt to settle the question as to what the tropopause is, which remains controversial. It defines, rather, an objective technique for locating the lowest height in the atmosphere where the lapse rate first decreases to an average lapse rate of 2°C/km for a two-kilometer layer. While the physical significance of this lowest height remains to be found, it does establish an international reference height to which other atmospheric phenomena can be empirically related. The main advantage is that the definition is objective, in that it allows the same height to be consistently selected by all technicians from a given sounding.

Various empirical and statistical relationships [34] [43] have been prepared in the past relating such things as the height of cirrus or the maximum wind to the height of the tropopause. These studies have probably been prepared using a more or less different definition of the tropopause than the WMO one. Before continuing to use these relationships, the difference(s) between the tropopause definition used and the current WMO definition should be determined to make certain that the relationships are still sufficiently valid when referred to tropopauses now being determined by the WMO definition.

6.10.1. WMO Tropopause Definition. As noted above, objective criteria for determining the tropopause height(s) transmitted in upper-air observations have been internationally standardized by the WMO. Within its definition, provision is made for identifying two or more tropopauses on a sounding. The WMO definition for the tropopause is as follows:

a. The "first tropopause" is defined as the lowest height at which the lapse rate[24] decreases to 2°C/km or less, provided also that the average lapse rate[25] between this height and all higher altitudes[26] within two

---

[24]The *lapse rate* is the rate of decrease of temperature with height.

[25]The *average lapse rate* is the difference between the temperatures at the respective end points divided by the height interval, irrespective of the lapse-rate variations in the layer between the end points.

[26]All higher altitudes means that no point on the sounding in the two- (one-) kilometer interval above the "lowest height" can fall to the left of the 2° C/km (3°C/km) line extending from the "lowest height."

kilometers does not exceed 2°C/km. This tropopause will be termed the *conventional tropopause*.

b. If above the first tropopause the average lapse rate between any height and all higher altitudes[26] within a one-kilometer interval exceeds 3°C/km, then another tropopause is defined by the same criteria as under "a" above. This second tropopause may be either within or above the one-kilometer layer. There is no specific name given to this second tropopause nor to still higher tropopauses.

c. There are three qualifying remarks attached to the definition. They are:

(1) Whenever the sounding terminates at less than two kilometers above the altitude which otherwise appears to be a tropopause, the ascent is classified as *tropopause not defined*. This applies to both the conventional and the higher tropopause determinations.

(2) A height below the 500-mb surface will not be designated as a tropopause unless it is the *only* height satisfying the definition, and the average lapse rate in any higher layer fails to exceed 3°C/km over at least a one-kilometer layer. Further, the sounding must reach at least the 200-mb pressure surface. (The intention here is to admit that a discontinuity in the lapse rate at a height below the 500-mb surface is a tropopause only if it is reasonably certain that no other choice is possible.)

(3) When determining the second or higher tropopauses, the one-kilometer interval with an average lapse rate of 3°C/km can occur at *any* height above the conventional tropopause and not only at a height more than two kilometers above the conventional tropopause.

Figure 57 illustrates how to apply the WMO tropopause definition to a sounding. The conventional tropopause is defined by criterion "a" of the definition. This criterion is satisfied above Point B of Figure 57. That is, the average lapse rate between Points B and D, the next two higher kilometers above Point B, is less than 2°C/km for all points of the two-kilometer lapse rate (see Footnote 26). Thus, the conventional tropopause is established at Point B of the sounding.

There also is a possibility of a "second" tropopause at Point D. To find out, criterion "b" is used. This criterion requires a one-kilometer layer with a lapse rate greater than 3°C/km below the second tropopause height. This requirement is met through the layer CD, and in this particular case, qualifying remark "c(3)" applies also. When criterion "b" is met, then criterion "a" is again used to determine the location of a higher tropopause. Above Point D, the lapse rate DE again decreases to less than 2°C/km for the next two higher kilometers. Thus, a second tropopause is determined at Point D.

6.10.2. Character of the Tropopause. A special code for the character of the tropopause (symbol S_t) has also been adopted by the WMO to help describe the tropopause more completely. This code is described in Table 3.

The following remarks are needed to help decide which code figure to select when describing any given tropopause:

a. All lapse rates should be determined over a one-kilometer interval when using the criteria in the table.

b. If the conventional tropopause does not coincide with any marked change in lapse rate and a marked change of lapse rate occurs at heights both above and below the conventional tropopause, then the larger of these changes should be used to determine whether code figure 5 or 6 is appropriate.

c. When the conventional tropopause is best characterized by code figure 6 in arctic and antarctic regions in winter, a special case exists. Then the height of the marked change in lapse rate below the conventional tropopause should be referred to as an "arctic" or "antarctic" tropopause and recorded as such.

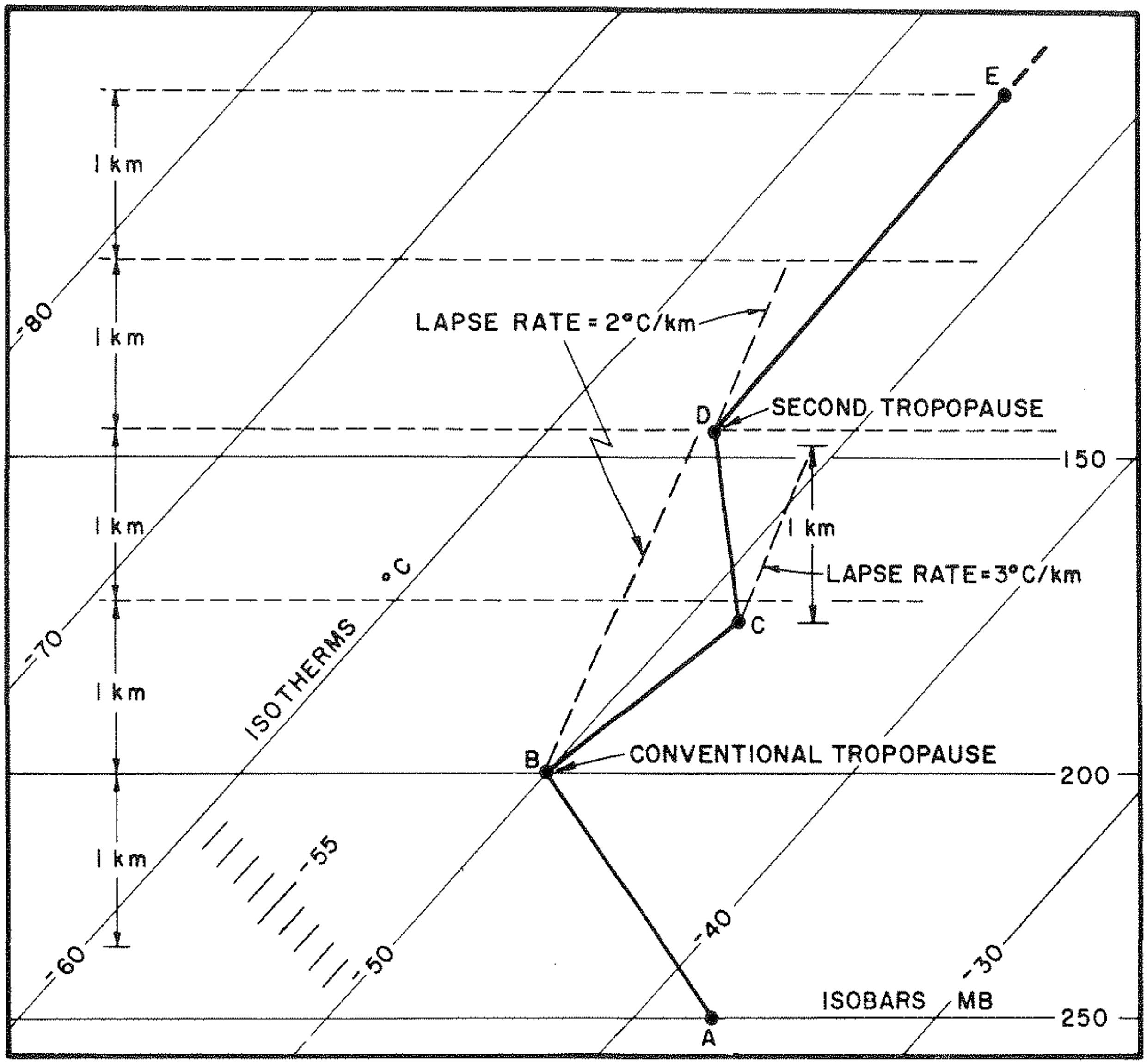

Figure 57. Tropopause Determinations Based on the WMO Definition.

This is done when there is not a one-kilometer interval between the "conventional" and "arctic" or "antarctic" tropopauses where the lapse rate exceeds 3°C/km.

If this occurs, the character of the "arctic" or "antarctic" tropopause should be given by code figure 9.

It is suggested that whenever a character of a conventional tropopause is given as code figure 5 through 9, the sounding be plotted and interpreted according to the use to be made of the tropopause information. In some cases it may well be that a tropopause with such a characteristic has no operational significance.

The determination of the character of the tropopause is rather straightforward. For example, in Figure 57 the character of the conventional tropopause at Point B is established by noting the lapse rate for the one-kilometer layer above and below it. Above Point B, the lapse rate is less than 0°C for a one-kilometer layer, while below Point B

TABLE 3

S_t - CHARACTER OF THE TROPOPAUSE

CODE FIGURE		CODE FIGURE DESCRIPTION	
1.	CONVENTIONAL TROPOPAUSE COINCIDES WITH A MARKED CHANGE IN LAPSE RATE	LAPSE RATE ABOVE TROPOPAUSE $\leqslant$ 0°C/km LAPSE RATE BELOW TROPOPAUSE $\geqslant$ 5°C/km	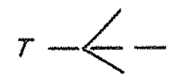
2.		LAPSE RATE ABOVE TROPOPAUSE $>$ 0°C/km LAPSE RATE BELOW TROPOPAUSE $\geqslant$ 5°C/km	
3.		LAPSE RATE ABOVE TROPOPAUSE $\leqslant$ 0°C/km LAPSE RATE BELOW TROPOPAUSE $<$ 5°C/km	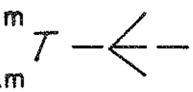
4.		LAPSE RATE ABOVE TROPOPAUSE $>$ 0°C/km LAPE RATE BELOW TROPOPAUSE $<$ 5°C/km	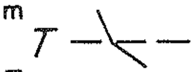
5.	CONVENTIONAL TROPOPAUSE DOES NOT COINCIDE WITH ANY MARKED CHANGE IN LAPSE RATE	BUT A MARKED CHANGE IN LAPSE RATE $>$ 3°C/km OCCURS AT A HEIGHT ABOVE THE CONVENTIONAL TROPOPAUSE	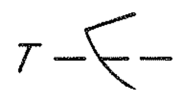
6.		BUT A MARKED CHANGE IN LAPSE RATE $>$ 3°C/km OCCURS AT A HEIGHT BELOW THE CONVENTIONAL TROPOPAUSE;	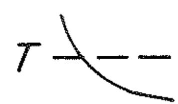
7.		AND NO MARKED CHANGE OF LAPSE RATE $>$ 3°C/km OCCURS AT ANY OTHER HEIGHT.	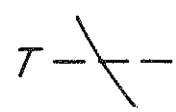

8. HEIGHT OF TROPOPAUSE UNCERTAIN BECAUSE TOP OF ASCENT IS LESS THAN 2 km ABOVE THE HEIGHT WHICH APPEARS TO BE THE TROPOPAUSE.

9. TROPOPAUSE IS NOT ALLOCATED TO ANY OF PRECEDING CATEGORIES.

the lapse rate is greater than 5°C for a one-kilometer layer. Thus, the character of the conventional tropopause is properly described by code figure 1 of the table.